SEPT. - DEC. 2000
Volume VI Number III

ISSN 0859 144X

THE ASEAN JOURNAL OF RADIOLOGY

Published by The Radiological Society and
The Royal College of Radiologists of Thailand,
Bangkok, Thailand

Started through an educational grant from Bracco since 1995

Leading-Edge Technology and Power

Computed Tomography Systems

TOSHIBA

GLOBAL IMAGING • MEDICAL SYSTEMS

Toshiba developed helical scanning which has become the global standard for CT. Other firsts include the real-time reconstruction technology known as AspireCI and other patented innovations creating the heart of the CT scanner. Acting now as a leader in CT technology, Toshiba continues its climb to the top in the area of clinical results.

The half-second CT scanner features a totally new concept in which the gantry has a cylindrical structure. This combines with revolutionary new multislice technology to collect multiple slices simultaneously in a single scan. The result is amazing volume data in a short time over a broad range. The CT has extended its range from diagnosis to treatment, and is now active over a wide range that includes the head region, cardiovascular, lung and abdomen, and limbs. Toshiba will continue to chart new paths in CT technology with new advances.

- 1998 Achieves cumulative global total of 10,000 systems.
- 1998 Development of multislice helical technology and half-second helical CT.
- 1996 Development of subsecond helical CT.
- 1993 Development of AspireCI real time technology.
- 1987 Obtains patent in Europe for helical scanning.
- 1986 Obtains patent in U.S.A. for helical scanning.
- 1979 Starts research on helical technology.

Evolving Step by Step Towards Tomorrow

Half-Second Real-Time Helical CT

- By creating the world's first 0.5 second full scan, Toshiba has realized use in the cardiac region.
- Toshiba has also realized 12 frame/second real-time reconstruction and 0.5 second/frame high-speed reconstruction.
- Equipped with highly definitive 3D display software.
- Designed for multislice technology.

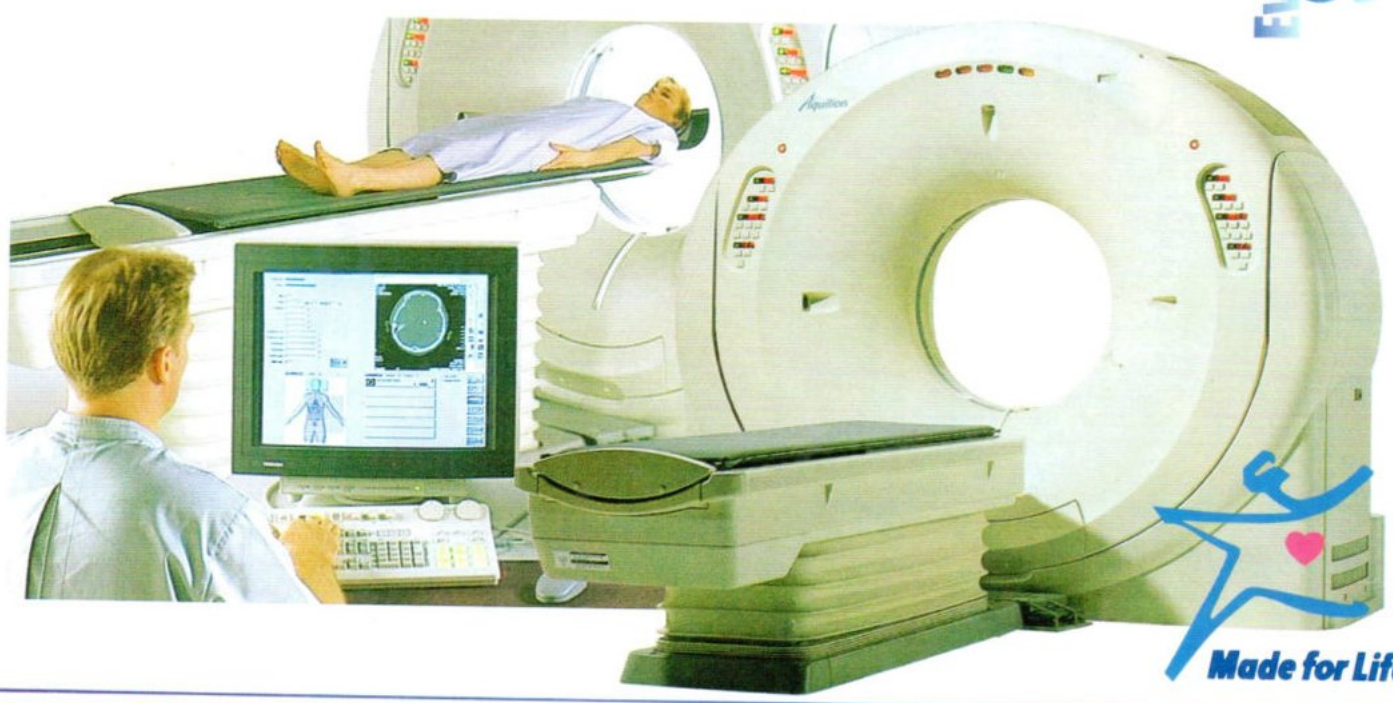

Made for Life

CMC BIOTECH

(SOLE DISTRIBUTOR)

CMC BIOTECH CO., LTD.

364 Muban Town-in-Town, Soi Ladphrao 94, Ladphrao Road, Wangthonglang, Bangkok 10310

Tel.(662) 530-4995-6, 559-2179-80, 538-4102, 538-0710, 559-3261-2 Fax: 539-6903

SEPT. - DEC. 2000
Volume VI Number III
ISSN 0859 144X

THE ASEAN JOURNAL OF RADIOLOGY

**Published by The Radiological Society and
The Royal College of Radiologists of Thailand,
Bangkok, Thailand**

Started through an educational grant from 1995

Chief Editor

Professor Kawee Tungsubutra
Kaweevej Hospital, 318 Taksin Road, Dhonburi, Bangkok 10600, Thailand.

Asean Journal of Radiology.
Instructions for Authors.

1. The Asean Journal of Radiology publishes the papers on Radiological Sciences, such as research work, review articles, case reports, innovations in Medical Sciences related to all branches of Radiology, and letters to the editor. The aforementioned materials can be written in English only.

2. The authors have to submit 2 copies of the manuscript and a diskette: **to Prof. Dr. Kawee Tungsubuttra.** 318 Kaweevej Hospital, Taksin Road, Dhonburi, Bangkok 10600, Thailand.

3. The original copy to be submitted must be typed in a double space on one side of the page of 8.1/2" x 11.1/2" paper.

4. The format of the article must include :

a. Title page and address of the author (s)
b. Abstract
c. Introduction (Background)
d. Material and Method
e. Results and discussion (Tables and Illustrations)
f. Acknowledgement (if any)
g. References (Follow the Vancouver style developed by ICMJE)

5. We will provide 10 copies of reprints for the author (s) who submit (s) an article for publication in the Asean Journal.

6. The illustrations and tables must be clearly prepared with legends in English as they are the art works to be reproduced.

7. The authors are responsible for the contents of the article as to its facts and findings.

8. Ethics.

Paper reporting studies which might be interpreted as human experimentation (e.g. controlled trials) should conform to the standards of the Declaration of Helsinki (see British Medical Journal 1964:2:177) and should indicate that, approval that such studies may proceed, has been granted by the local or hospital Ethics Committee.

When reporting experiments on animals indicate whether the institution's or the National Research Council's guide for, or any national law on, the care and use of laboratory animals was followed.

THE ASEAN JOURNAL OF RADIOLOGY

Volume VI Number III SEPT. - DEC. 2000

CONTENTS

THE ASEAN JOURNAL OF RADIOLOGY

Volume VI Number III SEPT. - DEC. 2000

CONTENTS

PREVALENCE OF SACROILIITIS IN PSORIATIC PATIENTS

Suphaneewan JAOVISIDHA MD.[1]
Thitima KUNLAYANOPAKORN MD.[1]
Pimjai SIRIWONGPAIRAT MD.[1]

ABSTRACT

Purpose: 1) To assess the prevalence of sacroiliitis in patients with psoriatic skin disease or psoriatic arthritis 2) To study whether this finding precedes the symptom or radiographic change of the peripheral joint which is the hallmark of psoriatic arthritis.

Materials and Methods: Retrospective study was performed in patients diagnosed as psoriasis or psoriatic arthritis between January 1993 and May 1999 who had anteroposterior (AP) film of lumbar spine and/or pelvis and lateral film of lumbar spine available, to evaluate psoriatic bone change. The findings of the sacroiliac (SI) joint were classified into grades 0-4.

Results: Sixty one patients (21 females [mean age 45.3 years] and 32 males [mean age 48.5 years]) were included. Male: female ratio was 1.5:1. Eight patients were excluded from this study due to lack of AP film of pelvis. Prevalence of radiographic sacroiliitis (grade 2 or higher) was 23 of 53 patients (43.4%); among these, 20 had sacroiliitis alone without spinal bone change. The incidence of bilateral symmetrical and asymmetrical sacroiliitis was 46.2% and 53.8%, respectively. In patients with SI abnormalities; such abnormalities preceded the symptom or radiographic change of the peripheral joint in all cases.

Conclusions: The prevalence of radiographic sacroiliitis in this study is 43.4% (23 of 53). Among these 23 patients, SI abnormalities preceded the symptom or radiographic change of the peripheral joint (which is the hallmark of psoriatic arthritis) in all cases. Early detection and diagnosis of psoriatic skeletal involvement may be from the SI joint or the symptom of back pain, which means proper treatment and may help to decrease subsequent complication.

INDEX TERM : Sacroiliac joint ; sacroiliitis Psoriasis

INTRODUCTION

Psoriatic arthritis produces distinctive abnormalities of synovial and cartilaginous joint as well as sites of tendon and ligament attachment to the bone.[1,2] Although the classic presentation is that of a polyarticular disorder with predilection for the distal interphalangeal joint, a variety

[1] Department of Radiology, Ramathibodi Hospital, Rama 6 street, Bangkok 10400, Thailand

of additional clinical patterns may be observed, including a symmetric seronegative polyarthritis identical in distribution to rheumatoid arthritis, arthritis multilan, oligoarthritis or monoarthritis, and sacroiliitis and spondylitis[1]

Prevalence of sacroiliitis on radiographic examination is approximately 10-25% in patients with moderate or severe psoriatic skin disease, and 14-84% (according to many authors) in patients with psoriatic arthritis. Bilateral symmetric abnormalities predominate.[1] Recent study in 1996 [3] stated that the prevalence of sacroiliitis in patients with psoriatic arthritis was 77%. A study in Thai population[4] reported that among the 28 admitted psoriatic patients in a given period, 21% had low back pain and 57% were found to have sacroiliitis by physical examination.

From the wide range of data mentioned above, the aims of our study were [1] assessing the prevalence of sacroiliitis in patients with psoriatic skin disease or psoriatic arthritis, and [2] studying whether this finding precedes the symptom or radiographic change of the peripheral joint which is the hallmark of psoriatic arthritis.

SUBJECTS AND METHODS:

Retrospective study was performed in subjects who were diagnosed as psoriatic skin disease (psoriasis) and/or psoriatic arthritis from January 1993 to May 1999. The radiographs included an anteroposterior (AP) view of lumbar spine and/or pelvis and lateral view of lumbar spine. The patient-film distance was 6 feet (72 inches). The radiographs were reviewed by one radiology resident and one radiologist who came to consensus agreement. The chart records were reviewed as well. The severity of sacroiliitis was graded according to the New York criteria [5] as (0) normal; (1) suspicious changes; (2) minimal abnormality - small localized areas with erosion or sclerosis, without alteration in joint space width; (3) unequivocal abnormalities - moderate or advanced sacroiliitis with one or more of : erosion, evidence of sclerosis, widening of joint space, narrowing of joint space or partial ankylosis; (4) severe abnormalities - total ankylosis. In cases of asymmetric involvement, we counted the more advanced grade of the two sides.

RESULTS

Sixty-one patients were collected. Every patient had radiographs. Eight patients were excluded from this study due to lack of AP film of pelvis. For the remaining 53 cases, there was a slight male predominance (M:F = 1.5:1[32:21]). The mean age of the female is 45.3 years (range 26-73) and of male is 48.5 years (range 12-83). The duration of the disease averages 8 years (range 4 weeks- 40 years). The radiographs were available to evaluate sacroiliitis in all 53 cases. (Table 1). All 53 patients were sent for radiographs due to back pain.

Forty-four of 53 patients (83.0%) had psoriatic bone change in the SI joint and/ or spine. Other 3 of 53 (5.7%) had degenerative disease of the spine, and the other 6 of 53 (11.3%) had back pain from other causes i.e., renal stone, avascular necrosis of bilateral hip joints, and metastatic prostatic carcinoma. We will report the spinal bone change in psoriatic patients in another article separately.

Prevalence of sacroiliitis (grade 2 or higher) was 23 in 53 patients (43.4%); and 69.6% of these had grade 3 disease (Fig. 1 and 2). The incidence of bilateral symmetrical and asymmetrical sacroiliitis was 46.2% and 53.8%, respectively. Among these 23 patients, 20 had sacroiliitis alone, which could be the cause of low back pain, without radiographic spinal bone change. Duration of the disease did not correlate to the severity (grading) of sacroiliitis. Three patients had SI,

spinal and hand abnormalities, whose pelvic films were taken before the hands were filmed. Fifty patients did not have film of the peripheral joint and did not have record of peripheral joint symptom. Therefore, in patients with SI abnormalities; such abnormalities preceded the symptom or radiographic change of the peripheral joint in all cases.

Table 1. The distribution of radiographic grading of sacroiliitis in 53 patients*

SI joint abnormality			Number of patients (%)
Normal			29 (54.7)
Unilateral	Grade 2		6 (11.3)
	Grade 3		5 (9.4)
Bilateral	Symmetry	Grade 1	1 (1.9)
		Grade 2	1 (1.9)
		Grade 3	4 (7.5)
	Asymmetry	Grade 3	7 (13.2)

* No grade 4 was classified in this study

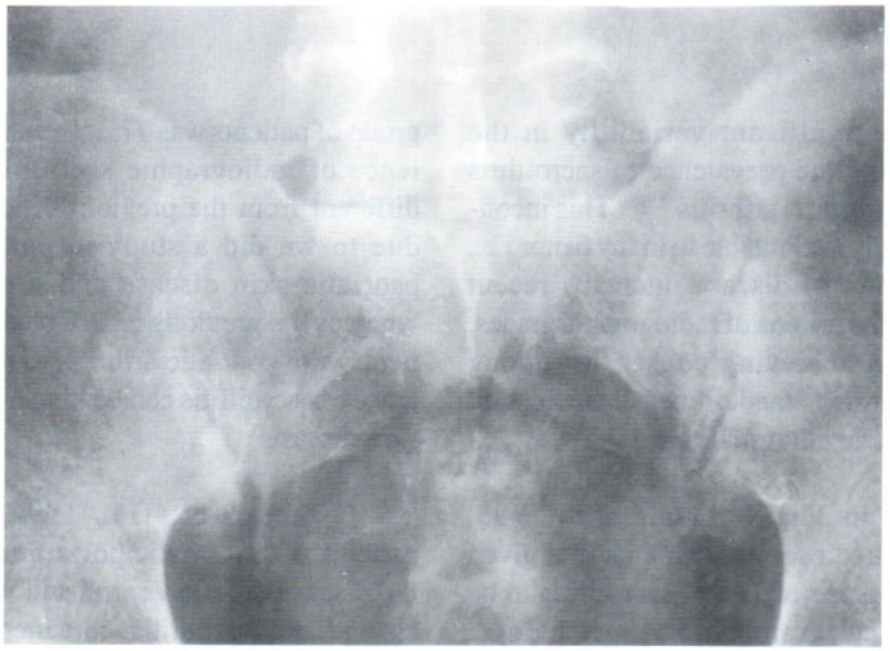

Fig. 1 AP view of pelvis reveals bilateral grade 2 changes : localized areas of erosion and sclerosis without alteration in joint space width

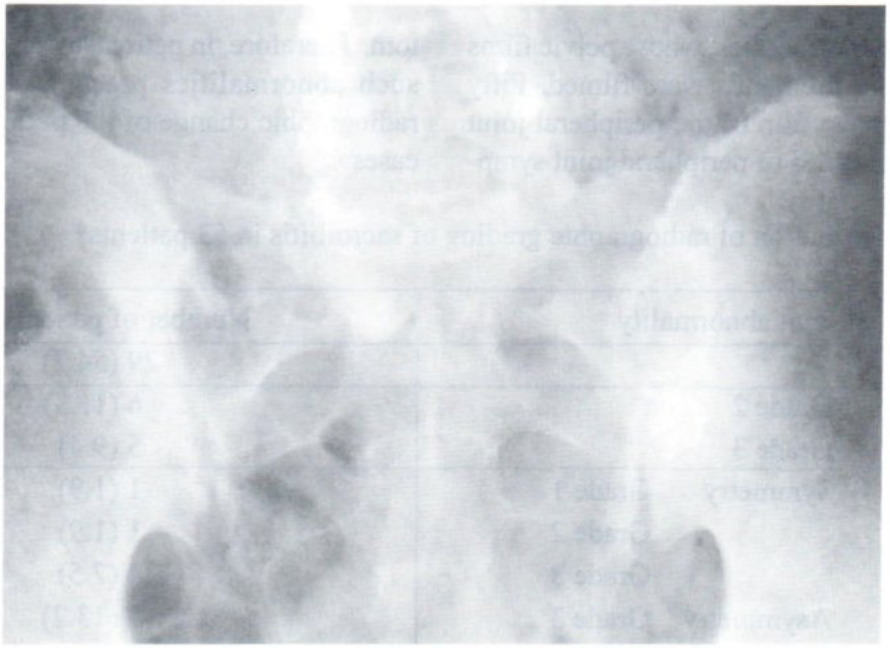

Fig. 2 AP view of pelvis reveals a definite abnormality (grade 3) of bilateral SI joints : advanced sacroiliitis with evidence of erosion & sclerosis

DISCUSSION

There is significant variability in the literature regarding the prevalence of sacroiliitis in patients with psoriatic arthritis.[3,6-10] This inconsistency is probably attributable to many factor i.e., the wide spectrum of disease intensity, recent modifications in the criteria of radiographic grades, and difficulty in achieving consensus among radiologists regarding standardized classification pattern of the sacral abnormalities.

A study in Thai population[4] in 1993, studied 28 admitted psoriatic patients in a given period, reported a prevalence of sacroiliitis to be 57.0% by physical examination. In radiologic literature, the prevalence of radiographic sacroiliitis in moderate to severe psoriatic skin disease was lower, 10-25%, compared to 14-84% in psoriatic arthritis.[1] Recently in 1996,[3] 202 patients with psoriatic arthritis were studied, and reported that the prevalence of sacroiliitis in this group of patients was 77%. In our study, the prevalence of radiographic sacroiliitis was 43.4%, different from the previous report. This may be due to we did a study in patients with both psoriatic skin disease and psoriatic arthritis, whereas the previous report[3] studied only in patients with psoriatic arthritis in whom the prevalence of sacroiliitis can be higher than in psoriatic skin disease.[1]

Taccari et al, in 1996,[7] studied 140 patients with psoriatic polyarthritis reported that the disease duration correlated with radiological change, and sacroiliitis score increased in patients with the longest disease duration. In addition, stage of sacroiliitis correlated with severity of peripheral joint changes and in all patients. In our study, the disease duration did not correlate with severity of radiographic sacroiliitis. And when the patients had SI abnormalities, such abnormalities

preceded the symptom or radiographic change of peripheral joint in all cases.

Bilateral symmetrical SI joint abnormalities were reported to be predominate.[1] In our study, the incidence of symmetrical and asymmetrical sacroiliitis was 46.2% and 53.8%, respectively. It seems that asymmetrical involvement was slightly predominates.

Limitations of this study are due mainly to the its retrospective type. The duration of the disease did not correlate with severity (grading) of sacroiliitis in this study. One reason could be inadequate data recorded; only 23 of 53 patients had record of duration of the disease. Second limitation is the rather small number of subjects.

In conclusion, the prevalence of sacroiliitis in psoriatic patients is 43.4% (23 of 53 patients studied). Among these 23 patients, SI abnormalities preceded the symptom or radiographic change of the peripheral joint which is the hallmark of psoriatic arthritis in all cases. Early detection and diagnosis of psoriatic skeletal involvement may be from the SI joint or the symptom of back pain, which means proper treatment and may help decrease subsequent complication.

REFERENCES

1. Resnick D, Niwayama G. Psoriatic arthritis. In: Resnick D ed. Diagnosis of Bone and Joint Disorder, 3rd ed, Philadelphia: WB Saunders 1995: 1075-100
2. Scarpa R, Oriente P, Pucino A, et al. The clinical spectrum of psoriatic spondylitis. Br J Rheumatol 1988; 27: 133-7
3. Battistone MJ, Manaster BJ, Redo D, Clegg DD. Prevalence of sacroiliitis in psoriatic arthritis: new prevalence from the largest cohort reported to date. Radiology 1996; 201(P): 331
4. Deesomchoke U, Tumrasvin T. Clinical comparison of patients with ankylosing spondylitis, Reiter's syndrome and psoriatic arthritis. J Med Assoc Thai 1993;76: 61-70
5. Green L, Myers OL, Gordon W, Briggs B. Arthritis in psoriasis. Ann Rheu Dis 1981; 40: 366-9
6. Braun J, Sieper J. The sacroiliac joint in the spondyloarthropathies. Curr Opin Rheumatol 1996;8:275-87
7. Taccari E, Spadaro A, Riccieri V. Correlation between peripheral and axial radiological changes in patients with psoriatic arthritis. Rev Rhum Engl Ed 1996;63:7-23
8. Gladmann DD, Brubacher B, Buskila D, Langevitz P, Farewell VT. Psoriatic spondyloarthropathy in men and women: a clinical, radiographic, and HLA study. Clin Invest Med 1992;15:371-5
9. Porter GG. Psoriatic arthritis: plain radiology and other imaging techniques. Baillieres Clin Rheumatol 1994;8:465-82
10. Bissoli E, Sansone V. Sacroiliitis in seronegative arthritis: The anatomicopathological aspects and imaging methods compared. Radiol Med Torino 1994; 88: 198-208

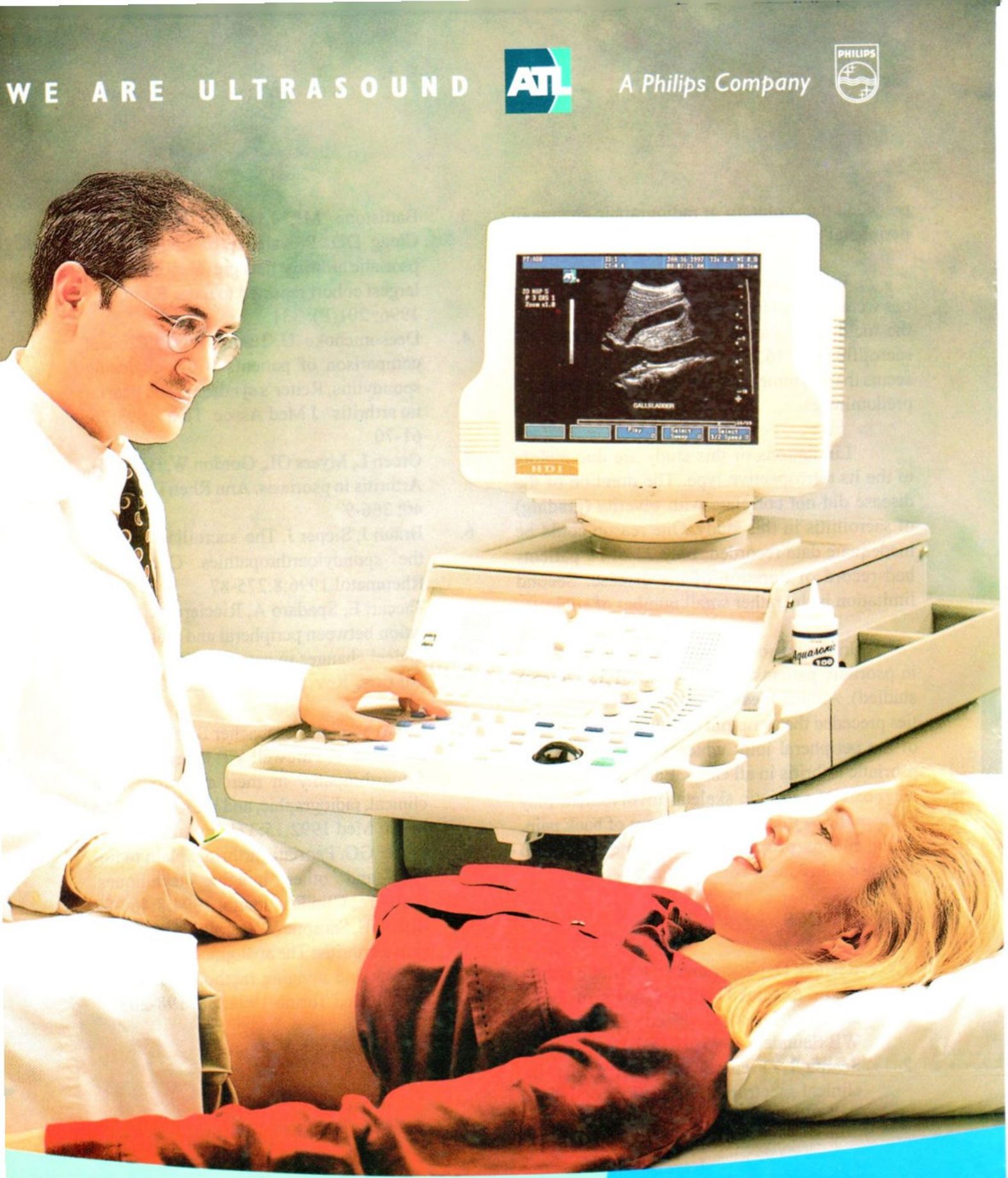

FOR MORE INFORMATION PLEASE CONTACT

PHILIPS MEDICAL SYSTEMS

- TEL. 745-4090 Ext. 3332
- FAX. 398-0792

Philips Electronics (Thailand) Ltd.
209/2 Sanpavuth Road, Bangna, Bangkok 10260

ฆพ. 78/2542

PHILIPS

Let's make things better.

PRENATAL DIAGNOSIS OF EXCENCEPHALY : A CASE REPORT

Wipaporn LIKKASIT, M.D.

ABSTRACT

Prenatal ultrasonographic diagnosis of 18 weeks gestational age fetus with Exencephaly is reported. Transabdominal ultrasound showed absence of fetal skull with presence of a large volume of brain tissue. The condition is rare and has a lethal outcome. Some authors have called Exencephaly as the variant or precursor of Anencephaly.

INTRODUCTION

Exencephaly is a rare,serious form of neural tube defects, which expresses by acrania (partial or total) and present of a large volume of brain tissue (with developmental anomaly). The incidence is very low and may confuse with the term "Anencephaly", which is absent of both cranial vault and cerebral tissue. Both conditions are serious and incompatible with life. Early diagnosis of these lethal abnormalities are required to minimize parenteral anguish and to reduce maternal morbidity from termination of pregnancy. Ultrasonographic diagnosis can be made as early as 10-11 weeks gestational age, especially by endo-vaginal ultrasound.

CASE REPORT

A 26-year-old woman (gravida 5, para 3, abortus 1, living children 3) last for 1 year; was referred from a health centre because of absence of fetal movement and negative fetal heart sound on examination. She had 5 months pregnancy. Threre was no significant family history of genetic or structural abnornalities.

Transabdominal ultrasonographic examination with 3.5 MHz,convex-sector realtime transducer showed a single, viable fetus with head presentation. The gestational age by femur length measurement was corresponding with 18 weeks. There was absence of normal fetal cranium with a large volume of brain tissue was noted, floating in amniotic fluid. (Fig.1) There was also deformity of cervical and thoracic spines (Fig.2), and mild polyhydramnios was revealed.The fetal face, heart, kidney, bladder, stomach and extremities appeared to be normal.

As the condition is serious and not compatible with life, pregnancy termination was done with maternal consent. Visual inspection of the abortus revealed a 300 grams non-viable fetus which confirmed the skeletal findings.

Department of Radiology, Sappasitthiprasong Hospital, Ubonratchathani, Thailand.

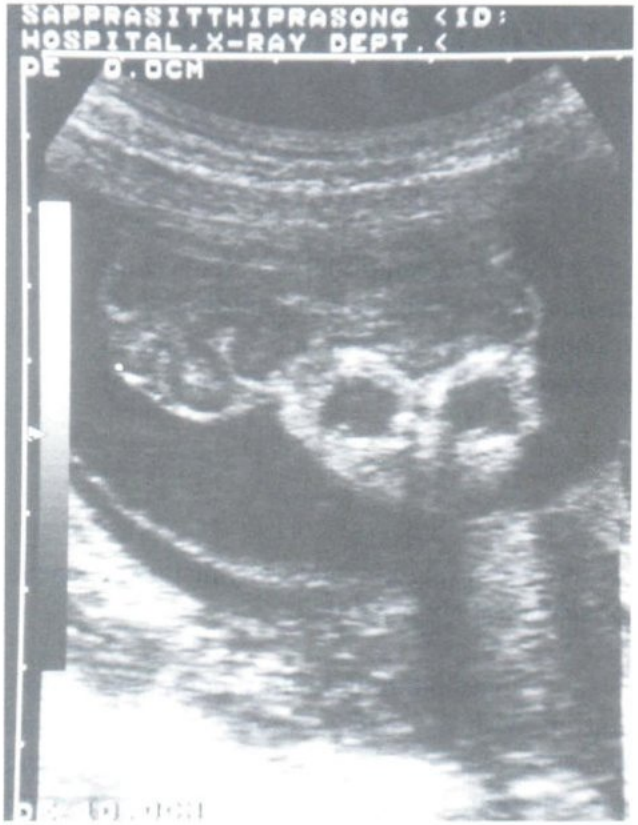

Fig.1 Coronal view at head of exencephalic fetus at 18 weeks gestational age by trans-abdominal ultrasonography. There is absence of normal fetal skull above the orbits, but a large amount of fetal brain tissue is noted and floating in amniotic fluid.

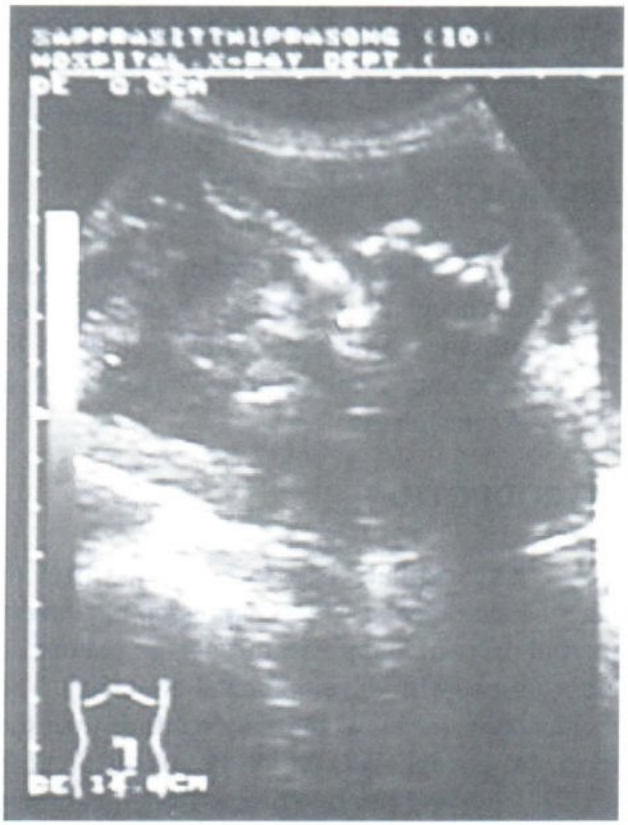

Fig.2 Sagittal view at spines of exencephalic fetus shows anomalous, deformed cervical and thoracic spines

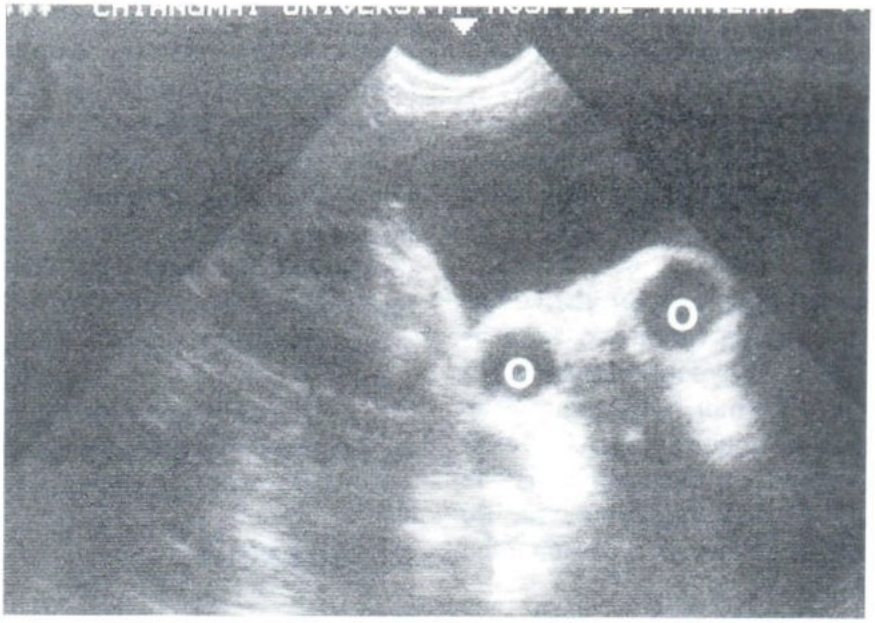

Fig.3 Coronal view at head of anencephalic fetus reveals absence of fetal skull and brain tissue. The orbits appear to be prominent, resembling like wearing sunglasses "Spectacle sign". (Theera Tongsong. Textbook&Atlas of obstetric ultrasound : P.B. Foreign Book Centre L.P.,1995:237)

DISCUSSION

Neural tube defects (NTD) are conditions that caused by failure of closure of the rostral portion of the neural tube during the sixth week of gestational age. Lack of closure of part or all of the neural tube leads to serious anomalies, some of which are incompatible with life, and resulted in abnormal forebrain development and a defective bony calvaria. The incidence of NTD is relatively high;1.2-1.7:1000 lifebirths. NTD is a multifactorial hereditary disorder, and may be suspected by increased meternal serum ∝ -feto-protein level, which are caused by leakage of this protein across the membrane covering the defect. The presence of NTD significantly increases the mother's risk of having another infant with NTD, and therefore warrants close monitoring of subsequent pregnancies. The NTD have many anomalous presentations, including anencephaly, exencephaly, iniencephaly, cephalocele and spina bifida.

Exencephaly is a rare cranial malformation that related to anencephaly,and the incidence is very low.In both disorders,the cranial bones are absent and the primary distinction between the two is the presence of a large amount of disorganized brain tissue in the former. It has been shown in animal studies that anencephaly can be resulted from exencephaly presumably from progressive reduction in the volume of the abnormal brain matter because of mechanical or chemical trauma. This same process have been documented in human fetuses. Some authors have mentioned that exencephaly is the variant of anencephaly which varying amount of brain tissue appear to be presented. If the entire brain is present but not confined within the skull,the term Acrania is used.

The prenatal ultrasonographic appearance of exencephaly has been reported infrequently, and those were previously described are

1. Absent calvarium with presence of large

mass of disorganized cerebral tissue without cranial bony covering.

2. Brain tissue volume is nearly normal but disorganized and may present with pseudosulci.

3. Preservation of bony base of the skull and normal facial structures.

The differential diagnoses are the conditions that have very thining calvarium, such as osteogenesis imperfecta or hypophosphatasia,but these conditions have normal brain tissue. The associated anomalies are abnormal vertebra, cleft lip,cleft palate and club foot. Exencephaly is one of serious anomaly that is incompatible with life and termination of pregnancy is recommended when diagnosed.

Mostly, reliable diagnosis was made at the beginning of the second trimester. Early diagnosis (first trimester) of exencephaly and other anomalies is clearly possible, by ultrasonography especially with the help of vaginal and other high resolution probes. There was one reported case of prenatal diagnosis at 10-11 weeks gestational age. However, caution is warranted because the fetal cranium is not completely calcified before 10-11 weeks gestational age. Therefore finding other than absent calvarium should also be sought.

Anencephaly is the most severe and most common form of NTD; occuring in 1 per 1000 births in the United states and 5 in 1000 births in Irerland and Wales. Female fetuses are affected more often than male (4:1). Anencephaly is a condition occuring with the absence of both normal formed brain and skull. (Fig.3) The base of skull and a portion of the occipital bone, which are formed in cartilage may be presented. The membranous neurocranium, which forms cranial vault, is absent .The rudimentary brainstem and a portion of the basal ganglia are usually presented. The facial bones are nearly normal. Anencephaly may be associated with rachischisis (congenital splaying of posterior spinal elements) depending on the extent of the neural tube defect.

The other associated anomalies are spina bifida, hydronephrosis, diaphragmatic hernia, congenital heart diseases and omphalocele. Anencephaly is also associated with polyhydramnios, presumably due to defective fetal swallowing. Ultrasonographic diagnosis of anencephaly may be made as early as 12 weeks on transabdominal ultrasound and it may be detected earlier with endovaginal ultrasound (may be as early as 8 weeks gestational age).

In conclusion,I have been reported a case of Exencephaly with prenatal ultrasonic diagnosis in a 18 weeks gestational age fetus.

REFERENCES

1. Beverly A. Spirt, Michael oliphant, Lawrence P. Gordon. Fetal central nervous system. Radiol clin North Am 1990;28:68
2. Cunningham FG, MacDonald PC, Gant NF, Leveno KJ, Gilstrap LC, Hankins GDV, Clark SV. Fetal abnormalities: inherited and acquired disorders In : Williams obstetrics. 20th ed. Norwalk : Appleton & Lange,1997:907-08
3. Glendon G. Cox, Stanton J. Rosentahl, James W. Holsapple. Exencephaly: sonographic findings and radiologic-pathologic correlation. Radiology 1985;155:755-56
4. Kathleen A. Kennedy, Kenneth J. Flick, RDMS, Amy S. Thurmond. First-trimester diagnosis of exencephaly. Am J Obstet Gynecol 1990;112:461-63
5. Roger C. Sanders. Prenatal ultrasonic detection of anomalies with a lethal or disastrous outcome. Radiol clin North Am 1990;28:163
6. Ruth B. Goldstein, Roy A.Filly. Prenatal diagnosis of anencephaly : spectrum of sonographic appearance and distinction from the amniotic band syndrome. AJR 1988;151:547-50
7. Theera Tongsong. Textbook&atlas of obstetric ultrasound : P.B.Foreign Book Centre L.P. 1995:235-49

BILATERAL FOCAL XANTHOGRANULOMATOUS PYELONEPHRITIS : A CASE REPORT AND LITERATURE REVIEW

Wipaporn LIKKASIT[1], Wannee ANANTRASIRICHAI[2]

ABSTRACT

Xanthogranulomatous pyelonephritis (XPN or XGP) is an uncommon entity, mostly unilateral. A case of bilateral focal xanthogranulomatous pyelonephritis is reported with literatures reviewed. Accurate preoperative diagnosis is difficult ; however ultrasound and CT may give the suggestion of this disease.

INTRODUCTION

Xanthogranulomatous pyelonephritis (XPN or XGP) is a rare atypical form of severe chronic renal parenchymal infection. Its manifestation mimics with those of neoplasm and other renal parenchymal infection,and often were misdiagnosed clinically. XPN is usually associated with stone formation (50-70%) and obstruction secondary to staghorn calculi. There is increased incidience in middle-aged female and diabetic.Pathologically, the kidney is enlarged with yellowish nodules containing Lipid-laden macrophages (Xanthoma cells). 80-90% of these kidneys have diffuse involvement. The disease is almost always unilateral and has no predilection for either side. Bilateral involvement which were previously reported in literatures, is only 8 cases.[9]

CASE REPORT

A 44-year-old female presented with on-and-off fever for 2 months.She had a feeling of fullness at right upper abdomen for 2 weeks,and lost of weight, 10 kg., within 2 months.She also had amenorrhea for 4 months.

Physical examination disclosed hepatomegaly and positive bimanual palpation at right side of abdomen.

Laboratory findings revealed anemia and leukocytosis.Urinalysis showed 1+ proteinuria and 1-2 white blood cells per high powered field.There was 2+ urine sugar. Mild elevation of BUN, Creatinine were noted and blood sugar was normal. Hepatic function test revealed chronic liver disease. Negative test for α - fetoprotein was noted.

Sonography revealed mixed echogenic mass with reniform shape (12 cm.in length) at right upper abdomen, inferior to the liver. (Fig.1) The mass had well defined border and the internal echo exhibited multiple foci of dense echoes with posterior acoustic shadowings. Upper pole of right kidney was spared. There was also 4 cm. cystic mass at upper pole of left kidney. The mass invaginated into the spleen, but not invading. Hepatomegaly with two silent gallstones are revealed. The sonographic diagnosis was renal cell carcinomas and Xanthogranulomatous pyelonephritis to be differentiated.

Liver scan with Tc^{99m}-SC showed hepatomegaly with decreased liver uptake at postero-inferior portion of right lobe liver.

[1] Department of Radiology, Sappasitthiprasong Hospital, Ubonratchathani, Thailand.
[2] Division of Diagnostic Radiology, Department of Radiology, Rajavithi Hospital, Bangkok, Thailand.

Excretory urography demonstrated a large intrarenal mass,involving nearly the entire right kidney, except the upper pole which some excretory function was preserved. The renal calyces were displaced and had distortion. There was normal size and excretory function of left kidney, with bulging renal outline at the upper pole and stretching of renal calyces. (Fig.2)

Plain CT scan revealed enlarged right kidney with hypodensity (12-16 HU.) mass, approximately 10 cm. in diameter, replacing almost the entire renal parenchyma sparing only the upper pole. (Fig.3 a) The renal outline was poorly defined, which indicated perinephric involvement of the disease. Left kidney was bulging at lateral aspect from relatively low density (16 HU.) mass, 3 cm. in diameter. (Fig. 3 b) No internal calcification or abnormal gas was noted.

Contrast enhancement CT scan showed no significant enhancement of the hypodense masses of both kidneys. The masses were more obvious due to peripheral rim enhancement of the lesions and there was also enhanced thick internal septations. The right renal mass involved ipsilateral right psoas muscle.The inferior vena cava and renal veins were normal. (Fig. 4 a,b)

Angiography revealed relatively hypovascular mass at lower pole of right kidney with neovascularization. Enlargement of renal capsular branch indicated perirenal extension was noted. (Fig. 5 a) There was cortical nephrogram defect at upper, lateral border of left kidney without any tumor vessel. (Fig. 5 b) The Inferior Vena Cava was patent. Both CT scan and angiography were suggestive of malignancy.

Right total nephrectomy demonstrated a large renal mass involving middle and lower portions of right kidney with direct extension outside renal capsule into the surrounding tissue including muscles. The mass grossly appeared firm and had yellowish nodules. Accidentally ruptured of the mass during the operation revealed yellowish pus, without any foul smell. Pus culture was negative, but hemoculture was positive for Klebsiella Pneumoniae.

Post-operative ultrasonographic guidance for percutaneous aspiration of left renal mass was failed.

Histologic study revealed thin renal parenchyma, hyalinized glomeruli,and fibrotic changes of renal pelvis, calyces and interstitium. Wall of the mass was composed of solid sheets of foamy histiocytes. (Fig. 6) There was also submucosal chronic inflammation of the ureter.

The conclusive diagnosis was bilateral XPN, focal form ,stage III (paranephric).

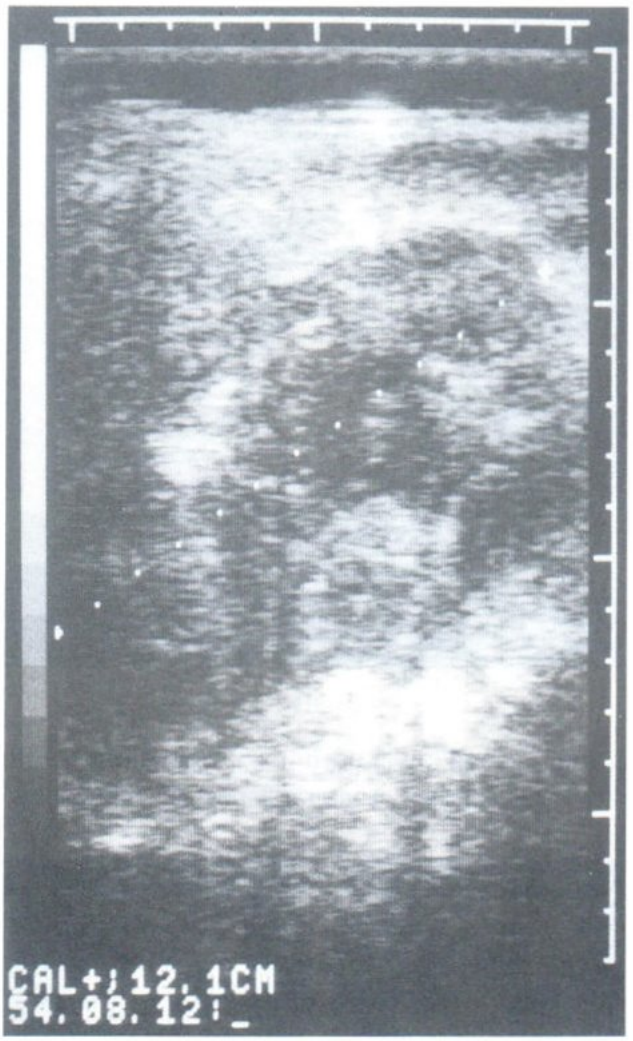

Fig. 1 Renal ultrasonography of right kidney shows a large mixed echogenic mass with dense internal echoes involving mid and lower portions with upper pole sparing.

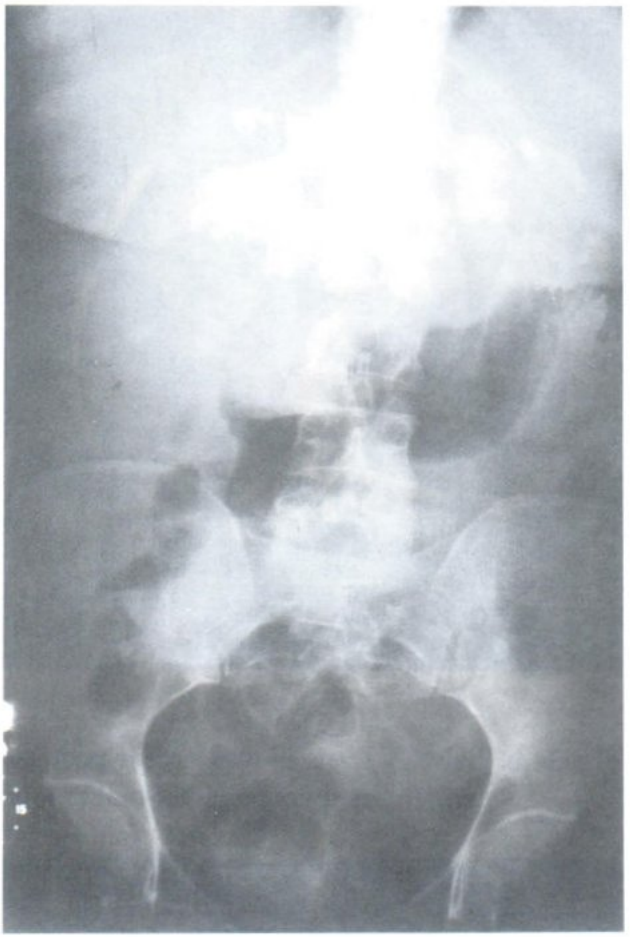

Fig. 2 Film IVP reveals a large intrarenal mass involving nearly entire right kidney with distortion of upper pole calyces and bulging renal outline of upper pole of left kidney.

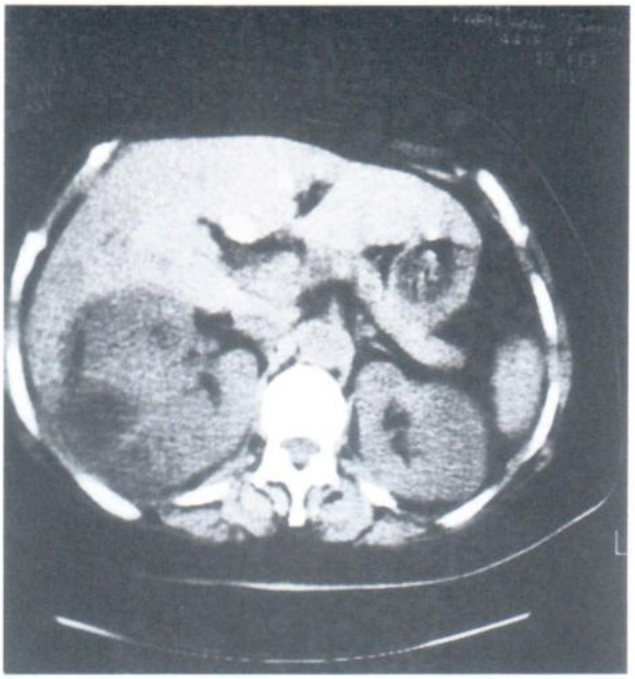

3A

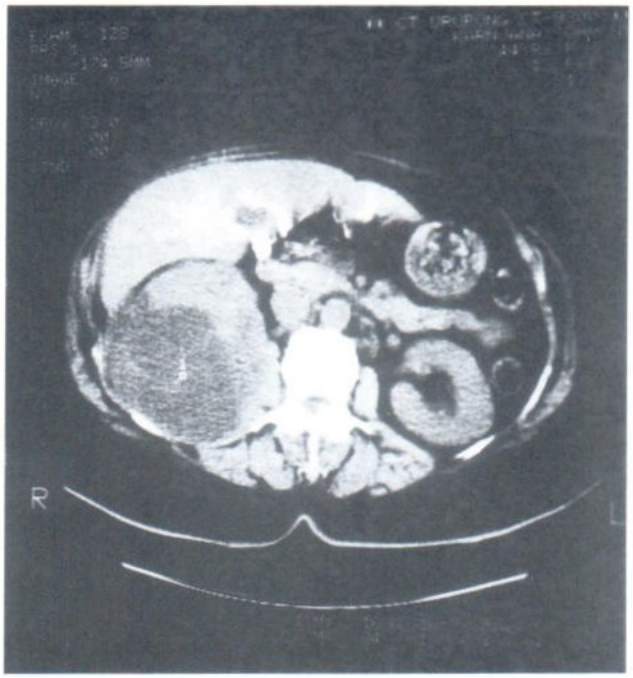

3B

Fig. 3a,b Plain CT scans show a large hypodensity mass at mid and lower portions of right kidney, with perinephric involvement. Smaller low density mass is noted at lateral aspect of left kidney.

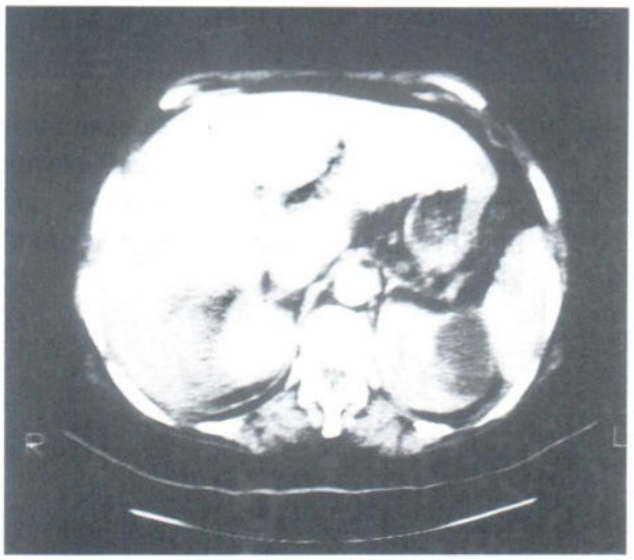

4A

Fig. 4a Contrast enhanced CT scan at level of left kidney shows non-enhancing hypodense mass at the lateral portion.

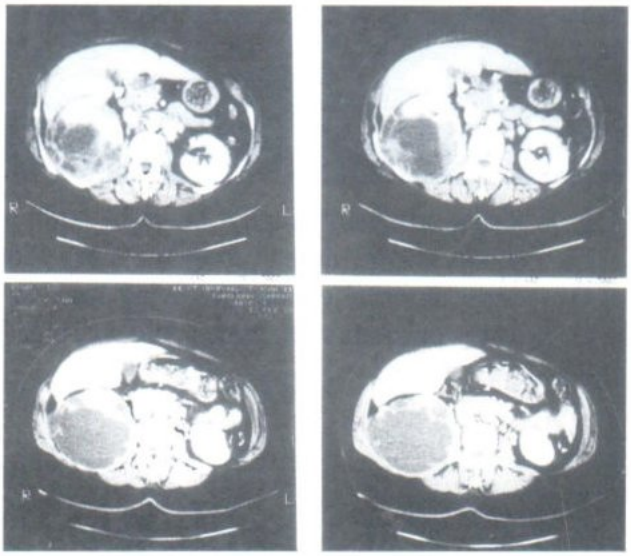

4B

Fig. 4b Contrast enhanced CT scans at multiple levels of right kidney reveal peripheral rim enhancement of non-enhancing hypodensity mass which has enhanced thick internal septations and also involves right psoas muscle.

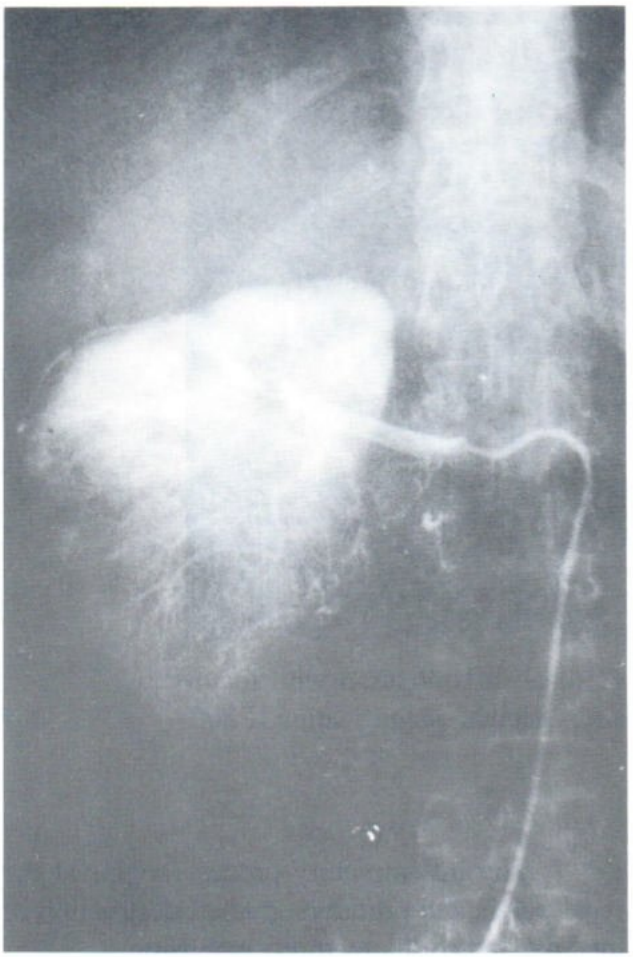

5A

Fig. 5a Right renal angiography demonstrates a large hypovascular mass with neovascularization, at lower half of right kidney and also reveals enlargement of renal capsular artery.

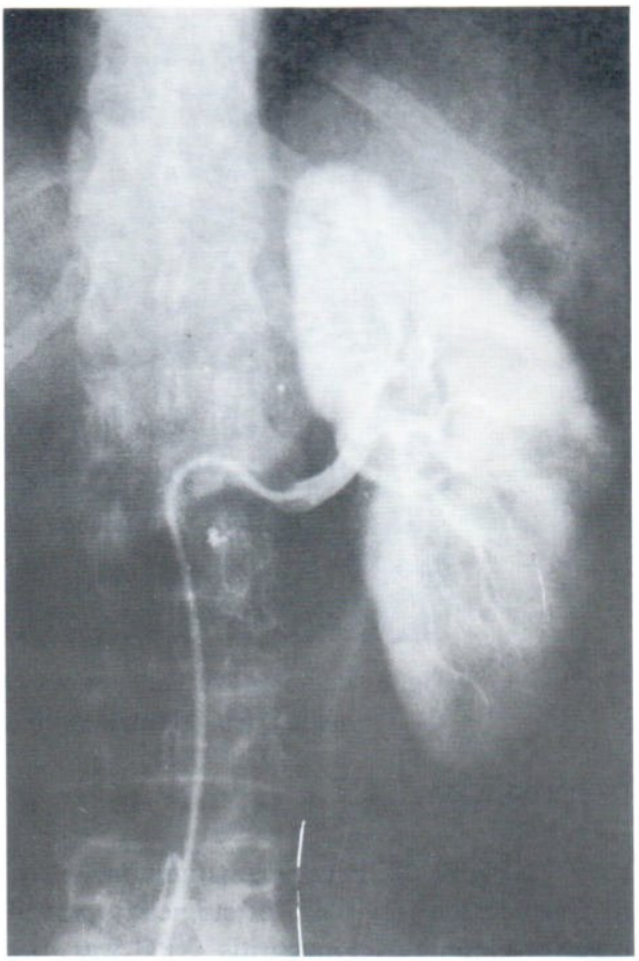

5B

Fig. 5b Left renal angiography shows a cortical nephrogram defect at upper lateral aspect of left kidney.

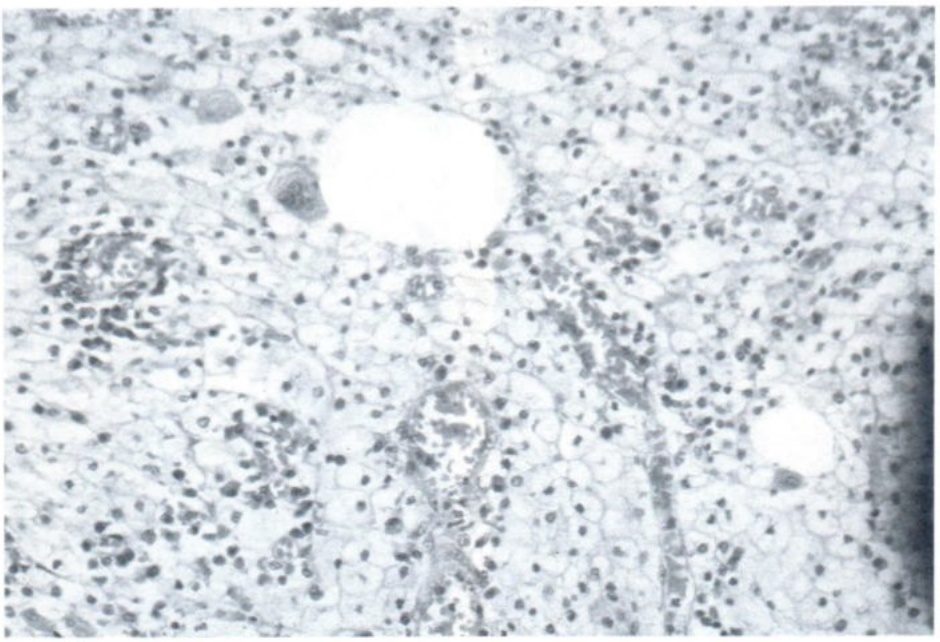

Fig. 6 Pathological slide shows chronic renal inflammation with foamy histiocytes. (Hematoxylin & eosin ; Original magnification X 200)

DISCUSSION

XPN or XGP is an uncommon entity, responsible for only 0.6% of surgically proved cases of chronic pyelonephritis. XPN was first described in 1916 by Schlagenhaufer. He used the term " Staphylomykosen " because of the macroscopic resemblance to Actinomycosis granuloma and the microscopic appearance of Staphylococci. Since 1916 to 1987, nearly 500 cases have been described in the literatures. It has apparently increased in frequency in more recent years.

ETIOLOGY

The etiology of XPN is unknown and usually associate with urinary tract obstruction and calculous disease (50-70% of cases). Abnormal lipid metabolism, lymphatic blockage, chronic renal ischemia with resultant localized alteration in renal metabolism, altered immune response, DM and finally, calculous or non-calculous urinary tract obstruction with prolonged antibiotic therapy have been suggested.

The inflammatory process begins at the renal pelvis and produces gradual destruction of medulla and cortex by direct extension.

XPN is almost always unilateral involvement, and equal incidence on each side. Bilateral involvement have been found only in 8 cases.[9] XPN is predominantly found in female (58-78%), with a peak of age incidence at 4^{th}-6^{th} decade of life.

TYPE AND STAGING

Type of involvement is divided into three forms.

1. Diffuse : This is the most common form (80-90%) and it is associated with staghorn calculi. It represents an entire renal involvement.

2. Segmental : The condition is confined to one pole of duplex kidney or the parenchyma which drains into an obstructed calyx.

3. Focal : It is also refered to as a Xantho-

granuloma. The inflammation usually originates within the renal parenchyma and does not communicate with the collecting system. In this case there will be a nonspecific solid or cystic renal mass.

There are three stages of XPN :

Stage I (nephric) : Inflammatory process was confined to the kidney.

Stage II (perinephric) : Involving kidney and gerota fascia

Stage III (paranephric) : Involving affected kidney and its surrounding fat with widespread retroperitoneal involvement

CLINICAL DATA

The presenting symptoms are generalized and composed of flank pain, flank mass, weight loss, malaise, fever, mild lower urinary tract symptoms and draining flank sinus.

The physical examinations of XPN are non-specific, such as flank mass and tenderness, fever, anemia, hepatomegaly, pyuria and hypertension.

Duration of the symptom is usually six months to one year. Several associated conditions have been held responsible for XPN, including renal stones (50-70%). hypernephroma, DM, multiple pregnancy and previous Urinary Tract Infection. No significant association with any systemic disease is noted.

BACTERIOLOGY

Bacteriology finding on urine or resected specimens mostly yielded Escherichia coli and Proteus mirabilis.

LABORATORY FINDINGS

No laboratory tests are specific for the condition ; anemia, leukocytosis, elevated ESR, pyuria, hematuria, proteinuria, rising BUN, Creatinine, and abnormal liver function test (nephrogenic and hepatic dysfunction).

ROENTGENOLOGIC FINDINGS

Plain film : The affected kidney is often enlarged and has staghorn renal calculi (or uretero-pelvic junction stone, or ureteric stone). The renal outline and psoas shadow are sometime ill-defined because of perinephric edema or infiltration (perirenal extension).

Intravenous pyelography : The stone bearing (70%) and functionless (80%) kidney have been the most frequent findings. The other findings are space occupying lesions, or intrarenal masses (focal form) with distortion of renal collecting system, or renal outline. Diffuse renal enlargement with transient rim nephrogram, indicating hydronephrosis, may be presented. Perinephric extension of the disease process produces ill -defined renal margin or a nondescripted renal mass.

Retrograde pyelography : The study may disclose obstruction at uretero-pelvic junction with gross dilatation of pelveocalyceal system. On occasion, irregular filling defect in a contracted renal pelvis with marked renal caliectasis may be noted.

Renal scintigraphy : The study generally reveals non-uptake of the affected kidney and no excretion.

Ultrasonography : In diffuse form;the affected kidney is enlarged and contains multiple cystic areas, with internal fine echoes. The renal calyces may be surrounded by thin zone of increased echogenicity. There may be central strong echogenic foci, with acoustic shadowings, correspond to staghorn renal calculi.The other findings

are hydro-or pyonephrosis,and echogenic areas due to the solid foci of granulomatous tissue;as well as debris and calculi. Sometime,the inflammation may extend into perirenal space or psoas muscle

Focal form reveals hypoechoic mass with irregular border and calculi in renal collecting system.

Computerized tomography : Diffuse form usually discloses a calculus in renal pelvis or collecting system with absence of contrast excretion in the involved kidney or focal area of i nvolvement. The other findings include (1) multiple non-enhancing rounded areas within medullary space (resemble hydronephrotic pattern) (2) discrete solid masses (3) area of fat density (4) diffuse renal enlargement with preserve reniform outline (5) the lesion may extend beyond the expected confines of the kidney into the perirenal space, pararenal space, psoas muscle, back muscle, diaphragm, colon or spleen.

Focal form demonstrates localized water-density mass adjacent to calyx, that contains calculus.

Angiography : Diffuse form reveals sparse, narrowed, and stretched intrarenal arteries around foci of granulomatous tissue. The intrarenal arterial pattern may resemble the neovascularity of hypernephroma. Renal capsular arteries are often enlarged, reflecting extrarenal extension of the inflammatory process.

Angiographic findings of focal form XPN usually resemble the diffuse form,with additional finding of irregular defect in nephrogram.

Four cases of renal vein thrombosis were previously reported.

PATHOLOGICAL CHARACTERISTIC

Macroscopic findings : - The kidney is usually enlarged with yellowish nodules and dilated collecting system containing purulent material. Perinephric inflammation and fibrosis may be present.

Microscopic findings : - The disease is characterized by Lipid-laden macrophages (Xanthoma cell) and granulomatous reaction. The abscess, focal calcification and cholesterol slits may be revealed.

The histology of XPN may resemble clear cell type of renal cell carcinoma.

PREOPERATIVE DIAGNOSIS

The correct preoperative diagnosis is range from 5-44% and the remaining patients were thought to have malignant tumors (hypernephroma, epidermoid carcinoma,or retroperitoneal tumor), hydronephrosis or pyonephrosis, renal tuberculosis, or renal abscess.

TREATMENT AND PROGNOSIS

The treatment of choice is nephrectomy (total or partial). Some patients were treated by percutaneous drainage before the major operation, due to extensive retroperitoneal involvement.

XPN doesnot seem to recur,metastasize, or involve contralateral kidney, and the prognosis is excellent. However, some of the conditions, associated with the disease, such as bacteremia and hypertension, may continue to be a problem.

CONCLUSION

XPN or XGP is an atypical, uncommon form of severe chronic granulomatous renal infection in chronic obstruction,and almost always

unilateral involvement. We reported one case of bilateral XPN which was one among small number of cases in worldwide literatures, and probably the first reported case of bilateral XPN in Thailand.

ABBREVIATION:

XPN, XGP = Xanthogranulomatous Pyelonephritis

REFERENCES

1. Albert Solomon, Zvi Braft, Joseph Papo, Ephraim Merimsky. Computerized tomography in Xanthogranulomatous Pyelonephritis. J Urol 1983;130:323-25
2. Bala R. Supramanyam, Alec J. Megibow, B. Nagesh Raghavendra, Morton A. Bosniak. Diffuse Xanthogranulomatous Pyelonephritis : Analysis by computed tomography and sonography. Urol Radiol 1982;4:5-9
3. Bhupendra M. Tolia, Alfredo Iloreta, Selwyn Z. Freed, Bernard Fruchtman, Boyce Bennett, Harry R. Newman. Xanthogranulomatous pyelonephritis: Detailed analysis of 29 cases and a brief discussion of atypical presentation. J Urol 1981;126: 437-42
4. F.R. Smith. Bilateral Xanthogranulomatous pyelonephritis. B J Urol 1981;53:81
5. H. Claes, R. Vereecken, R. Oyen, B. Van Damme. Xanthogranulomatous Pyelonephritis with emphysis on Computerized tomography scan. Urology 1987;29:389-93
6. I. Husain, A. Pingle, T. Kazi. Bilateral diffuse Xanthogranulomatous Pyelonephritis. Br J Urol 1979;51:162-63
7. J.C. Gingell, J. Roylance, E.R. Davies, J. B. Penry. Xanthogranulomatous Pyelonephritis. Br J Radiol 1973;46:99-109
8. Mason Goodman,Thomas Curry, Thomas Russell. Xanthogranulomatous Pyelonephritis (XGP): Local disease with systemic manifestation; Report of 23 patients and review of the literature. Medicine 1979; 58:171-81
9. Mohammed Akhtar, Wajeh Qunibi. Bilateral Xanthogranulomatous Pyelonephritis involving native kidneys in a renal transplant recipient: Association with renal cell carcinoma and amyloidosis. Am J of Kidn dis 1992;20(3):289-93
10. Owen C. Van Kirk, Raymundo T. Go, Victor J. Wedel. Sonographic features of Xanthogranulomatous Pyelonephritis. AJR 1980;134: 1035-39
11. Reza S. Malek, Jack S. Elder. Xanthogranulomatous Pyelonephritis: A critical analysis of 26 cases and of the literature. J Urol 1978;119:589-93
12. R.G. Grainger, A.J. Longstaff, M.A. Parsons. Xanthogranulomatous Pyelonephritis : A reappraisal. Lancet 1982;19: 1398-1401
13. Stanford M. Goldman, Davis S. Hartman, Elliot K. Fishman, Joseph P. Finizio, Olga M.B. Gatewood, Stanley S.Siegelman. CT of Xanthogranulomatous Pyelonephritis : Radiologic-pathologic correlation. AJR 1984;142:963-70

Nippon Electric Glass Co., Ltd.
Radiation Shielding Lead Glass

- ☐ Observation window for CT scanning room
- ☐ Observation window for angiography room
- ☐ Observation window for X-ray diagnosis room

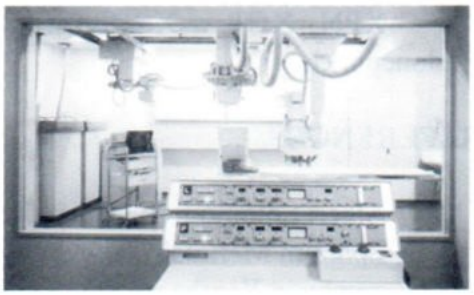

จำหน่าย กระจกตะกั่วกั้นรังสี แผ่นตะกั่วเรียบหนา 1 มม.-10 มม. รับกรุแผ่นตะกั่วที่ผนังห้องเอ็กซเรย์ รับทำบานประตูไม้อัด ประตูเหล็กบุแผ่นตะกั่ว ยินดีให้คำชี้แนะ

สอบถามได้ที่

ผู้แทนจำหน่ายในประเทศไทย

ห้างหุ้นส่วนจำกัด วิมิตรกิจ เอ็นจิเนียริ่ง
VIMITKIJ ENGINEERING LTD., PART.

42 ซอย 96/3 ถ.จรัญสนิทวงศ์ บางอ้อ เขตบางพลัด กทม. 10700

42 CHARANSANITWONG 96/3, BANG-AW, BANGPLAT, BANGKOK 10700

☎ **(02) 424-9775, 424-1009, 424-0977**

FAX : 435-7870, 424-1009

E-mail : napana@access.inet.co.th

CASE REPORT: EXTENSIVE BRAIN CALCIFICATION IN POSTSURGICAL HYPOPARATHYROIDISM

Wipaporn LIKKASIT,M.D.

ABSTRACT

Basal ganglia calcification is common in hypoparathyroid states. However, extensive brain calcifications from vascular and perivascular deposits in postsurgical hypoparathyroidism are rarely described radiologically. A case of 54-year-old woman with secondary hypoparathyroidism after long standing subtotal thyroidectomy is presented. CT-scan showed extensive bilateral symmetrical calcifications in the region of the basal ganglia, cerebellum, thalamus,cerebral white matter and cortex. The mechanism of metabolic disturbance leading to vascular deposits are reviewed.

INTRODUCTION

Calcification of the basal ganglia has been visualized by skull radiography for more than 40 years.In two-thirds of cases it has been associated with metabolic abnormalities. Twenty percent of the cases had been an incidental findings. Computed tomography (CT) is 5 to 15 times as sensitive as plain skull radiography in detecting intracerebral calcification. Calcification confined to the globus pallidus,of basal ganglia, of a patient older than 40 should be considered physiological and does not warrant further investigation.

Extensive bilateral intracerebral symmetrical calcification is known to occur in idiopathic hypoparathyroidism (IHP), in pseudohypoparathyroidism (PHP), in postoperative hypoparathyroidism and without any detectable cause (Fahr's syndrome). However, the condition is believed to be relatively rare in postsurgical hypoparathyroidism, presumably because patient with this order are treated more expeditiously than patients with other form of hypoparathyroidism.

This is a case with a far more extensive brain calcification in a patient of postsurgical hypoparathyroidism after subtotal thyroidectomy for 24 years.

CASE REPORT

A 54-year-old woman was admitted after recent episode of syncope without any aura. She had previously 5-times attacks of syncope during the past one year. The duration of each syncope is about an hour. She had previously subtotal thyroidectomy for treatment of toxic goiter twenty-four years ago. She developed tetany in the immediate postoperative period and spontaneous recovered. She was treated with antithyroid drug for one year. No further bouts of tetany occurred and no medication was given for 23 years.

Physical examination showed a thyroidectomy scar. The patient had hoarseness, but no neurological deficit, dementia or symptom of basal ganglia dysfunction. Serum calcium level was 8.0 mg/dL (norm: 8-11 mg/dL) and serum inorganic phosphate was 6.4 mg/dL (norm: 2.5-5.0 mg/dL). Other biochemical tests were normal, including

Department of Radiology, Sappasitthiprasong Hospital, Ubonratchathani, Thailand.

thyroid function test. The electrocardiography showed sinus tachycardia. The electroencephalography revealed no epileptic discharge or abnormal slow activity.

Computerized tomography of the brain without contrast medium demonstrated a symmetrical pattern of intracerebral calcifications without mass effect. There were widespread calcifications involving both caudate nuclei, globus pallidus, putamen, thalami, dentate nuclei and cerebellar hemispheres. Calcifications of subcortical white matter were presented at frontal lobe, and cortical calcification of occipital lobe was revealed. The caudate body calcification extended laterally into the corona radiata (white matter radiation). The wispy configuration of this lateral extension indicated the vascular nature of calcification.

She was treated with short course of oral calcium and had complete recovery.

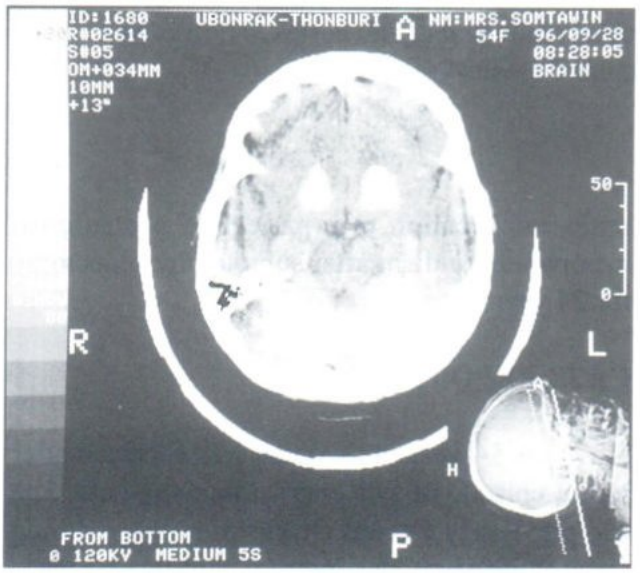

Fig. 1 Noncontrast computed tomography of brain. A slice through the posterior fossa demonstrates calcifications of dentate nuclei and cerebellar white matter.

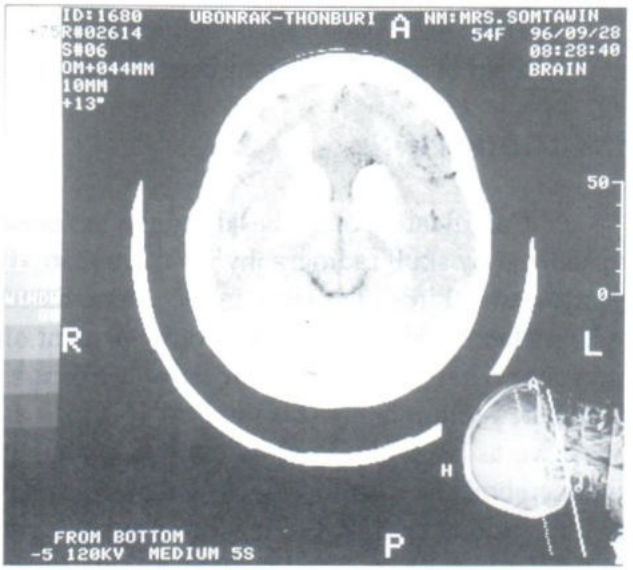

Fig. 2 A central slice through the frontal horns and third ventricle reveals thick calcifications of the basal ganglia (caudate and lenticular nucleus). Subcortical white matter calcifications are present in the frontal lobe.

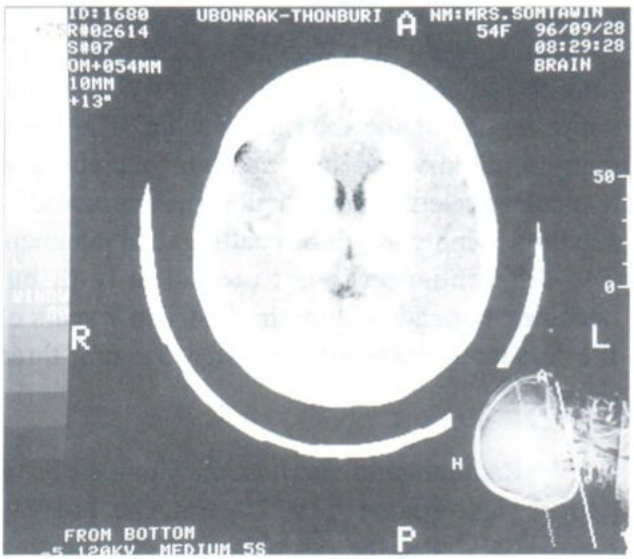

Fig. 3 A slice at higher level shows bilateral, symmetrical basal ganglia and thalamic calcifications.

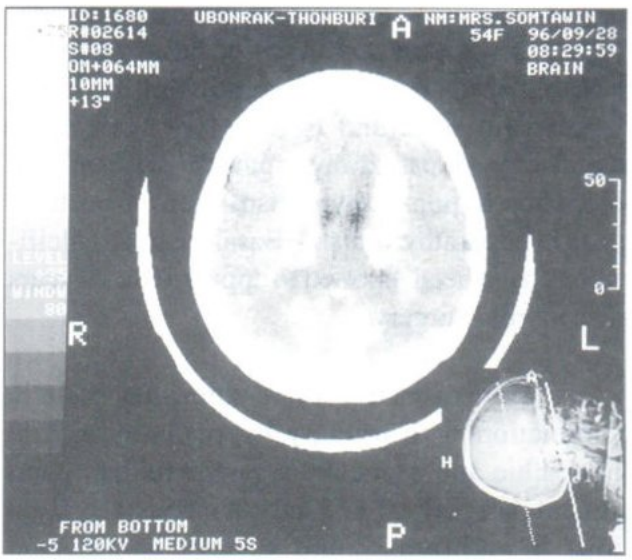

Fig. 4 A slice through the top of lateral ventricles demonstrates caudate body calcifications extending laterally into the corona radiata. Cortical calcifications of occipital lobe are present.

DISCUSSION

Hypoparathyroidism is a clinical disorder characterized by hypocalcemia and hyperphosphatemia in the absence of renal failure and hypomagnesemia. The causes of hypoparathyroidism can be classified as two groups : (1) insufficient parathyroid hormone secretion (hypoparathyroidism) :and (2) impaired parathyroid hormone action (pseudohypoparathyroidism). The hypopara -thyroidism may be idiopathic, but is more often a complication of thyroid surgery. Postsurgical hypoparathyroidism was first described in 1879. The incidence of temporary hypoparathyroidism (lasting six months or longer) following thyroidectomy varies widely in surgical series (a range of 0.2-33% has been reported). As far as thyroid disorders that require bilateral thyroidectomy, a tendency to have persistent hypoparathyroidism is more frequent in patients operated on for Graves' disease and thyroid cancer than in other thyroid disorders. Hypoparathyroidism in patients after radioactive iodine therapy of Graves' disease is extremely uncommon.

Diminution of parathyroid hormone action on kidney and bone leads to hypocalcemia and hyperphosphatemia. Decreased serum ionized calcium concentration increased neuromuscular excitability and the symptom may range in severity from mild paresthesia to severe tetany with muscle cramps, carpopedal spasms, laryngeal stridor and convulsions. Sometimes choreoathetosis is also induced and the symptom is presumably due to calcification of the basal ganglia. Also in some instance there are signs of a cerebellar lesion. Occasionally there may be a long latent period before symptoms will develop and before hypocalcemia is diagnosed. The occurrence of intracerebral calcification in patients with hypoparathyroidism is well known. This calcification occurs not only in the basal ganglia, but also in the dentate nuclei of the cerebellum and/or other areas of the brain, particulary the frontal lobes.

Development of calcified basal ganglia is probably a function of the duration of the hypoparathyroid state and is therefore seen more commonly in pseudohypoparathyroidism and idiopathic hypoparathyroidism than in postsurgical hypoparathyroidism. Basal ganglia calcifications have been reported to appear 10 to 20 years after thyroid surgery.

More extensive calcification may occur in conjunction with primary hypoparathyroidism (idiopathic and pseudohypoparathyroidism) and cortical, subcortical and subcutaneous calcifications in addition should suggest parathyroid diseases. In one serie, 93% of the cases of primary hypoparathyroidism had basal ganglia calcifications. Of the cases with calcifications, 47% had calcification in the cerebral cortex and 21% had calcification in the cerebellum.

The basal ganglia are cental gray matter structures, readily distinguished on CT and MRI from the adjacent lateral ventricles and from the white matter of the internal capsule. The basal ganglia are divided into caudate nucleus and lenticular nucleus. The lenticular nucleus is readily subdivided innto the globus pallidus and putamen. The differentiation is not present at birth but becomes evidence within the first 1 to 2 years of life, gradually increasing through the first three decades.

Radiographic calcification within the basal ganglia was reported in 1935 by Fritzche. In 1939, Eaton et al. noted the association of calcification of the basal ganglia with hypoparathyroidism, and in 1945, Sprague et al. reported its occurrence with pseudohypoparathyroidism. It has since been described in association with many pathological conditions, the most common of which are listed in TABLE 1. [1]

TABLE 1: Conditions Associated with calcification of the basal ganglia

Endocrine	Congenital/ Developmental	Inflammatory	Toxic/Anoxic
Hypoparathyroidism	Familial cerebral vascular	Cytomegalic inclusion disease	Carbon monoxide
Pseudohypoparathyroidism	ferrocalcinosis(Fahr's disease)	Encephalitis(measles,	intoxication
Pseudo-pseudohypoparathyroidism	Cockayne syndrome	chicken pox)	Lead intoxication
	Tuberous sclerosis	Toxoplasmosis	Birth anoxia
	Oculocraniosomatic disease	Cysticercosis	Therapeutic radiation
			Methotrexate therapy

Basal ganglia calcifications are usually small in extent and bilateral, symmetrically confined to the globus pallidus, and are rarely associated with calcification of the other areas of brain. Symmetrical calcifications of the basal ganglia occur in upto 1.5 % of individuals examined by CT-scan. It is most commonly found in patients older than 40 years, who only rarely have symptoms associated with it. The manifestation may be dismissed as an aging phenomenon of no clinical significance and perhaps classified as "physiologic calcification". When calcification occurs early in life (under the age of 40) and is of such degree as to be visible in plain film of the skull, it must always be regarded as abnormal. Patients of any age with calcification in the lenticular nucleus and elsewhere in the basal ganglia, dentate nucleus, or multiple areas of the cerebral cortex should be evaluated for pathological disorders. Thus, the "physiologic calcification" differs from pathological calcification in their density, volume and distribution.

The exact etiologic factor(s) responsible for calcification deposits in the basal ganglia, dentate nuclei and other areas of the cerebral and cerebellar hemispheres are still obscure. Because of generally accepted that 70-80% of cases of basal ganglia calcifications are associate with hypoparathyroidism, a generalized disturbance of calcium metabolism has been suggested. Cerebral anoxia has also been considered solely because the basal ganglia, particulary the globus pallidus, are known to be susceptible to various anoxic and metabolic injuries. It has been postulated that this sensitivity may be a result of the high metabolic activity of the central nuclei, their vascular anatomy, and their autoregulatory physiology. One suggestion has been that basal ganglia calcification may be secondary to an elevated" calcium-phosphorus product" (Ca. x P. value). But, Illum and Dupont found no significant difference in serum Ca. x P. among their 10 idiopathic hypoparathyroidism patients with brain calcinosis compared to their 5 patients without calcinosis. Therefore, the factors governing calcification remain to be elucidated.

The sequence of events in this calcification process apparently begins with the deposition of a colloid protein material in and about the walls of the small cerebral vessels. The substrate is subsequently impregnated first with iron and later with calcium that can coalesce into large masses which obliterate completely the usual microscopic structures and become visible a large calcareous mass. Twenty percent of patients with calcification showed extrapyramidal syndrome, possibly due to calcium salt deposits in the metasynaptic dopamine receptors. Parkinsonism associated with basal ganglia calcification differs from idiopathic parkinsonism in being resistant to levodopa therapy.

CONCLUSION

Basal ganglia calcification which confined to the globus pallidus of patient older than 40 should be considered physiologic, with a prevalence of 0.6-1.5% of the CT-studies. Calcification elsewhere in the basal ganglia, dentate nucleus or multiple areas of the cortex in a patient of any age should also be considered pathological. The extensive calcification of brain have been found in patient with hypoparathyroidism and Fahr's d isease. The mechanism of cerebral calcification remain unknown. There are two main possible factors which alone or in combination may cause cerebral calcification, first : perivascular deposits of an albuminoid matrix attracting calcium ions, second : an imbalance of electrolyte yielding low calcium and high phosphorus levels.

This report describe a case of extensive cerebral calcifications in postsurgical hypoparathyroidism, in which the calcifications not only located in basal ganglia but also in dentate nuclei, central cerebellar white matter zones, corona radiata, thalamus, cortical layer of occipital lobe and subcortical white matter of frontal lobe. The finding is not yet frequently found and has some differences from the previous reports.

REFERENCES

1. Chad R. Cohen, Paul M. Duchesneau, Meredith A. Weinstein. Calcification of the basal ganglia as visualized by Computed tomography. Radiology 1980;134:97-99
2. Charlotte Sachs, Hans-Erik Sjoberg, Kaj Erikson. Basal ganglia calcifications on CT: Relation to hypoparathyroidism. Neurology 1982;32: 779-82
3. C. Lang, W. Huk, J. Pichl. Comparison extensive brain calcification in postoperative hypoparathyroidism on CT and NMR scan. Neuroradiology 1989;31:29-32

4. F. Illum,E. Dupont. Prevalences of CT-detected calcification in the basal ganglia in idiopathic hypoparathyroidism and pseudohypoparathyroidism. Neuro-radiology 1985;27:32-37
5. Iraj Derakhshan. Basal ganglia calcification and hypoparathyroidism : Case report. Neurology 1979;29:1191-92
6. Milford Fulop, Barbara Zeifer. Case report : Extensive brain calcification in hypoparathyroidism. Am J Med Sci 1991; 302(5):292-95
7. Solomon Posen, Phillip Clifton-Bligh, Thomas Cromer. Computerized tomography of the brain in surgical hypoparathyroidism. Ann Intern Med 1979;91(3):415-17
8. William C. Koller, John W. Cochran, Harold L. Klowans. Calcification of the basal ganglia : Computerized tomography and clinical correlation. Neurology 1979; 29:328-33

ULTRASOUND & CT PICTURES OF CHOLANGIOCARCINOMA

Warinthorn PHUTTHARAK [1] Jiraporn SRINAKARIN[2]
Supinda PUNTACE[3] Vallop LAOPAIBOON[4]

Presented at 34th annual radiological scientific meeting on March, 1997 at the Royal Golden Jubilee Building, Soi Soonvijai, Bangkok, Thailand.

ABSTRACT

Our hospital, Srinagarind hospital, is located in the highest prevalence area of Cholangiocarcinoma (CHCA). The aim of this study is to present the findings of 110 ultrasound and 49 conventional CT images of 132 cases with histopathologically proven CHCA seen during 1991-1997. There were 2 major types; peripheral type 105 cases (US & CT = 22, US only = 65 and CT only = 18); extrahepatic type 27 cases (US & CT = 5, US only = 18 and CT only = 4). The peripheral type was divided into nodular and infiltrative forms. The nodular form was the most common US finding ; solitary mass (95.12%), large size > 5 cm. (71.5%), ill-defined border (53.65%), hyperechogenicity (68.29 %) and 23.17% of the cases had peripheral halo. The CT pictures were ill -defined hypodense mass with minimal peripheral enhancement. Most tumors located at posterior segment of the right lobe of liver. Peritumoral bile duct dilatation (41.46 % by US, 52.5 % by CT) was a useful finding in helping to distinguish CHCA from the other liver tumors. The infiltrative form was much less common (5 cases), can not be differentiated from hepatocellular carcinoma or liver metastases. The extrahepatic type CHCA (27 cases) was commonly located at hepatic duct confluence. The hilar mass could either be visualized or non – visualized.

(**Keywords;** Liver tumor, Bile duct carcinoma, cholangiocarcinoma, US – liver and bile duct, CT – liver and bile duct)

INTRODUCTION

Primary intrahepatic cholangiocarcinoma (CHCA) is known as an uncommon liver tumor in most parts of the world including several regions of Thailand (except the northeastern part) when it was compared to hepatocellular carcinoma in the past. The prevalence of CHCA is highest in the northeast Thailand. The people living in this region of Thailand have highest risk in developing CHCA in relation to liver fluke (Opistorchis viverrini, OV) infestation and nitrosamine (source of carcinogen) contamination.[4] Culturally - bound habits of eating ground raw fresh-water fish (Koi

[1, 2, 4] Department of Radiology, Faculty of Medicine, Srinagarind Hospital, Khon Kaen University, Khon Kaen, Thailand 40002
[3] Department of Pathology, Faculty of Medicine, Srinagarind Hospital, Khon Kaen University, Khon Kaen, Thailand 40002

Correspondence to

Warinthorn PHUTTHARAK Department of Radiology, Faculty of Medicine, Srinagarind Hospital, Khon Kaen University, Khon Kaen, Thailand 40002 Telephone : 043-348389 Fax : 043-348389

pla) and fish fermented in salt (Pla ra) as daily foods and even feeding them to infants,make the local people of the northeast predisposed to these risk factors in their early lives. This relationship is not different from association between Clonorchis sinensis infection and CHCA in the previous reports of other countries,[5] particularly Asia. CHCA may be classified as (a) peripheral type, which originates in an interlobular duct; and (b) extrahepatic type, which originates at major right or left hepatic duct, the main hepatic bifurcation, common hepatic duct and common bile duct.

The aim of this study is to analyze the US and CT findings of CHCA treated at our hospital which may be useful for future diagnosis and treatment planning.

MATERIAL AND METHOD

The ultrasound and CT images of 132 patients with histopathologically proven cholangiocarcinomas seen at Srinagarind Hospital, Khon Kaen University, during 1991-1997 (110 US, 49 conventional CT images) were retrospectively reviewed. The specimens were obtained either by surgery or biopsy. At microscopic examination, all tumors were diagnosed as CHCA; composed of acinar structures with atypia in a pattern characteristic of adenocarcinoma with the frequent presence of mucin, fibrosis, and calcification. Cholangiocarcinomas were classified as peripheral type in 105 patients (performed US - 65, CT - 18, US & CT - 22 cases); and extrahepatic type in 27 patients, (performed US - 18, CT - 4, US & CT - 5 cases). The study included 78 men and 54 women with an age range of 22 – 77 years (average age 53.5 years). One case had fascioliasis coinfection.

Ultrasonographic examinations were performed with a real time scanners (EUB – 40 Hitachi, or SSD 650 Aloka, Tokyo). The 3.5 MHz transducers (convex array) was used in all patients. The scanning was performed across the entire upper abdomen by the intercostal subcostal approaches, mainly transverse plane and additional sagittal oblique plane.

CT examinations were mostly performed with a CT 9800 (General Electric Medical System, Milwaukee, WI, USA). After obtaining a precontrast scan, a bolus hand injection of 100 ml., 60 % iodinated water soluble contrast agent was given and the scan was performed dynamically. The remaining small number of patients had CT from the outside hospitals.

All images of the peripheral type were analyzed for; a). number of tumor mass, size, margin, echo or density, degree of contrast enhancement, location; b). presence of peritumoral bile duct dilatation, calcification or cystic degeneration within the mass, retraction of the adjacent liver capsule, irregularity of adjacent diaphragm or nearby vascular involvement; c) presence of metastatic lesion.

All images of the extrahepatic type were analyzed for; a). site of obstruction, determined by pattern, distribution of dilated ducts; b). presence of a mass, echo or density of tumor mass, degree of contrast enhancement; c). associated findings; d). presence of extrahepatic metastases; e). comparing diagnostic accuracy for site of obstruction between CT and US (correlate with operative findings)

RESULTS

We found the peripheral type cholangiocarcinoma (105 cases, 79.54%) more than the central type (27 cases, 20.46%). US and CT findings were analyzed, regarding the anatomic location and tumor characteristic, respectively.

SONOGRAPHIC FINDINGS OF PERIPHERAL TYPE (87 cases)

Peripheral type was divided into two group; nodular form 82 cases (94.25%) and infiltrative form 5 cases (5.57%). The ultrasonographic (US) findings of nodular form were summarized in table 1.

Most of nodular form of the peripheral type CHCA presented as solid solitary mass (fig.1, 2). Four patients had multiple masses, the largest one with adjacent smaller satellite nodules were shown. The size of tumor ranged from 2 cm. to 15 cm. The tumor larger than 5 cm. were most frequently encountered. The tumor margin was either ill defined or well defined (fig.1, 2).

Echogenicity varied by tumor size. We found the highest frequency of the the big tumor size, larger than 5 cm. (59 of 82 cases, 71.5%). The big tumor size was likely to be hyperechogenic. (fig.1b)

Nineteen patients had peritumoral halo (23.17%) (fig.2). Peritumoral duct dilatation was shown in 34 cases, 41.46 % (Fig 1a). Most of the tumors were in the right lobe, particularly the posterior segment, and only 15 cases (18.29%) in the left lobe. The tumors rarely had calcification or cystic degeneration (2.44%,12.19%) (fig.1b)

Only one case (1.2%) was a cystic tumor by evidence of homogeneously hypoechoic mass with posterior enhancement with mural hyperechoic portion of the mass (fig. 3). Four cases (4.87%) of bright echoic spots without acoustic shadowing within the mass, possibly representing mucin products were depicted (fig.3, 4). In three cases (3.66%), atrophic change of the involved liver part was found. Irregularity of adjacent diaphragm was demonstrated in only 5 cases (6%) by US .

INFILTRATIVE FORM (5 cases)

Five patients (5.75%) had distorted parenchymal echo with inhomogeneous pattern involving the entire lobe of the liver. (fig.5) They were in RT. lobe (n = 2), LT. lobe (n = 2), and both lobes (n = 1). The extrahepatic extension were lymph nodes (n = 2), and diaphragm (n = 1).

SONOGRAPHIC FINDINGS OF THE EXTRAHEPATIC TYPE (23 cases)

In this type, the mass could be visualized in 12 patients (52.17%), and non-visualized in 11 patients (47.83%) (fig.6,7). The echogenicity of the mass were isoechoic in 3 cases (25%) and hyperechoic in 9 cases (75%). The site of obstruction were found mainly at the main hepatic duct bifurcation in 12 cases (52.17%), LT.main hepatic duct in 3 cases (13.04%), RT.main hepatic duct in 2 cases (8.59%), CBD in 6 cases (26%). The gallbladders were not able to be demonstrated in 2 cases (8.70%), contracted in 4 cases (17.39%), normal size in 10 cases (43.48%) and distended in 7 cases (30.43%). The extrahepatic extension was lymph nodes (n = 2, 8.69 %). The other findings were hepatic lobar atrophy (n = 3, 3.04%), increased periportal echo (n = 6, 26.08%).

CT FINDINGS OF PERIPHERAL TYPE (40 cases)

Almost all of these cases were nodular form with solitary mass , (n = 38, 95%) (fig.8). Two cases had multiple masses (5%), one dominant mass and adjacent satellite nodules in one patient (fig. 9). The tumor boundary was found to be ill defined (n = 28, 70%) more than well defined (n = 12, 30%). The tumor density varied; mainly hypodense (n = 37, 92.5%). Most enhancement pattern was mostly slightly enhanced (n = 30, 75%) (fig. 8b). The tumor size was commonly larger than 5 cm. (n=29, 72.5%). The tumor location was the RT. lobe (n = 2, 80%), particu-

larly posterior segment, more than the Lt. lobe. We found peritumoral duct dilatation in about half of the cases (n = 21 cases, 52.5%) (fig. 1a, 11b); calcification 8 cases (20%) (fig. 11); cystic degeneration (n = 2, 5 %); adjacent vascular involvement (n = 8, 20%); retraction of adjacent liver capsule (n = 7, 17.5%) (fig.5). The other findings were hepatic lobar atrophy (2 cases) ; gall stone (1 case) ; focal fatty liver (1 case). The extrahepatic extensions were involvement of adjacent diaphragm, 12 cases (30%) (fig. 10), lymphadenopathy 19 cases (47.5%) (fig. 12a), adjacent gastric wall involvement 1 case (fig. 12b), pulmonary metastases 1 case and pleural effusion 6 cases (15%).

CT FINDINGS OF EXTRAHEPATIC TYPE (9 cases)

The hilar mass was visualized in 7 of the 9 cases. They were mainly isodense (6 cases) (fig.13a). The remaining 1 case was a hyperdense mass. All lesions were slightly enhanced after the contrast injection. The common obstructive location was at main hepatic duct bifurcation (7 cases) (fig. 13, 14) and the remainings were at main duct 1 case and CBD 1 case.

The gallbladder size was normal in 4 cases, contracted 3 cases, enlarged 2 cases. The extrahepatic extensions were lymphadenopathy 2 cases, ascites 2 cases. Hepatic lobar atrophy was shown in 2 cases (fig. 14a).

Table 1 Us findings of nodular form of the peripheral type (82 cases)

	Number	%
NUMBER OF LESIONS		
- Solitary	78	95.12
- Multiple	4	4.87
TUMOR SIZE		
> 5 cm.	59	71.50
3-5 cm.	16	19.50
< 3 cm.	7	8.54
TUMOR BOUNDARY		
- Ill defined	44	53.65
- Well defined	38	46.35
- With peripheral halo	(19)	(23.17)
ECHOGENICITY		
- Hyperecho	59	68.29
- Hypoecho	13	15.85
- Isoecho	18	12.19
- Mixed echo	2	2.43
- Cystic Tumor	1	1.20
LOCATION		
- RT.lobe	67	81.7
Posterior segment	48	71.60
- LT.lobe	15	18.29
OTHER FINDINGS		
- Peritumoral duct dilatation	34	41.46
- Cystic degeneration	10	12.19
- Bright echo spots of mucin products	4	4.87
- Atrophy of involved liver segment	3	3.66
- Calcification	2	2.44
EXTRAHEPATIC EXTENSIONS		
- Regional node enlargement	10	12.19
- Irregularity, involved adjacent diaphragm	5	6

Table 2 CT findings of nodular form of the peripheral type 40 cases

	Number (n)	%
NUMBER OF LESIONS		
- Solitary	38	95
- Multiple	2	5
TUMOR SIZE		
> 5 cm.	29	72.5
3-5 cm.	7	17.5
< 3 cm.	4	10
TUMOR BOUNDARY		
- Ill defined	28	70
- Well defined	12	30
DENSITY		
- Hypodensity	37	92.5
- Isodensity	2	5
- Hyperdensity	1	2.5
ENHANCEMENT		
- Slightly	30	75
- Intermediate	10	25
- Markedly	-	-
LOCATION		
- Rt.lobe	32	80
- Posterior segment	(21)	(65.63%)
- Lt.lobe	15	20
OTHER FINDINGS		
- Peritumoral duct dilatation	21	52.5
- Cystic degeneration	2	5
- Bright echo s[ots of mucin products	7	17
- Atrophy of involved liver segment	2	5
- Calcification	8	20
EXTRAHEPATIC EXTENSION		
- Regional nodes Enlargement	19	47.5
- Irregularity of adjacent diaphragm	12	30
- Stomach	1	2.5

Table 3 Accuracy in the detection of extrahepatic type of CHCA by sites in the patients who had both US & CT

	CT		SONOGRAM	
Location	Surgical findings	CT detection	Surgical findings	US-detection
	(n)	total(%)	(n)	total(%)
-Main hep.Duct	2	2 (100%)	4	3 (75%)
-Bifurcation	3	3 (100%)	11	8 (72.73%)
-CHD	-	-	-	-
-CBD	2	1 (50%)	6	4 (66.67%)

** No surgical notes 2 cases

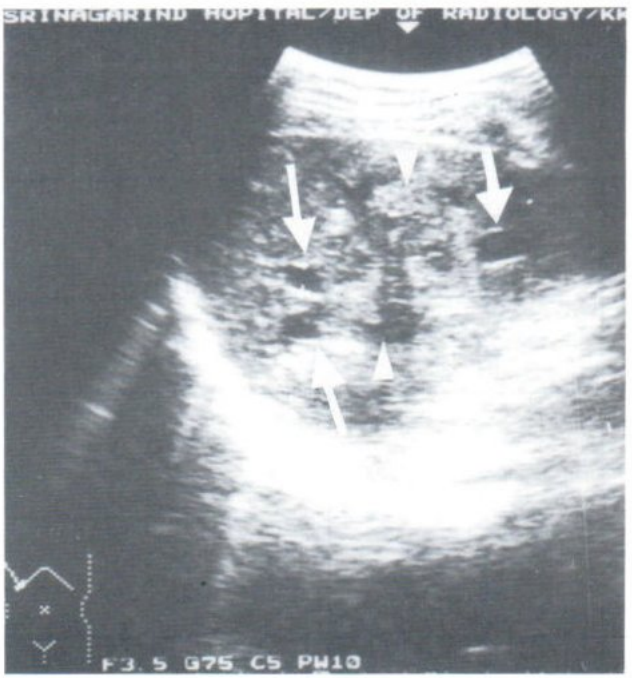

1A.

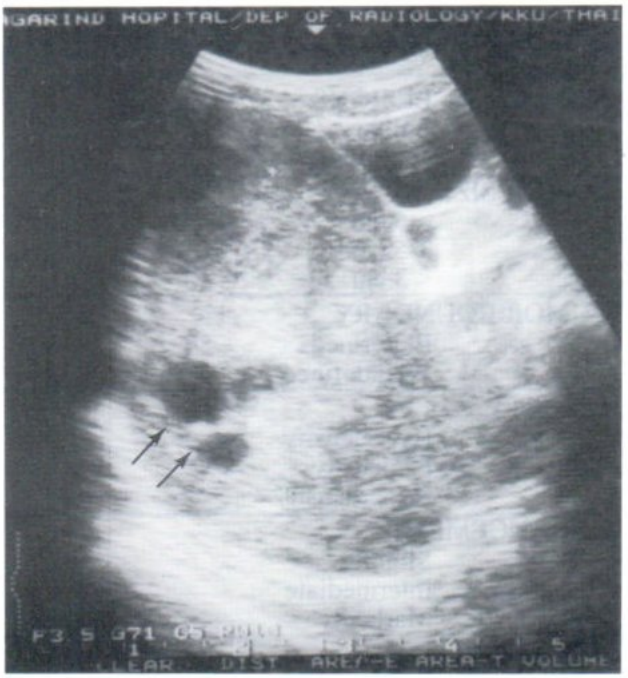

1B.

Fig. 1. US of nodular form of peripheral CHCA with ill defined margin a). Slightly hyperechoic mass at posterior segment, right lobe liver (white arrowheads), with peritumoral bile duct dilatation (arrows). Intercostal approach scanning. (b). The larger hyperechoic mass with small areas of cystic degeneration (arrows).

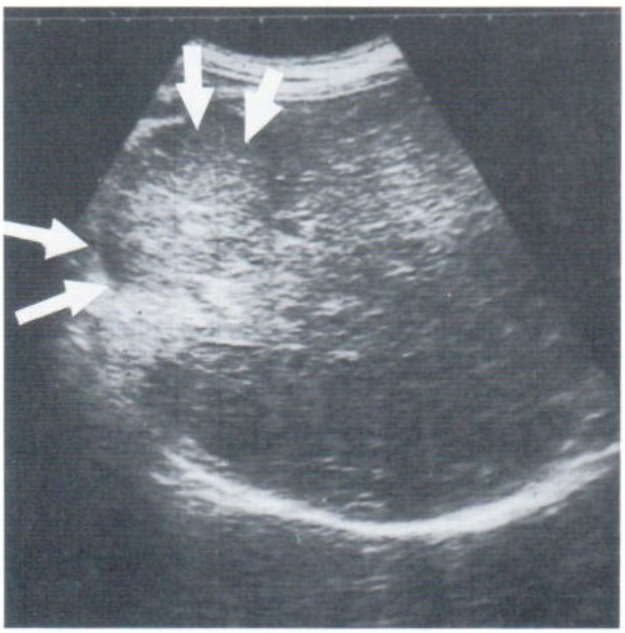

Fig. 2. Peripheral CHCA with well defined margin : Echoic right lobe mass with peripheral halo (arrows)

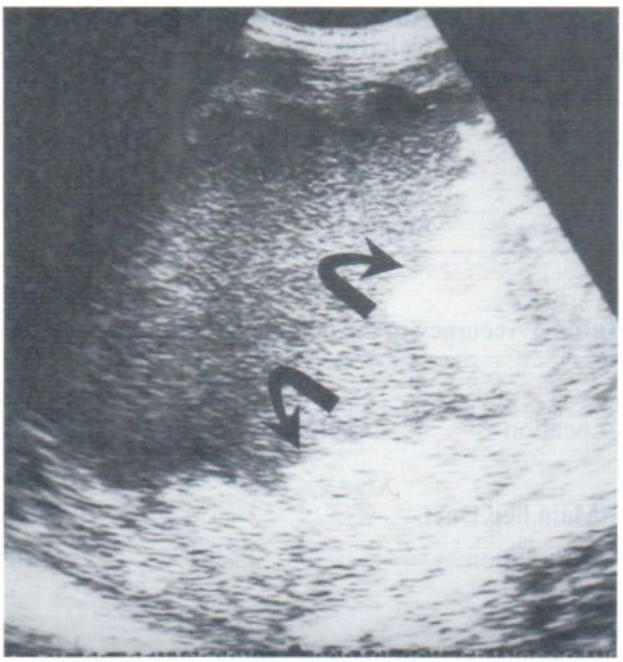

Fig. 3. Cystic CHCA : Large cystic tumor in the right lobe (by evidence of posterior enhancement) with visualized mural hyperechoic portion (curve arrows).

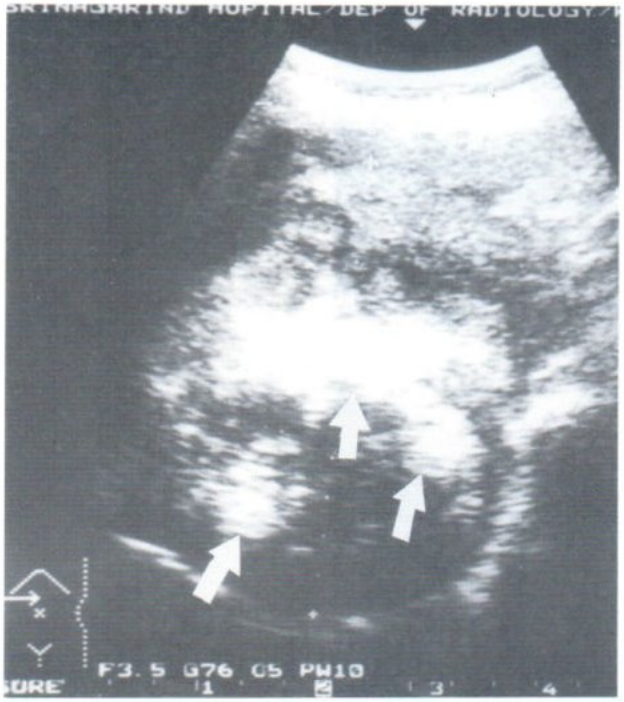

Fig. 4. Peripheral CHCA with mucin products : Large hyperechoic mass with bright echo areas (without acoustic shadowing) within the mass (arrows), probaby represent mucin products.

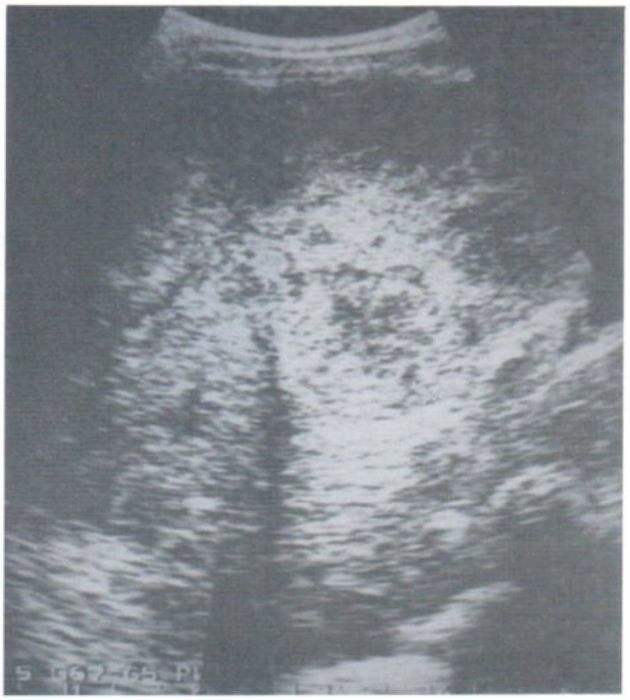

Fig 5. US of infiltrative form of peripheral CHCA : inhomogeneous echo pattern of the entire right lobe liver

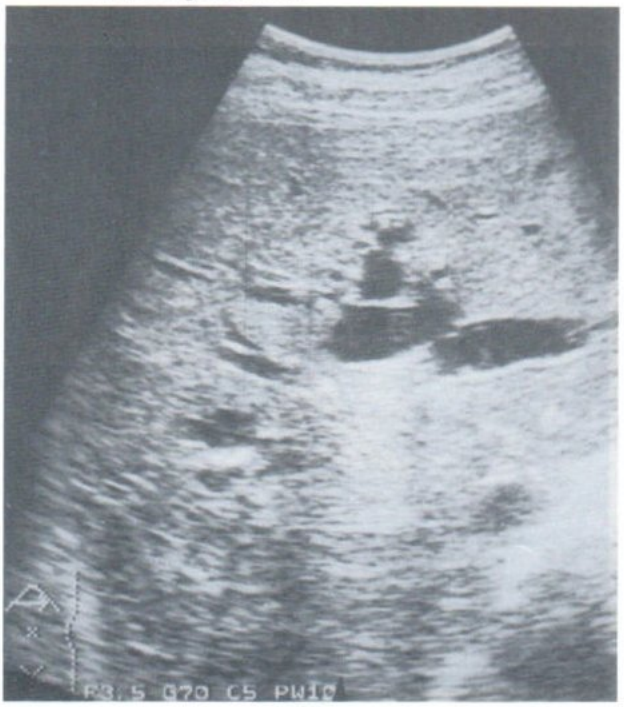

6A

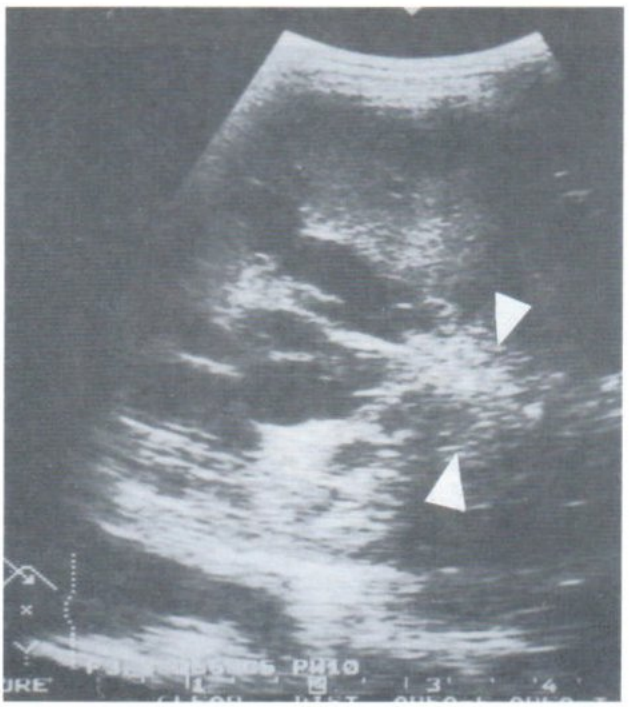

6B

Fig 6. Extrahepatic type CHCA (proximal duct) (a). CHCA at porta hepatis by visualized nonunion of dilated intrahepatic ducts both lobes of liver and non-visualized mass lesion (b). CHCA at porta hepatis with visualized hyperechoic mass (white arrow heads)

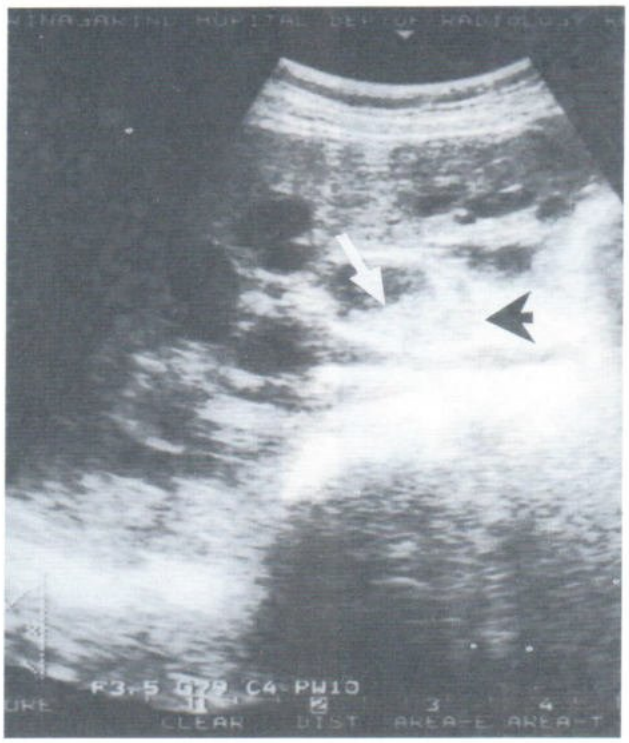

Fig. 7. Extrahepatic type CHCA (distal duct carcinoma) : Dilated CBD (black arrow) with obstruction by intraluminal mass (white arrow)

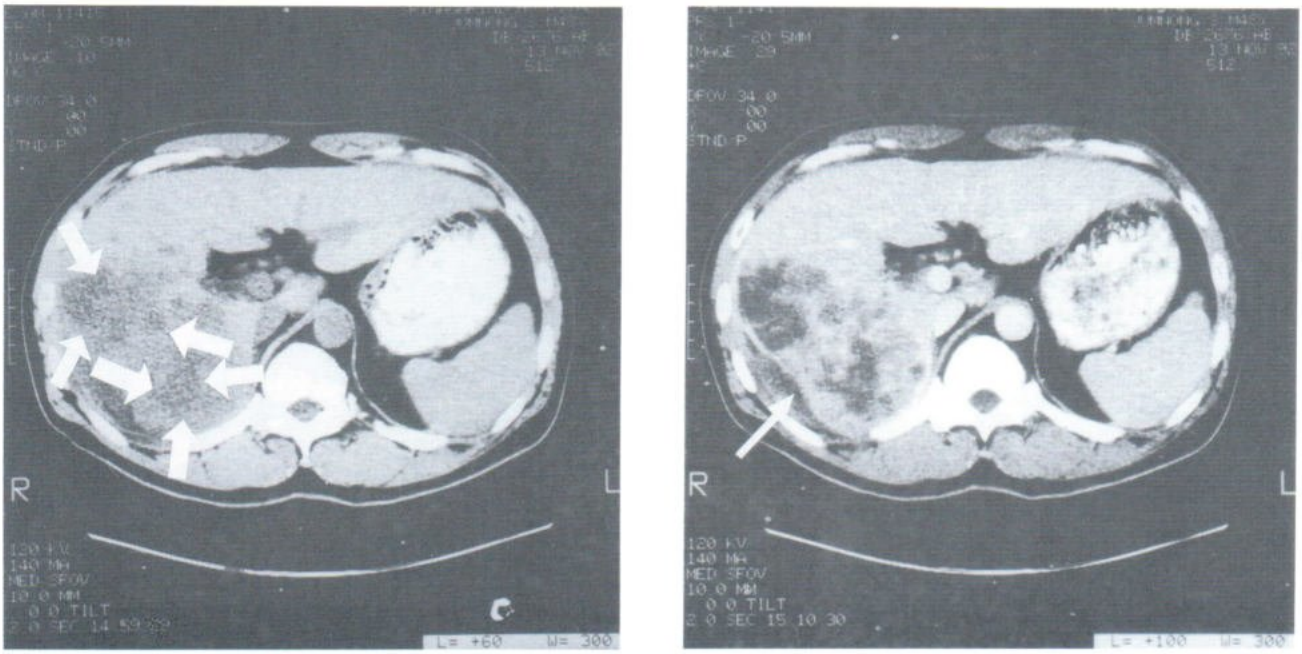

8A **8B**

Fig. 8. CT of solitary, peripheral CHCA
(a). Ill defined hypodensity-mass (arrows) at posterior segment, right lobe liver on pre-contrast CT scan. (b). Slightly contrast enhancement of the mass with retraction of adjacent liver capsule (long arrow).

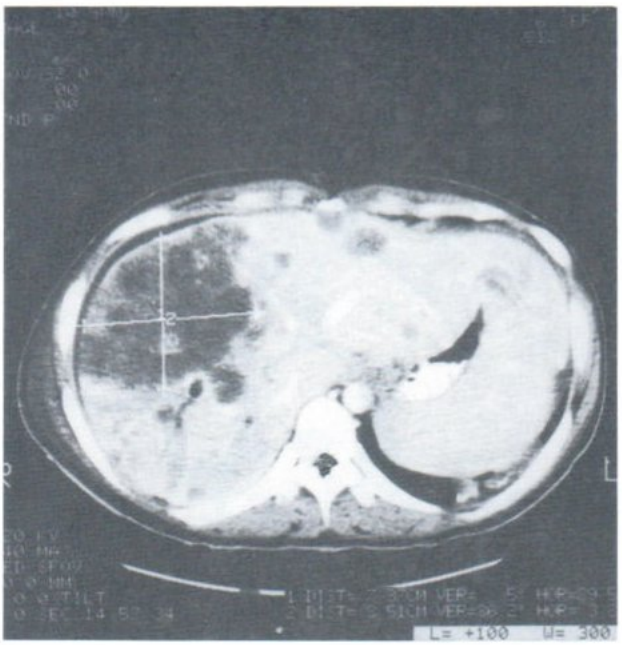

Fig. 9. Multiple masses of peripheral type CHCA The biggest mass at anterior segment of RT.lobe of liver with multiple small satellite nodules. Lesions at LT.lobe probably due to metastases.

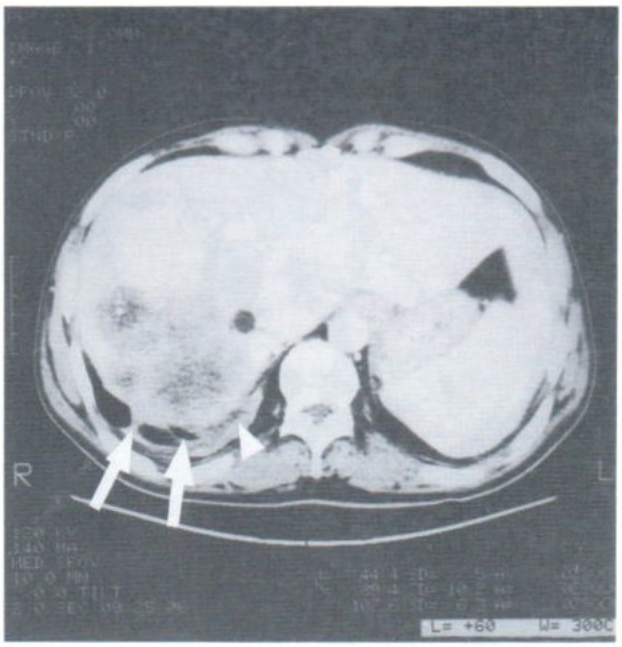

Fig. 10. Superoposterior segment, right lobe CHCA with involved adjacent diaphragm : By visualized evidence of irregular, thickening of diaphragmatic outline (arrows), minimal pleural effusion and /or pleural thickening (arrowheads).

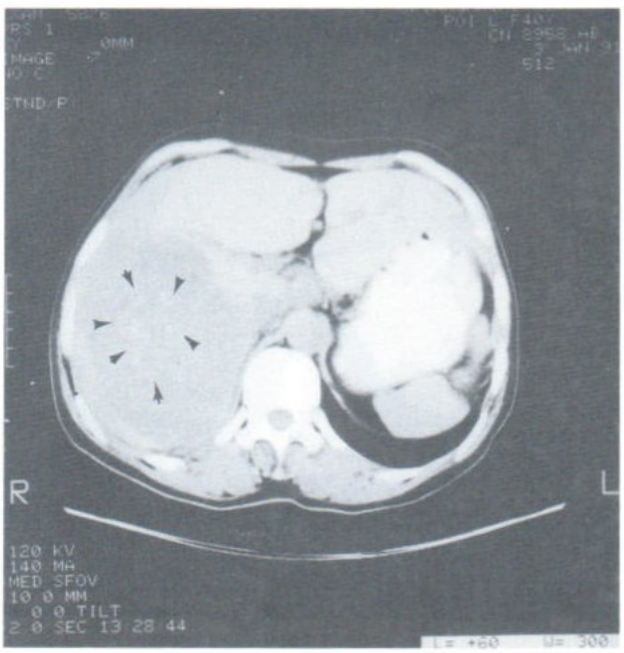

11A

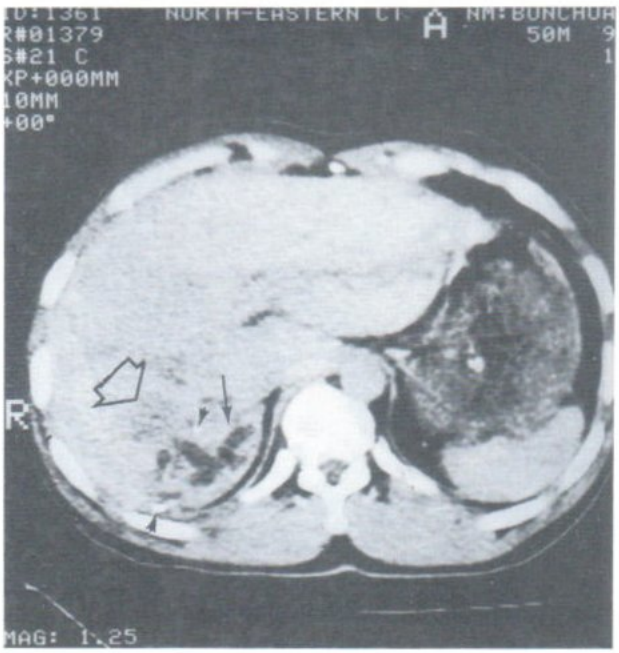

11B

Fig. 11. Peripheral CHCA with hyperdensity areas (a). powerlike high attenuation areas (arrowheads) within low attenuation mass in RT. lobe, mucin products or calcification (b). Right lobe mass (opened arrow) with peritumoral duct dilatation (black arrow) and a few tiny high density spots (arrowheads)

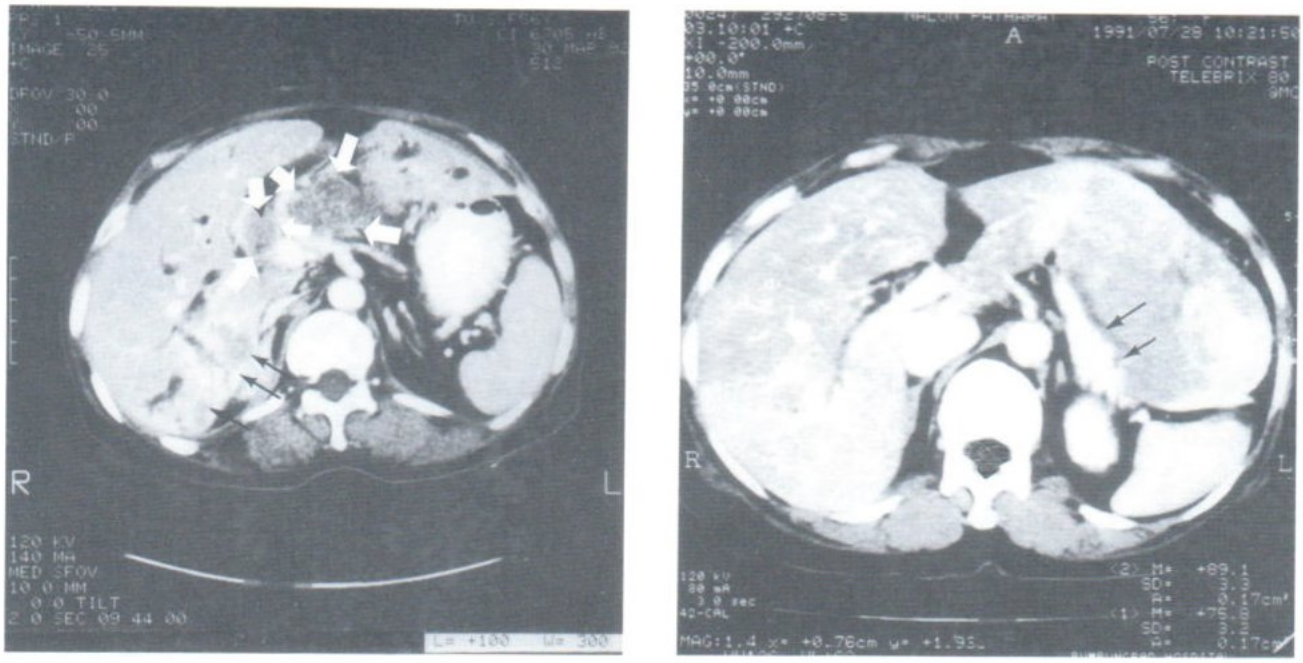

12A 12B

Fig. 12. Extrahepatic extension of CHCA
(a). Peripheral enhanced mass at posterior segment right lobe (arrow) with enlarged lymph nodes at celiac region (white arrows). (b). Large masses in both lobes of liver and involvement of adjacent gastric wall (black arrows) by left lobe mass lesion .

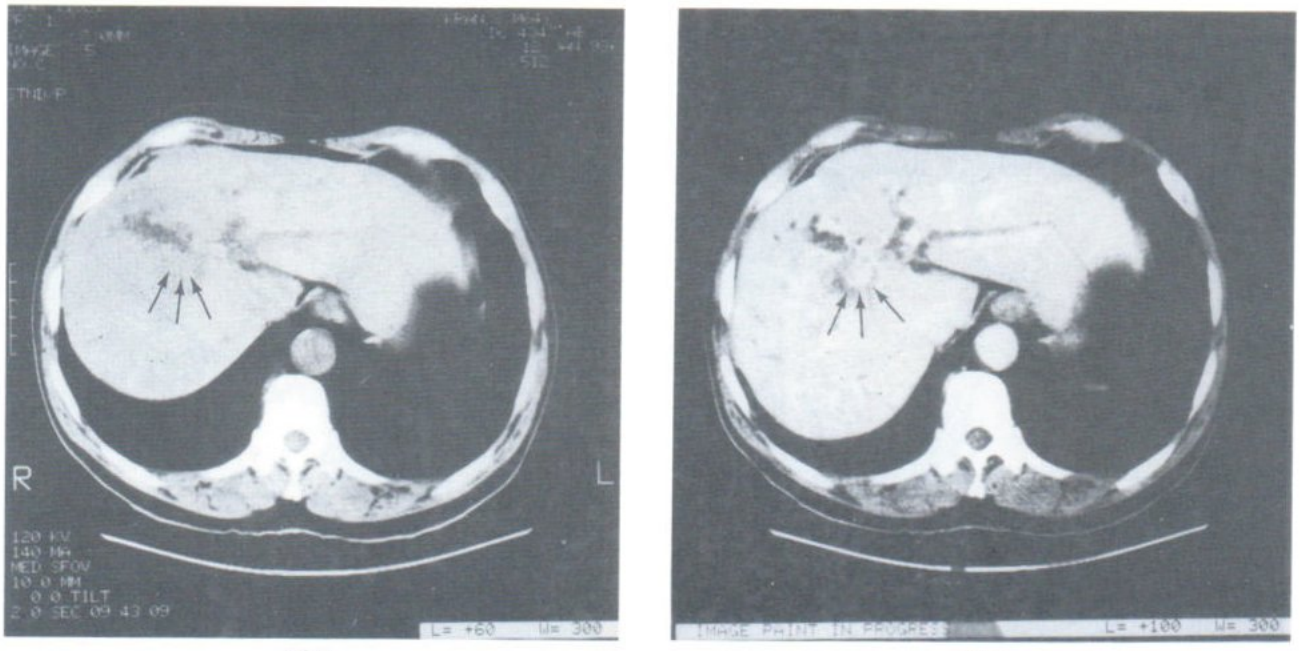

13A 13B

Fig. 13. CT findings of CHCA at porta hepatis with visualized mass lesion
(a). Non-union of dilated intrahepatic ducts in both lobes of liver with abrupt termination at the bifurcation by an isodense mass on pre-contrast study (black arrows) (b). slight enhancement on post-contrast study (black arrows)

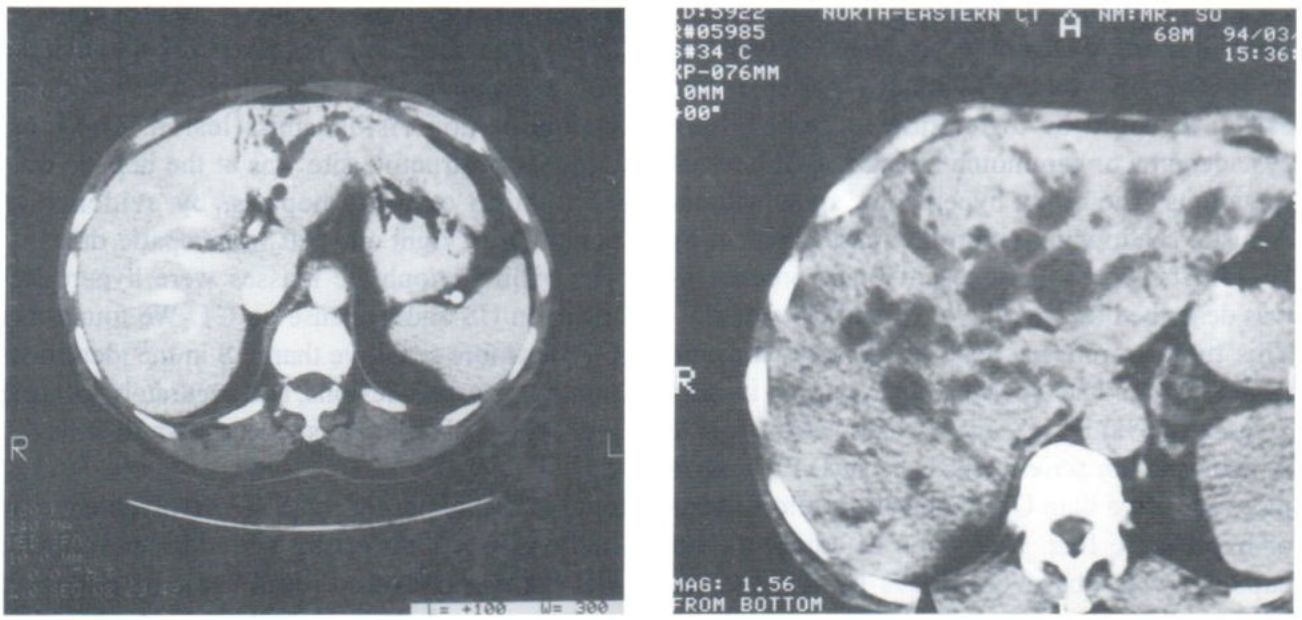

14A 14B

Fig. 14. CT of extrahepatic type CHCA with non-visualized mass lesion
(a). Isolated dilatation of left main hepatic duct and branches indicates obstructive site at left main hepatic duct ,no mass is visible. Slightly atrophic change of involved liver at medial segment LT. lobe. (b). Marked dilatation of the intrahepatic ducts both lobes without extrahepatic duct dilatation by CHCA at porta hepatis, non-visualized mass .

DISCUSSION

In our series, we found a slightly male predominance, as was described in the previous literatures.[1, 2, 5, 9] The male : female ratio is about 1.44 : 1, with the average age of 53.5 years, which is lower than the studies at many institution, particularly Okuda et al. Series (62.2 yrs.),[1] but approximate with series of Choi et al. & Wibulpolprasert et al.[5, 9] The lowest age of our patient is 22 years old. We found more cases of peripheral type more than central type significantly because a large number of cases of operated central type underwent surgical bypass without biopsy. The US findings of peripheral type are two patterns of nodular and infiltrative forms (the former is more common). In the majority of cases, tumors were located in the right lobe, particularly posterior segment. Peritumoral duct dilatation was seen in nearly half of all cases. The CT findings of peripheral type are mainly the nodular form with solid hypodense mass. In more than half of cases, CT show peritumoral bile duct dilatation. Lymphadenopathy was detected by CT better than US. The US and CT findings of nodular form of the peripheral type in our study was not different from the previous reports, mainly solid, solitary, large size (>5 cm.) mass, ill or well defined margin with increased echogenicity and ill defined low density, slightly enhanced mass respectively. The common location is at the posterior segment of right lobe of liver. The tumor size was mostly large because they were rarely producing symptoms early in their course. We see dilated peritumoral intrahepatic ducts more often than the previous reports (41.46% by US, 52.5 % by CT). This is a helpful,although not definite finding for distinguishing CHCA from other liver tumors. We

have one case of cystic CHCA from US which is an uncommon type as previously reported by Lee et al.[13] It could be differentiated from biliary cystadenoma or carcinoma by lacking of internal septations. The bright hyperechoic spots without acoustic shadowing within the mass depicted by US (4.87%) probable represent mucin product, as was described by Kokubo et al. and Choi et al.[7, 8] This tumor rarely has calcific density or cystic degeneration. The calcification was seen in only 2 cases (2.3%) by US and 8 cases (20%) by CT imagings in our series. This is because CT scan is more sensitive than US in detecting calcification or hyperdense foci. Retraction of adjacent liver capsule was observed 17.5% by CT, as was reported by Soyer.[11] Multiple masses were found on US (4 cases) and CT (2 cases). The CT images revealed a dominant mass and adjacent satellite nodules, which could mimic with metastatic tumor. Liver atrophy was less uncommon in peripheral type than in central type CHCA.

In one case, fascioliasis was found, which may imply relationship between liver fluke and CHCA, or it may be an incidental findings. We could not definitely concluded.

When comparing CT with US findings in 22 patients who underwent both investigations, we found that CT was more sensitive than US for detecting a local extrahepatic extension, particularly diaphragmatic involvement and lymphadenopathy. Peripheral CHCA is commonly located at the posterosuperior part of right lobe of liver where it is difficult to detect by US unless a careful intercostal approach is performed, the same as previously mentioned by Wibulpolprasert et al.[9]

The infiltrative form of peripheral type CHCA (5 cases) could not be differentiated from infiltrative hepatoma or infiltrative metastases by US or CT.

Of 27 patients who had extrahepatic type CHCA, the images findings were dilatation of the bile ducts above the obstructive site, and either visible or non-visible mass lesion. The most frequent obstructive site was at the hepatic duct bifurcation or porta hepatis, by evidence of nonunion of right and left intrahepatic ducts.[7,16] The visible exophytic masses were hyperechogenic on US and isodense on CT. We found that CT was more sensitive than US in the identification of metastatic lesions, and accurately locating the level of obstructive site as shown in table 3.

Evaluation of vascular involvement was limited in our study because no additional doppler US were performed and lack of accurate portovenous phase in every case studied by CT. Doppler US and helical CT scan (two phases) are more effective in this regard.

CONCLUSION

We found : (1). high percentage of peritumoral duct dilatation in peripheral type of CHCA. (2). CT scan is more sensitive than US in the detection of local extrahepatic extension. (3). The images findings of infiltrative form of peripheral type can not be differentiated from infiltrative hepatoma or infiltrative metastases. (4). The extrahepatic type of CHCA, commonly affected at the main hepatic duct bifurcation with visible or non-visible mass lesion. (5). CT is more sensitive than US for the identification of the level of biliary obstruction and extrahepatic extension for extrahepatic type of CHCA.

We, therefore, use sonography as a screening examination and CT as a complementary study in the evaluation of CHCA and for tumor staging.

ACKNOWLEDGEMENT

We thank Professor Tula Dhiensiri, for editing the manuscript.

REFERENCES

1. Kunio Okuda, Yasuhiko Kubo, Nobuo Okazaki, Tsuneaki Arishima et al; Clinical aspects of intrahepatic bile duct carcinoma including hilar carcinoma: Cancer 1977; 39: 232-246
2. Edmondson HA, Peter RL; Tumor of the liver: pathologic features: Seminar Roentgenology 1983 ; 18: 75-83
3. P. Jongsuksuntigul and T. Insomboon; Epidemiology of Opisthorchiasis and national control programme in Thailand : Southeast-Asian-J-Trop-Med-Public-Health 1998, June; 29 (2): 327-32
4. Pairojkol C., Sithithaworn P., Sripa B., Thamawit W., Ito N., Itoh M. ; Risk groups for opisthorchiasis – associated cholangiocarcinoma: indicated by a study of worm burden related biliary pathology. Kan Tan Sui 1991; 22(3): 393-402
5. Byung Ihn Choi, Jae Hyung Park, Yong Il Kim: Peripheral Cholangiocarcinoma and Clonorchiasis: CT findings: Radiology 1988; 169: 149-153
6. Ana M. Viamonte Ros., William W. Onnsteu: Intrahepatic Cholangiocarcinoma: Radiology 1988; 167: 689-693
7. Byung Ihn Choi, Jeong Hun Lee, Man Chung Han; Hilar Cholangiocarcinoma; Comparative study with sonography and CT: Radiology 1989; 172: 689-692
8. Takashi Kokubo, Yuji Itai, Kuni Ohtomo; Mucin – hypersecreting Intrahepatic Biliary neoplasms : Radiology 1988; 168: 609-614
9. Busanee Wibulpolprasert, Tula Dhiensiri; Peripheral cholangiocarcinoma: Sonographic Evaluation: J Clin Ultrasound 1992; 20: 303-314
10. Yasuyuki Yamashita, Mutsumasa Takahashi, Susumu Kanazawa, Chusilp Charnsangavej and Sidney Wallace; Parenchymal Changes of the Liver in Cholangiocarcinoma: CT Evaluation: Gastrointest Radiology 1992; 17: 161-166
11. Phillippe Soyer, David A. Bluemke, Christiane Vissuzaine; CT of hepatic Tumors : Prevalence and specificity of Retraction of Adjacent Liver Capsule: AJR 1994; 162: 1119-1122
12. Steven J.Garber, Jennifer J. Donald, and William R. Lees; Cholangiocarcinoma: Ultrasound Features and Correlation of Tumor Position with Survival: Abdominal Imaging 1993; 18: 66-69
13. S.K. Lee, B.I. Choi , J.M. Cho ,J.K. Han ; Cystic peripheral cholangiocarcinoma : Sonography and CT: Abdominal Imaging 1995; 20: 131-132
14. Phillippe Soyer, David A. Bluemke, Ralph Reichle; Imaging of Intrahepatic Cholangiocarcinoma : AJR 1995; 165: 1427-1431
15. B.I. Choi, J.K. Han, Y.M. Shin; Peripheral Cholangiocarcinoma: Comparison of MRI with CT: Abdominal Imaging 1995; 20: 357-360
16. Carlo Emanuele Neumaier, Michele Bertolotto, Rosaria Perrone; Staging of Hilar Cholangiocarcinoma with Ultrasound: J Clin Ultrasound 1995; 23: 173-178.

ABDOMINAL PREGNANCY : REPORT OF 1 CASE AND REVIEW OF THE LITERATURES

Piyanan APIWANTANAGUL, MD.

ABSTRACT

Abdominal pregnancy is a rare form of ectopic gestation. When it occures, its early diagnosis is difficult, owing to the atypical presentation and the low index of suspicion for the condition.

A 31-year-old woman case of abdominal pregnancy at hepatoduodenal ligament, just below to left lobe liver, presenting with dyspepsia was reported and the literatures were extensively reviewed.

CASE REPORT

A 31-year-old Thai farmer woman in Amphur kumtakar, Sakon Nakhon province, G3 P2-AO-2, last 6 years, LMP = 2 December 1999 x 3 days, was admitted at medical ward on 24 January 2000 due to right upper quadrant abdominal pain for 3 weeks without nausea, vomitting, diarrhea, fever or abnormal vaginal bleeding. Physical examination shows a women of her age. Blood pressure = 110/70 MM.Hg, pulse rates = 80 beats/min, Body temperature = 37 °C
Not pale, no jaundice
Heart and Lungs are normal

Abdomen : Mild generalized tenderness
Liver and spleen are impalpable
No abnormal mass
Normal bowel sound

Per Vaginal examination [PV] = normal size of uterus
No abnormal mass
Cervix is close uneffaced, no bleeding per os
Cervical excitation test = negative

She was sent to radiological department for transabdominal ultrasound examination, with an impression of Dyspepsia R/o acute cholecystitis.

Ultrasound finding : as figure 1 and 2

- abdominal pregnancy with viable active heart beats fetus, at just below left lobe of liver and portal vein, medial to IVC
- gestational sac = 3.3 cm. in diameter and crown rump length [CRL] = 20 mm., According to about 8 weeks gestational age
- normal size of uterus, no intrauterine gestational sac
- no free fluid in cal de sac
- normal : liver, gall bladder, CBD, pancreas, spleen, kidneys and urinary bladder.

Department of Radiology, Sakon Nakhon Hospital Amphur Muang, Sakon Nakhon 47000, Thailand.

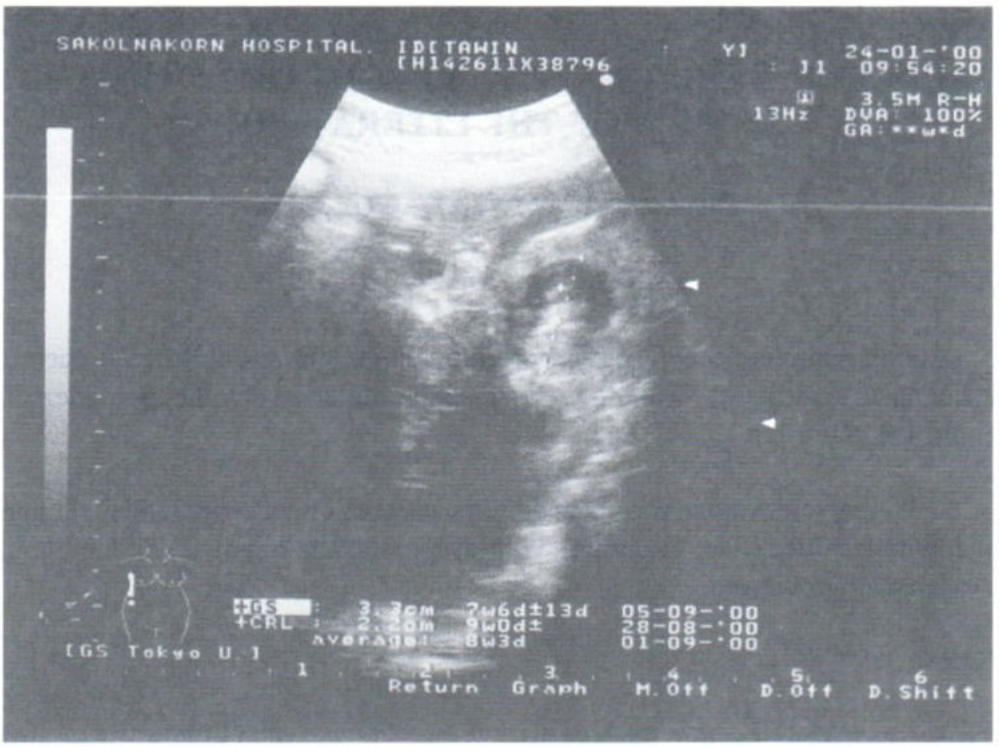

Fig.1 longitudinal scans at mid upper abdomen show abdominal pregnancy with viable fetus at just below left lobe liver and portal vein

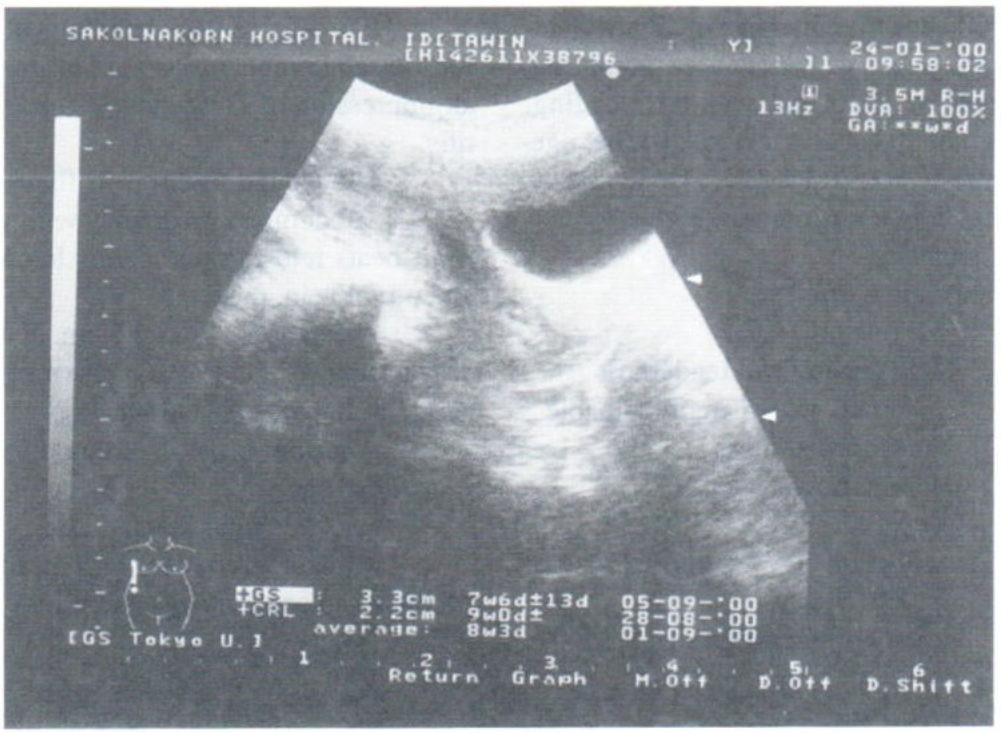

Fig. 2 longitudinal scans of uterus show normal size of uterus without intrauterine gestational sac

Urine pregnancy test is positive.

The final diagnosis is unruptured abdominal pregnancy with viable fetus.

Emergency laparotomy show :

1. Abdominal pregnancy : gestational sac adhere to hepatoduodenal ligament and in Foramen of Winslow.

2. placenta adhere to portal vein and duodenal loop

Gestational sac was removed and the placenta was left intra-abdominally.

DISCUSSION

Abdominal pregnancy is relatively rare. The incidence is estimated at 1 in 8000 births, and abdominal pregnancy represents 1.4 % of ectopic pregnancy.[1] In the united states[2] it has been estimated that there are 10.9 abdominal pregnancies per 100,000 births, and 9.2 abdominal pregnancies per 1000 ectopic gestations. It is more commonly seen in patients of low socio-economic status and in developing countries, age between 24-35 years, mean age 26 years.[3]

The prognosis is poor, with an estimated maternal mortality rate 0.5-18 % and perinatal mortality rate 40-95 %. The risk of dying from an abdominal pregnancy is 7.7 times higher than from other forms of ectopic pregnancy and 90 times of normal pregnancy.

Abdominal pregnancy has been classified by Studiford criteria as primary and secondary.

I. primary abdominal pregnancy : where by definition the tubes and ovaries are normal, there is no evidence of uteroplacental fistula and the pregnancy is related exclusively to the peritoneal surface early enough in gestation to eliminate the possibility of secondary implantation after a primary nidation else where.

II. Secondary abdominal pregnancy : which by definition usually occurs after tubal abortion or rupture, with subsequent implantation of the conceptus on a nearby peritoneal surface or intraligamentary extension.[4]

However, treatment is depend on presenting symptom and not depend on classification.

RISK FACTORS

1. Pelvic infection. There was one report of recurrent abdominal pregnancy in genital TB.
2. Ectopic gestation
3. Endometriosis
4. History of infertility
5. Prior tubal surgery[5]
6. Threatened abortion

DIAGNOSIS

Diagnosis of abdominal pregnancy is frequently difficult, may be delayed or missed diagnosis. Early diagnosis requires a high index of suspicion and clinical features includes :

1. abdominal pain[6] (80% of cases) : this is noticed in early pregnancy and varies from mild discomfort to severe and unbearable pain and there is often abdominal tenderness

2. fetal movement may be painful or absent with fetal death.

3. Vaginal bleeding (30% of cases) : especially in early pregnancy.

4. nausea, vomiting and general malaise (20% of cases) in some there may be additional features of bowel obstruction.

5. fetal parts are easily palpable.

6. abnormal lie (15-20 % of cases)

7. Vaginal examination often reveals a closed uneffaced cervix occasionally displaced anteriorly.

8. absence of palpable uterine contractions to oxytocin stimulation or to induction of labour by prostaglandins is one of the most helpful clinical clues to the diagnosis.

Other atypical presentation were reported are :

1. Hemoperitoneum[7] with shock
2. Hemothorax[8] by implanted on the diaphragm.
3. Rectal bleeding[9] by implanted on rectum
4. Lower GI. Bleeding[10]
5. Delayed diagnosis and was transformed to be lithopedian[11]

Laboratory finding

1. Urine pregnancy test is positive
2. Elevated maternal serum alpha fetoprotein.

Utrasound : Diagnostic tool of choice ; should reveal one or more of the following features.

1. the fetal head is located outside the uterus
2. the fetal body is outside the uterus as is the ectopic placenta
3. Failure to demonstrate a uterine wall between the fetus and the urinary bladder
4. recognition of a close approximation of fetal parts and the maternal abdominal wall
5. atypical sites of gestational sac such as liver[12-14] spleen, appendix[15] ,diaphragm

Radiography should reveal one or more of the following features :

1. absence of a definite uterine shadow around the fetus.
2. maternal intestine shadows intermingling with fetal parts in the anteroposterior view.
3. overlapping of the maternal spine by fetal small parts in the lateral film.

MRI : Magnetic resonance imaging can safely produce images in different planes without use of ionizing radiation. This method seems to be a very sensitive diagnostic tool where facilities exist.

DIFFERENTIAL DIAGNOSIS

1. complications in pregnancy such as abortion
2. gynecological condition such as ovarian cyst
3. non-gynecological [medical or surgical] such as acute appendicitis

Management : summary of management options

1. with dead fetus : delivery by laparotomy, possibly with a delay to reduce complication rates
2. with a live fetus before 24 weeks : delivery by laparotomy
3. with a live fetus after 24 weeks
   - consider a conservative approach after careful counseling possibly undertaken as in-patient.
   - consider laparotomy and delivery if oligohydramnios and/or compressional deformites
4. Laparotomy and delivery :
   - ideally performed jointly with general / vascular surgeon
   - several units of blood available
   - mid-line vertical incision in abdomen
   - incision of sac away from placenta
   - avoid placental manipulation during delivery
   - if blood supply to placenta can be secured, remove placenta completely
   - if blood supply to placenta cannot be secured, ligate cord only [greater post operative morbidity]

CONCLUSIONS

Abdominal pregnancy is rare which is life threatening and interesting conditions. Clinical presentation, physical examination and laboratory findings are non-specific causing pre-operative diagnosis is rarely made. Suggestive

diagnostic abdominal pregnancy are abdominal tenderness, closed uneffaced cervix and palpation of a pelvic mass distinct from the uterus. The initial clinical manifestations are often like that of an ectopic pregnancy. The commonest sign elicted in most series was abdominal tenderness.[16-18] The main complication is sudden haemorrhage which can occur at anytime.

This case report shows a case of abdominal pregnancy at hepatoduodenal ligament which developed clinical GI symptom for 3 weeks. She was not suspected to have ectopic pregnancy, but diagnosis of abdominal pregnancy was made by chance by radiologist from transabdominal ultrasound. Transabdominal ultrasound was successfully used to make the diagnosis preoperatively.

This paper also shows the important role and usefullness of ultrasound in acute abdomen both gynecological and surgical condition. In ectopic pregnancy or abdominal pregnancy, the ultrasound can be of help in the diagnosis of viable or non-viable fetus and complication such as ruptured ectopic pregnancy from intra-abdominal hemorrhage. Nowaday, Ultrasound is widespread in community hospital and provincial hospital which is non-expensive, portable and no radiation risk. Ultrasound training in the diagnosis of acute abdominal condition is recommended.

REFERENCE

1. Pisarska M.D. , Carson S.A. ecopic pregnancy. Scott J.R. Disia P.J, Hammond C.B. Spellacy W.N. et al editor : Danforth's obstetris & Gynecology, 8th editor: Lippincott Williams & Wilkins 1999(11): 157-8
2. Mahomed k, Abdominal pregnancy in Abdominal pain in pregnancy, James D.K., Stee PJ, Weiner CP, Gomik B et al editor : High risk pregnancy 2nd editor : W.B. SAUNDER 1999(55):996-8
3. Bonfante-Ramirez-E; Bolanos-Anconc-R; Simon-Pexeyra-L; Juarez-Garcia-L; Garcia -Benitez-CQ, Abdominal Pregnancy, Institutional Experience, Ginecol-obstet-Mex. 1998 Jul ; 66 : 287-9
4. Cordero-DR; Adro-A; Yasin-S; O'sullivan –MJ, Intraligamentary pregnancy; obstet-Gynicol-Surv. 1994Mar; 49(3):206-9
5. Fisch-B; Peled-Y; Kaplan-B Zehavi-S; Neri-A; Abdominal pregnancy following in vitro fertilization in a patient with previous bilateral salphingectomy : Obstet-Gynecol. 1996 oct;88(4pt2):642-3
6. Agizza-S; Miranda-L; Grassia-M, Abdominal pregnancy, clinical case in surgical emergency; Minerva-Ginecal. 1998 Apr; 50 (4):157-160
7. Paternoster-DM; Santarosso-C; Primary Abdominal pregnancy A case report; Minerva-Ginecal. 1999 Jun; 51(6):251-3
8. Fishman DA, et al; Ectopic pregnancy causing Hemothorax Managed by thoracoscopy and Actinomycin D; obstet Gyneal. 1998 May, 91(spt2):837-8
9. Saravanam C, et al; Rectal bleeding: a rare complication of abdominal pregnancy; Aust N.8 J. obstet Gynecol. 1997 Feb; 37 (1):124-5
10. Salines A, et al; abdominal pregnancy causing massive lower gastrointestinal bleeding, case report: Mt. Savai J Med 1985 May, 52(5):371-4
11. Frayer-CA; Hibbert-Ml; Abdominal pregnancy in a 67-year-old woman undetected for 37 years. A case report: J-Report-Med. 1999 Jul;44(7):633-5
12. Leshchevko-AP; Sapline-OI; Timoshenko-LD; Leehko-VL, Abdominal pregnancy with implantation of the ovum in the liver, vestn-Khir-Im-I-I-grek. 1994 Jan-Feb; 152 (1-2):47-8
13. Borlum KG, Blom R. Primary hepatic pregnancy. Int J Gynaecol obstet 1988 Dec; 27(3) ; 427-9.

14. Barbosa Junior A de A, de Freitas LA, Mota MA. Primary pregnancy in liver. A case report. Pathol Res Pract 1991 Mar ; 187(2-3) : 329-31 ; discussion 332-3.

15. Ben-Rafael Z, Dekel A, Lerner A, Orvieto R, Halperm M,Powsner E, et al. Laparoscopic removal of an abdominal pregnancy adherent to the appendix after ovulation induction with human menopausal gona dotrophin. Hum Reprod 1995 Jul ; 10(7) : 1804-5.

16. Stojak-I; Ulasick-P; Undiagnosed Abdominal pregnancy resulting in fetal death and surgical removal of the fetus; Ginecol-Pol. 1996 Aug ; 67(8) : 419-80

17. Zahi-ZM; An unusual presentation of Ectopic pregnancy; Ultrasound-obstet-Gynecol. 1998 Jun ; 11(6) :456-8

18. Rani-PR; Pandiasajan-T; Raghavan-ss; Rajasam-P, secondary abdominal pregnancy; Asia-Oceania-J-obstet-Gynecol. 1994 Jun ; 20(2) : 161-3

PEDIATRIC RADIOLOGY WEB PAGES

Pannee VISRUTARATNA, MD

ABSTRACT

Nowadays information technology is a vital part of everyone's daily life; it is also becoming an increasingly vital part of the daily practice of radiologists. The Pediatric Radiology Web Pages went online at the Faculty of Medicine, Chiang Mai University in December 1998. Their purpose has been to help medical students and radiology residents learn more by themselves about the fascinating field of pediatric radiology. These web pages have 3 sections: Pediatric Abdomen, PED-RAD Review, and Publications. The first section is about common abnormalities of the pediatric abdomen such as duodenal atresia, necrotizing enterocolitis, and intussusception. In the second section there are interesting cases and a list of topics in pediatric radiology. The third section has abstracts of articles about various research topics; all this research was done at the Department of Radiology, Faculty of Medicine, Chiang Mai University. For more details visit the web pages at <http://www.medicine.cmu.ac.th/dept/radiology/pedrad/pedrad.htm>.

BACKGROUND

Teaching files are important in teaching and studying radiology; however there are many problems with film-based files such as limited access, high cost of reproduction, ease with which they are lost or damaged, and difficulty when searching through the file.[1] We tried to eliminate these problems by the use of information technology, which has become a vital part of everyone's daily life and the daily practice of radiologists. We started to create our Pediatric Radiology Web Pages in December 1998. The purpose of these web pages has been to help medical students and radiology residents learn more by themselves about the fascinating field of pediatric radiology.

METHODS

Our Pediatric Radiology Web Pages were done on an IBM-compatible personal computer, which was used to both acquire images and create text files. Each web page was created in HyperText Markup Language (HTML) format with Netscape Composer versions 4.5-4.6 (Netscape Communications, Mountain View, CA). Images were entered into the computer with either a 35-mm slide scanner or a digital camera. Once the images were in the computer, they were cropped and labeled using Adobe Photoshop version 5.0 (Adobe Systems, Cupertino, CA). The images, which ranged from 5.2 to 63.2 kilobytes, were saved in Joint Photographic Experts Group (JPEG) format or Graphics Interchange Format (GIF). For one particular image GIF Animator (Microsoft, Redmond, WA) was used to create a cine MRI, which was 130 kilobytes, to show aortic regurgitation in a patient with Marfan syndrome.

The completed HTML files and the corresponding image files were transferred over a local area network from our computer to our

Department of Radiology, Faculty of Medicine, Chiang Mai University Chiang Mai 50200, Thailand

Faculty's World-Wide-Web server for storage. Our web pages can be found at <http://www.medicine.cmu.ac.th/dept/radiology/pedrad/pedrad.htm>. At present we have 120 pages and 138 images, including radiographs, ultrasonograms, computed tomographic scans, and magnetic resonance images.

DESCRIPTION OF THE WEB PAGES

The web pages (Fig. 1) are divided into 3 sections: Pediatric Abdomen, PED-RAD Review, and Publications. The first section, Pediatric Abdomen, is about common abnormalities of the pediatric abdomen such as duodenal atresia (Fig. 2), necrotizing enterocolitis, and intussusception. The objective of this section is to get medical students to review these abnormalities by themselves. There are short explanations of each abnormality with illustrative images.

In the second section, PED-RAD Review, there are interesting cases and a list of topics in pediatric radiology. Each case has a short clinical history, one or several pertinent "unknown" images, a discussion of the pertinent findings with appropriately labeled images, a short discussion of the diseases, and references (Fig. 3). Some cases also have images of other patients with the same disease. For each topic, there are a short discussion of the disease, a short discussion of the imaging findings, and relevant images (Fig. 4).

The third section has abstracts of articles about various research topics (Fig. 5); all this research was done at the Department of Radiology, Faculty of Medicine, Chiang Mai University.

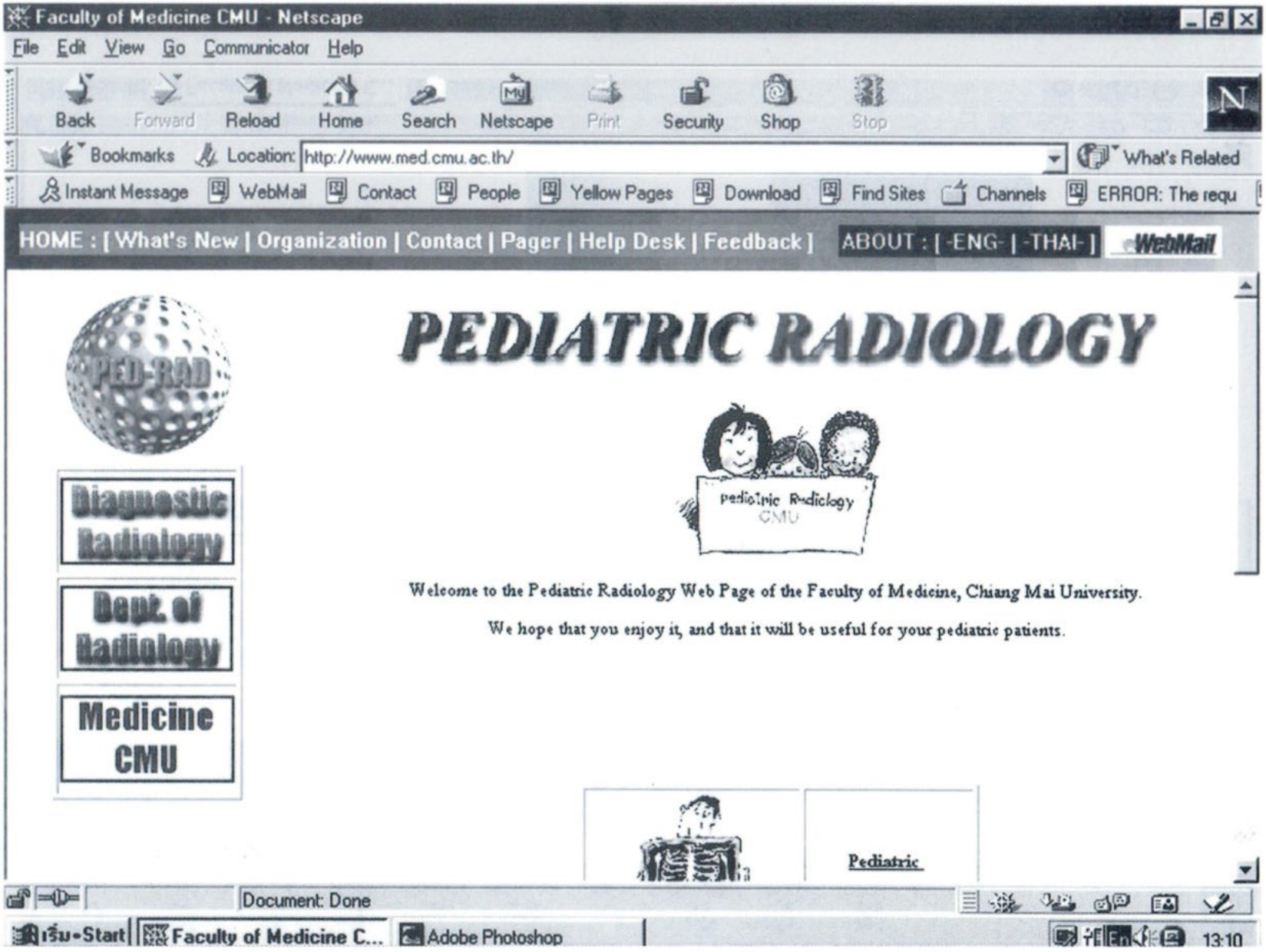

Fig. 1. The first page of our Pediatric Radiology Web Pages.

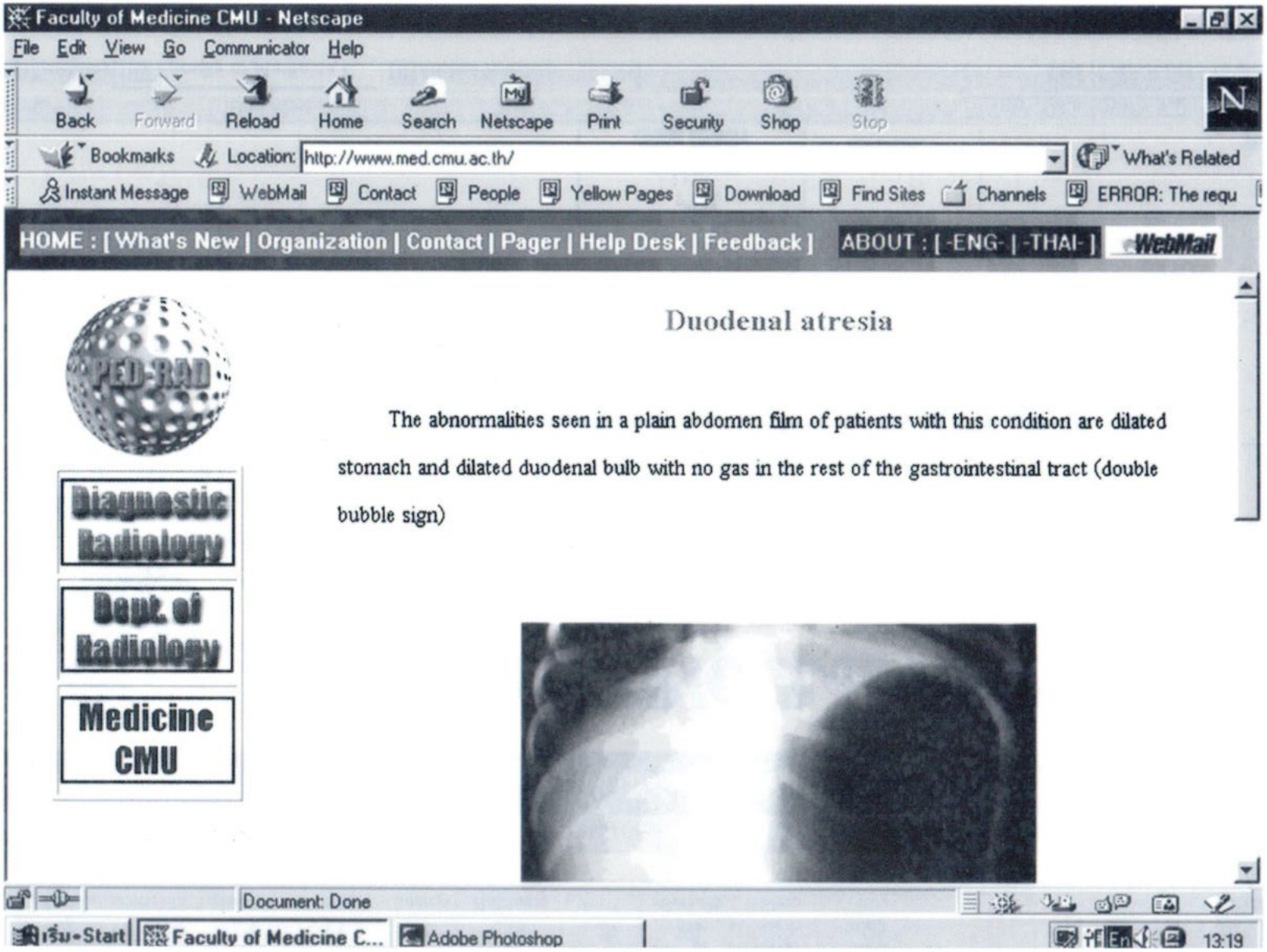

Fig. 2. A sample page from Pediatric Abdomen.

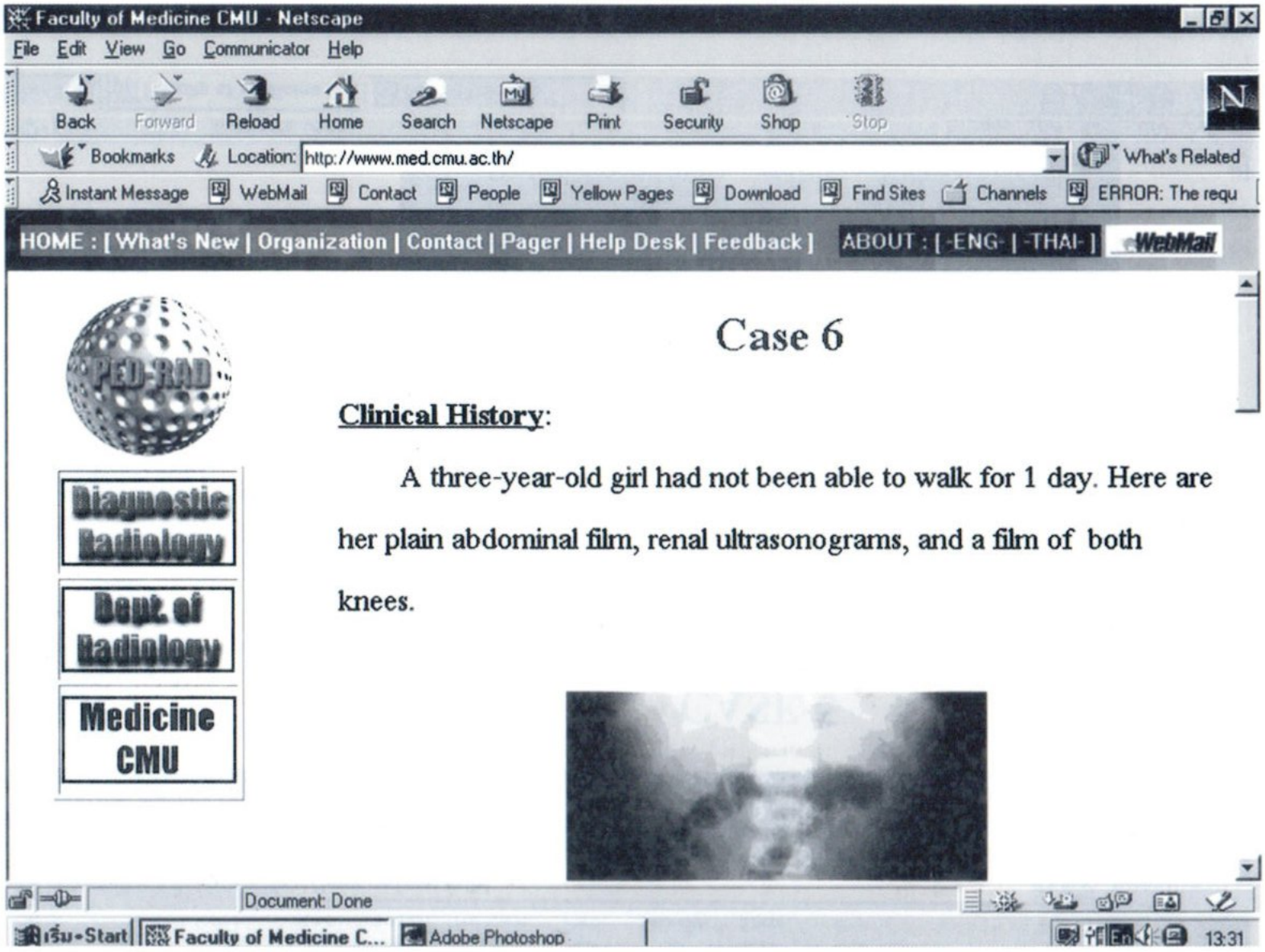

Fig. 3 Case 6 from Interesting Cases.

Fig. 3A Short clinical history and pertinent unknown image.

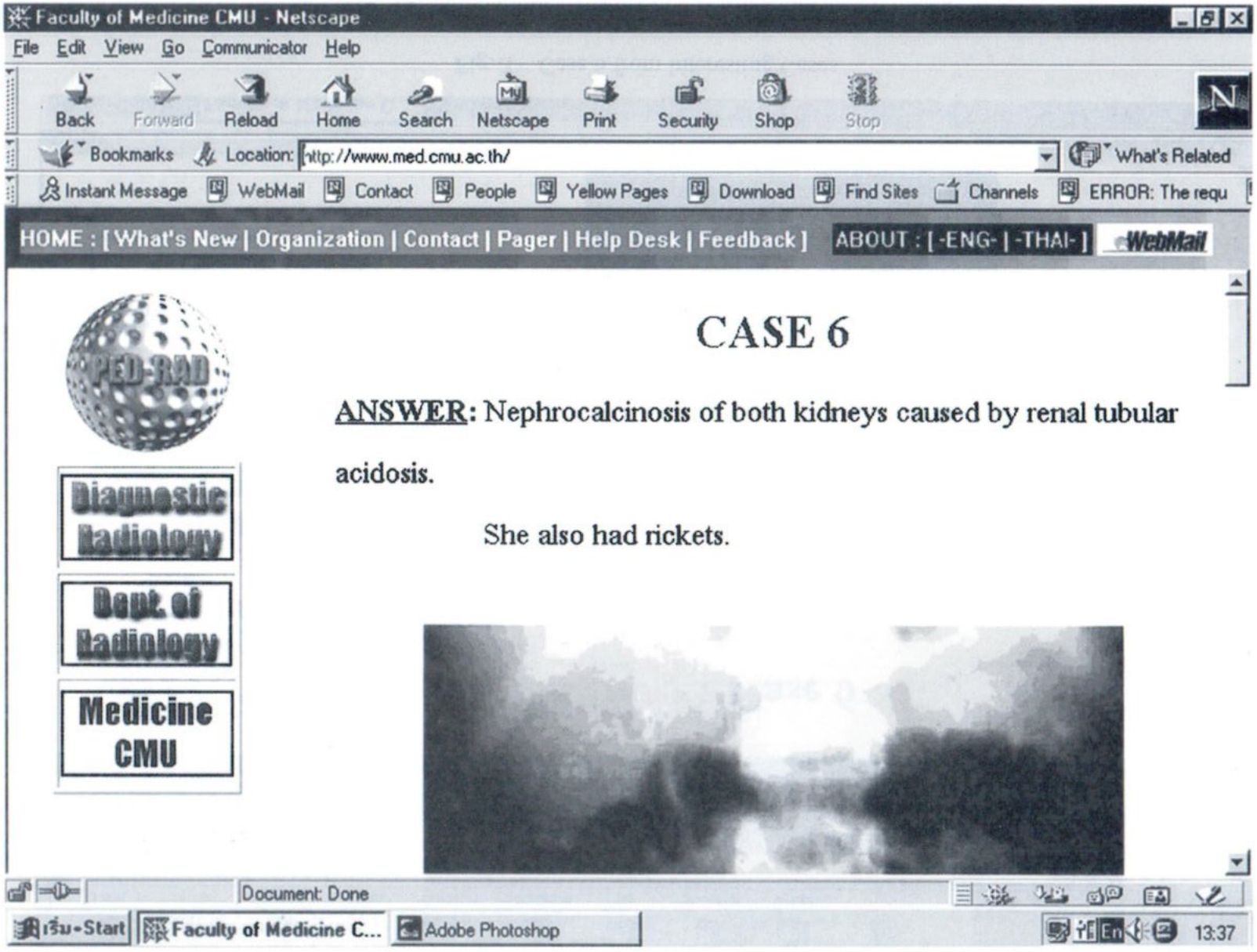

Fig. 3B Answer.

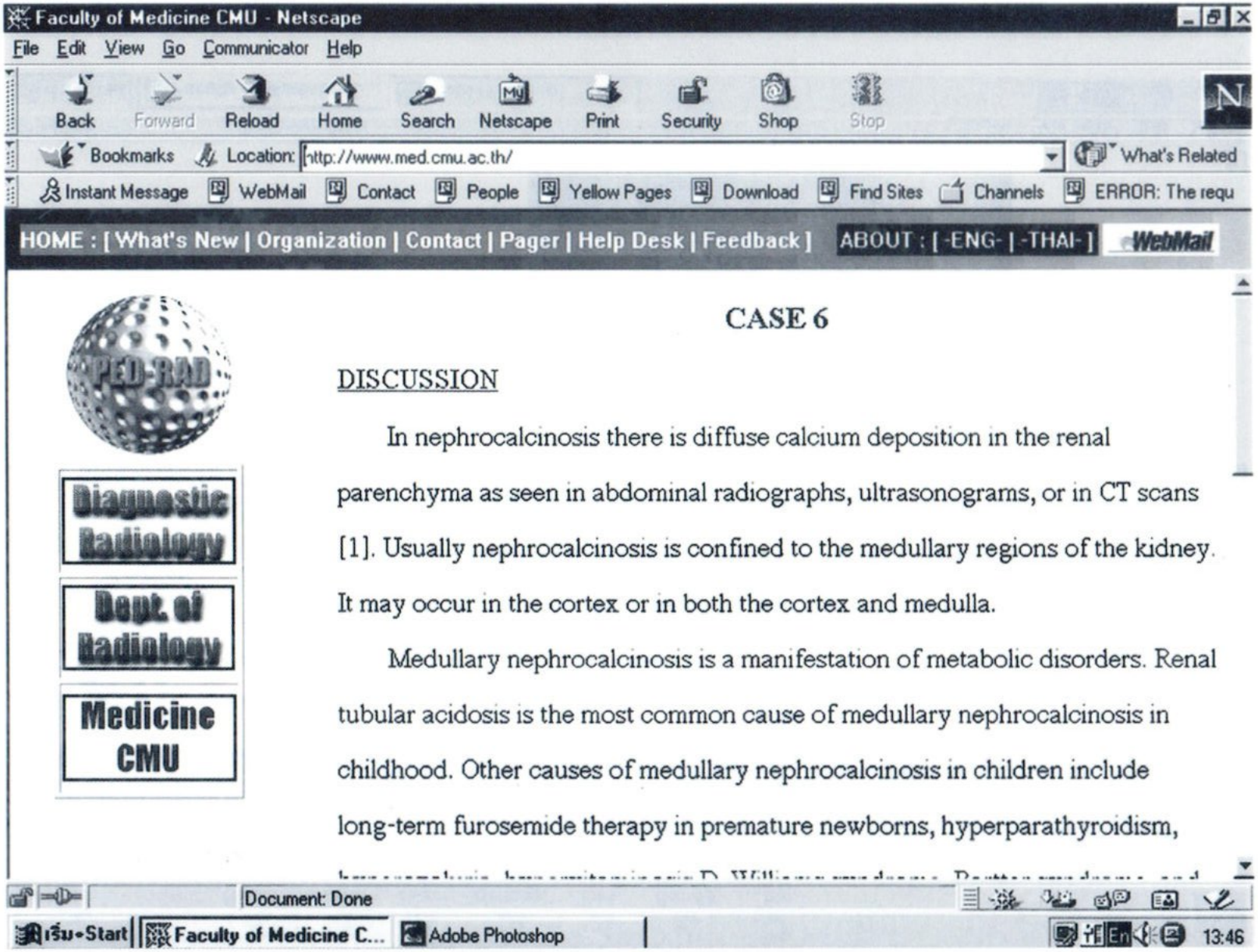

Fig. 3C Short discussion of the disease .

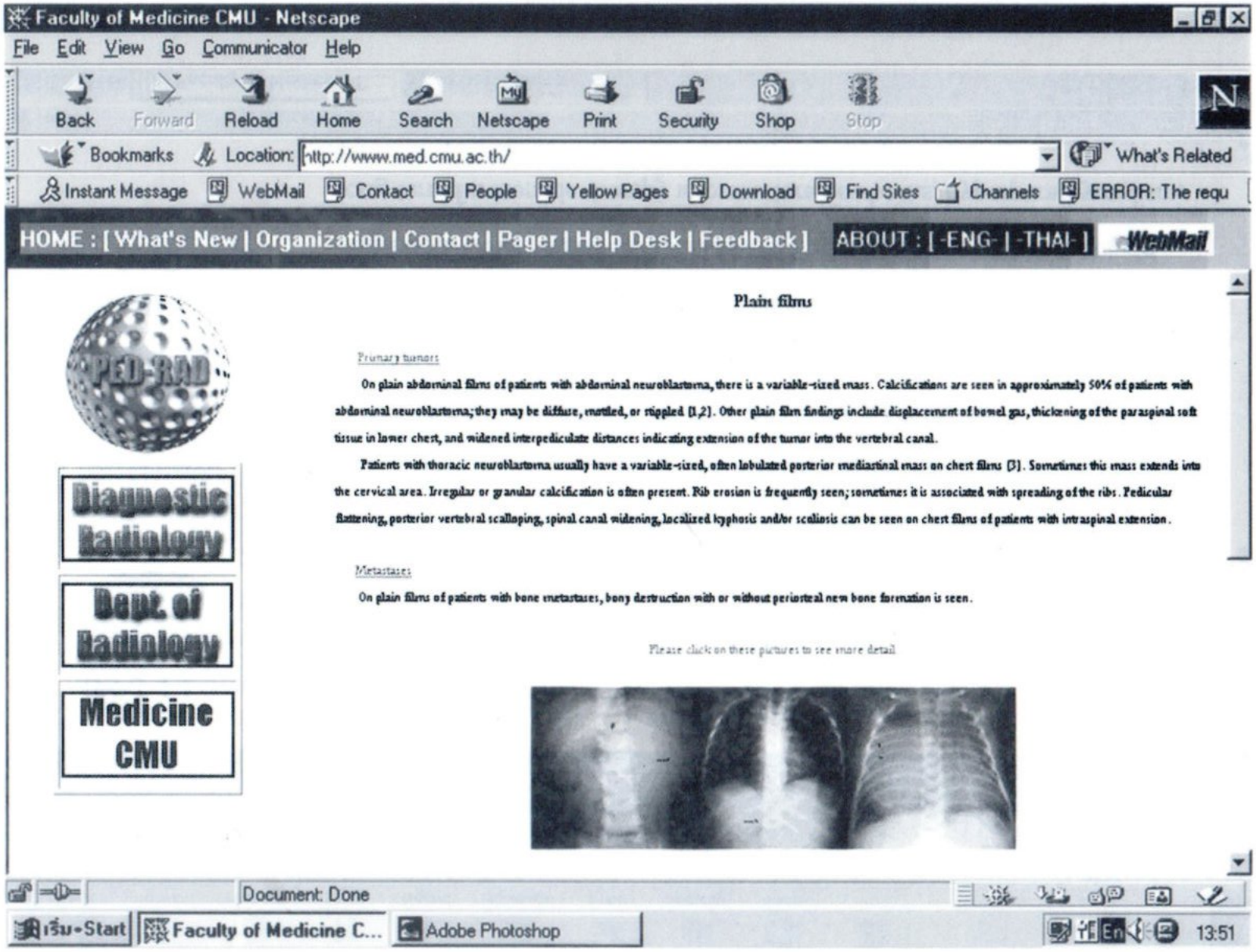

Fig. 4. A sample page from Interesting Topics.

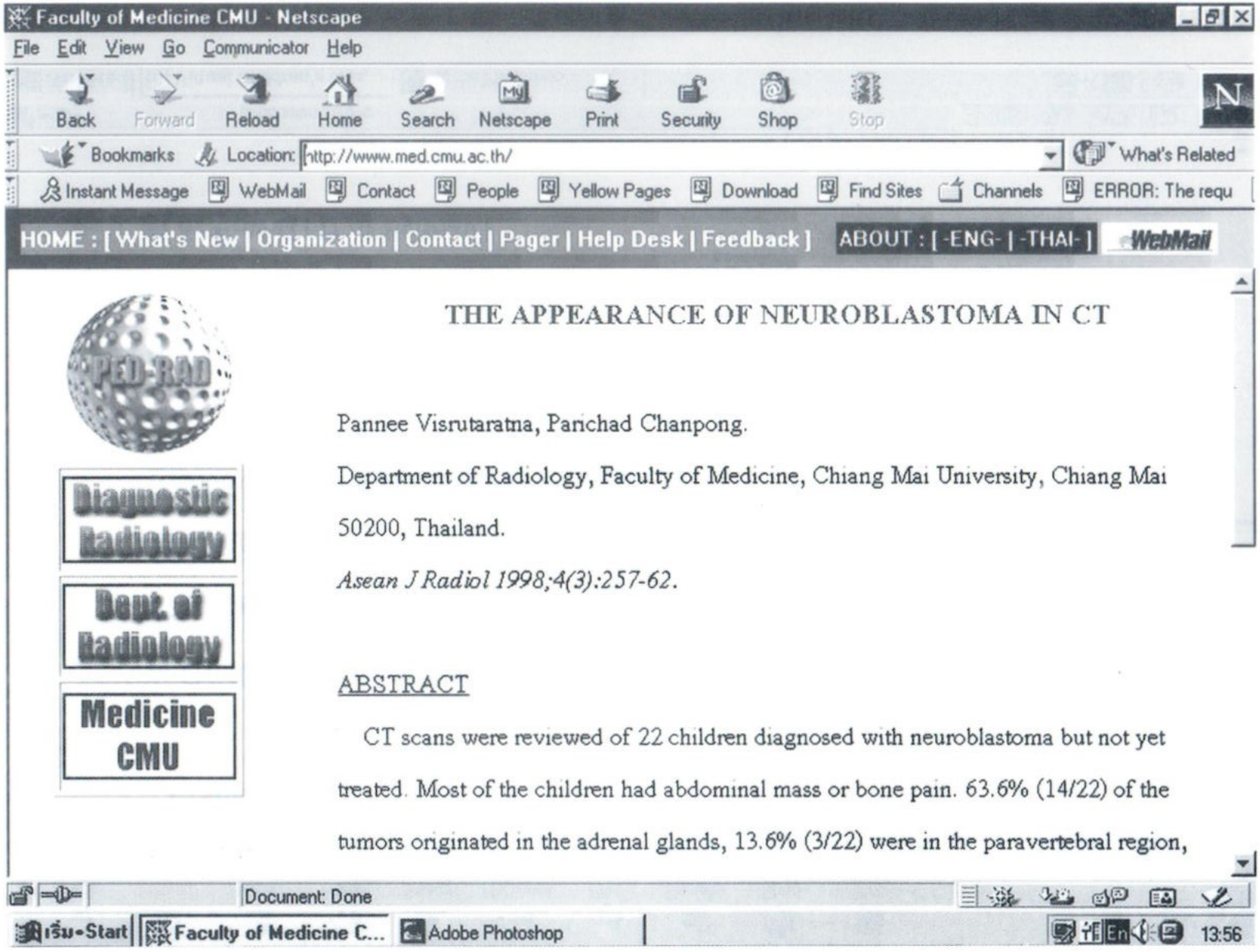

Fig. 5. A sample page from Publications.

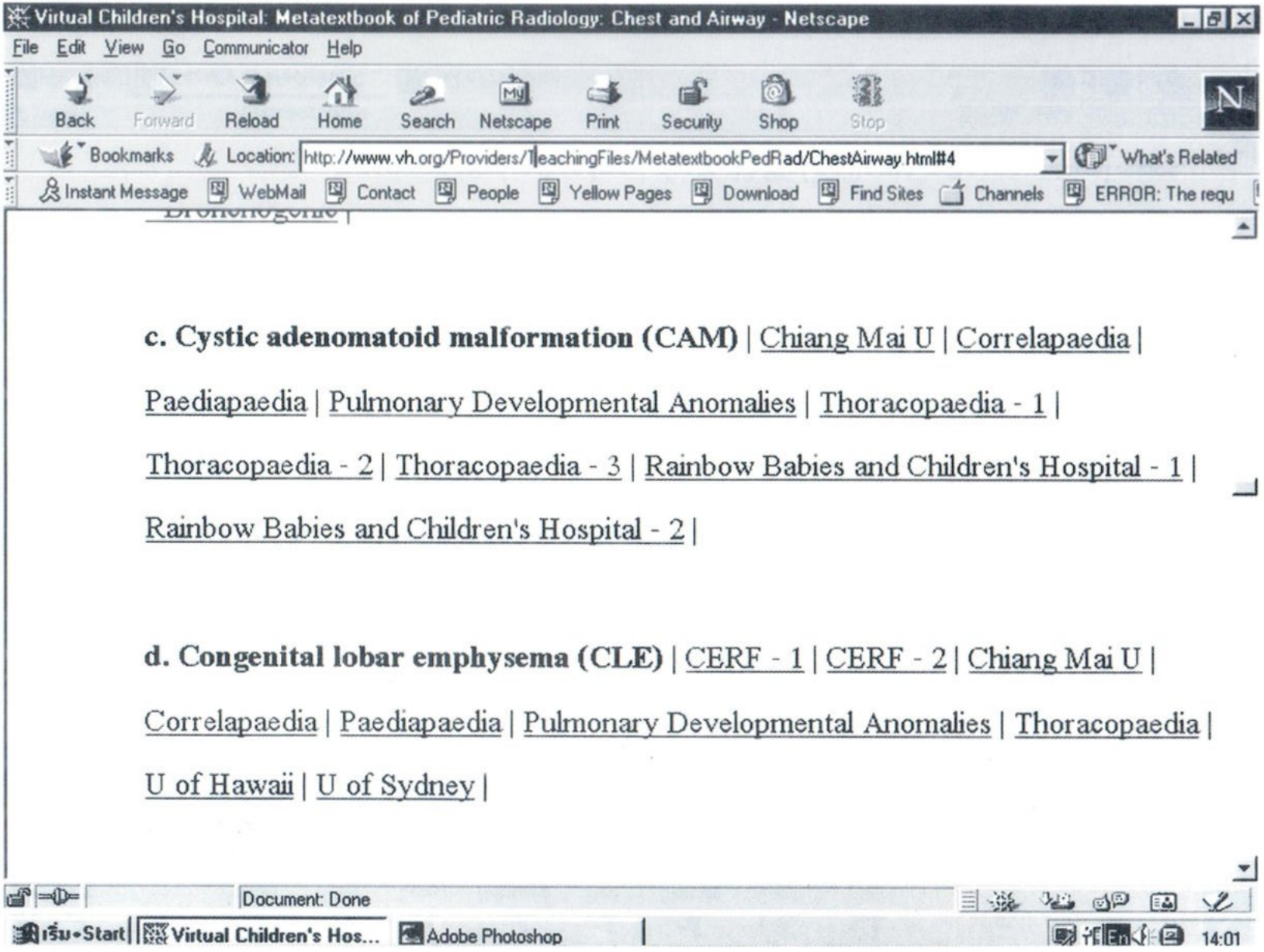

Fig. 6. A page from the PediatricRadiology.com web site with links to our web pages.

RESULTS

It was found that placing our web pages on the Internet has simplified distribution of teaching files to all parts of our hospital. Our medical students and residents can bring up our web pages using computers in our department, the hospital's computer laboratory, or common study rooms in their dormitories anytime they would like to. When there are questions about imaging findings or imaging techniques at meetings or when seeing patients, images from our web pages can be brought up immediately instead of having to search through the file of teaching films or textbooks for them.

DISCUSSION

For radiologists, images are the basic source of information. When making a diagnosis, radiologists frequently access image collections for reference. The most commonly used sources of radiologic reference images are textbooks and teaching files. Computer-based references such as electronic textbooks and teaching files on Intranets or the Internet are other sources of images.[2,3]

Nowadays WYSIWYG (what-you-see-is –what-you-get) editor software helps to produce documents in HTML easily.[4] The HTML format allows the combining of text, images, sound, movie files and other files into a single document. It also allows persons with little computer experience to navigate through the Internet, read text files, view images (stills and movies), and download files by merely pointing with the mouse and clicking on items of interest.[5] This has allowed us to maintain a teaching file that is physically small and easy for residents and students at our university and radiologists elsewhere to access. Our web pages were accepted by the web site PedaitricRadiology.com on March 4, 2000 and have been incorporated into the list of imaging appearances of common pediatric diseases there (Fig. 6).

We plan to add more cases to our web pages and to provide on-line continuing medical education courses for radiologists in Thailand.

REFERENCES

1. Galvin JR, D'Alessandro MP, Kurihara Y, Erkonen WE, Knutson TA, Lacey DL. Distributing an electronic thoracic imaging teaching file using the Internet, Mosaic and personal computers. AJR 1995;164:475-8.
2. Macura KJ, Macura RT, Morstad BD. Digital case library: a resource for teaching, learning, and diagnosis support in Radiology. RadioGraphics 1995;15:155-64.
3. Jaffe CC, Lynch PJ. Computer-aided instruction in radiology: opportunities for more effective learning. AJR 1995;164: 463-7.
4. Richardson ML, Norris TE. On-line delivery of continuing medical education over the World-Wide Web: an on-line needs assessment. AJR 1997;168:1161-4.
5. Richardson ML. A World-Wide Web radiology teaching file server on the Internet. AJR 1995;164:479-83.

UNUSUAL CLINICAL AND IMAGING FINDINGS IN PANCREATIC PSEUDOCYSTS

Somrak LOWANITCHAI, MD.

ABSTRACT

Four cases of pancreatitis, with the presence of pancreatic pseudocysts were presented. All were clinically not indicative to be pancreatitis. They came to the hospital with a chief complaint of epigastric pain, left flank mass, enlarge scrotum, and massive bilateral pleural effusion. Sonography and Computed Tomography were performed and revealed pancreatic pseudocysts at the superior recess of omental bursa, subcapsular region of left kidney, in splenic hilum and at area posterior to left lobe of liver anterior to the stomach, which suggested to be in the hepatogastric ligament. Careful observation of the image findings in these cases will be helpful to make a differential diagnosis from other diseases.

INTRODUCTION

Pseudocyst is a fluid collection composing of necrotic material, proteinaceous debris, and enzymatic material that is confined by a fibrous capsule. They vary greatly in size, and are round or oval in shape which develop late, usually after repeated episodes of pancreatitis. At the time of diagnosis,most other signs of acute pancreatitis have already subsided. The incidence of pseudocysts following acute pancreatitis is 2% -4%, and in chronic pancreatitis is 10–15%.[13] Their clinical significance are related to their size and to dangerous complications, such as rupture, bleeding, or abscess formation. In patients with history of heavy alcoholic intake, pseudocyst are often detected in asymtomatic individuals. Spontaneous resolution of pseudocysts can occur simply from resorption of fluid or drainage into a loop of bowel. Internally drainage of pseudocysts may occur if it is greater than 5 cm in size.[4] With modern imaging procedures, the unusual sites of pancreatic pseudocysts seem to be increasing. Followed were 4 patients being sent for sonography and Computed Tomography without clinical symptoms suggesting to be pancreatitis. They presented with mid epigastric pain, left flank mass, enlarge scrotum and bilateral pleural effusion. The first two cases turned out to be pseudocysts at the superior recess of omental bursa, subcapsular pseudocyst of left kidney, and the last two cases, findings were fluid in scrotum from pancreatic ascites, and bilateral pleural effusion from pancreatitis. The sonographic and Computed Tomographic imaging features are described and the possiblitics how the pancreatic secretion entered into these organs are discussed.

CASE ONE

A 45-year-old man presented with a chief complaint of abdominal pain and discomfort at the epigastrium 10 hours before admission and intensified 2 hours before his coming to the hospital. Physical examination showed tenderness at the epigastrium and RUQ of abdomen. Plain abdomen showed only small bowel ileus. Sonographic study revealed low echoic to anechoic

Department of Radiology, Sapprasitthiprasong Hospital, Mueng, Ubonratchathani, 34000 THAILAND.

mass near or at the caudate lobe of liver, size 1.6 cm. (fig. 1). 2 days later, sonography was done due to clinically increasing in abdominal pain. This time, the mass suspected to be in the caudate lobe showed moderately increasing in size to be about 5.0x4.5cm^2 (fig. 2). Other findings in this study were a moderate amount of ascites and bilateral pleural effusion. The pancreas looked normal in size and echogenicity. Computed Tomography at 8th day of admission revealed fluid attenuation mass size 5.0 cm. at the superior recess of omental bursa (fig. 3.) with minimal fluid along the porta hepatis (fig. 4). Mild dilated pancreatic duct and small pseudocyst at the pancreatic body (Fig. 5). Final diagnosis was pancreatic pseudocyst at the superior recess of omental bursa and small amount of fluid tracking along the porta hepatis.

Conservative treatment was done. The followed up sonography every 1 month showed some decreasing in size of the pseudocyst at the superior recess of omental bursa, and finally after 4 months, it showed to have a complete resolution of the pseudocyst.

CASE TWO.

A 32-year-old man was admitted to the hospital from a motorcycle accident. He was in the trauma ward for observation of any abnormal neurological sign. 6th day after admission, he complained to have left side abdominal pain. Physical examination revealed a palpable mass at the left flank and an initial clinical diagnosis was perinephric hematoma. Sonographic study showed a 10 cm. encapsulated fluid collection compressing the upper pole of left kidney. Some internal echo fluid contents were evidence. (fig. 6). Other findings were thickening of the mesentery at the upper abdomen, and only part of pancreatic head was visualized which appeared to have mild prominent duct.

Sonography diagnosis was subcapsular pseudocyst of left kidney VS renal abscess with rupture outside the renal capsule. Computed Tomography showed thin and some part thick wall cystic mass at upper pole of left kidney compressing normal renal parenchyma (fig. 7). Computed Tomography well demonstrated this cystic mass extending from the pancreatic tail (fig. 8) which now can be well seen in detail. There was a mild dilatation of the pancreatic duct with others small cystic masses, size 1-2 cm. at the left psoas muscle and root of mesentery which were also evidence (fig. 9). The diagnosis was subcapsular pancreatic pseudocyst of left kidney with small pseudocysts at the mesentery, and left psoas muscle. Cystogastrostomy was done, and the fluid revealed to have elevated amylase level. The patient eventually recovered after a long post operative course.

4 months later,there is a complication by having an extrapancreatic fluid collection at the left lobe of liver (fig. 10).

CASE THREE

A 32-year-old man with a history of a progressive swelling of the right scrotum about 2 weeks ago was referred for sonography of the scrotum without any other clinical detail. Tentative clinical diagnosis was hydrocele of the right scrotum, and tumour of testis was to be excluded. Scrotal sonography revealed a bilateral hydroceles with a moderate amount of fluid in the rightside and a small amount of fluid in the left side with a normal testis in both sides. (fig. 11). Additional sonography of the abdomen showed focal bulging contour of pancreatic head, size about 3.7cm. This could be focal pancreatitis, or pancreatic head mass (fig. 12), with mild prominent of pancreatic duct and a moderate amount of ascites was seen. Sonography diagnosis was focal pancreatitis or CA head of pancreas. Computed Tomography 3 day after that revealed a focal enlargement of pancreatic head (fig. 13), small pseudocysts at the splenic hilum, mesentery (fig. 14,15) and a small amount of fluid at the left

anterior pararenal space. Computed Tomography diagnosis was focal chronic pancreatitis with small pseudocysts. Follow up sonography 2 months later, the pancreatic head was reduced in size to 1.5cm., no ascites, and still presence of fluid in the scrotal sac, however, decreasing in amount.

CASE FOUR

A-28 -year-old man with a history of dyspnea for 3 months, without fever. Chest film showed right pleural effusion. Thoracocentesis revealed dark reddish color fluid, cell 1500 mm^3 ; PMN 31 % ; LYM 69 % ; Protein 1596 mg %, Sugar 63 mg % (Bs 52 mg %) ; Gram stain and AFB were negative. Pleural biopsy showed chronic pleuritis with abortive granuloma, no definite fungus. At this time anti TB drug was given. 1 month later his symptom was not improve. Chest film still presence of massive right pleural effusion. Intercostal drainage was done. Pleural fluid showed brownish color fluid, Celll 1500 mm3 ; PMN 42% ; LYM 54 % ; Mono 4% ; Protein 3950 mg %, Sugar 83 mg % (Bs 104 mg%) ; Cytology ; bloody with normal mesothelial cell and macrophage, negative for malignancy cell. Pleural biopsy revealed no granuloma, nor malignant cell. He was still treated as TB pleuritis. 2 weeks later he came to the hospital due to progressive dyspnea. Chest film showed bilateral pleural effusion (fig. 16). Sonography of the thorax and abdomen showed bilateral pleural effusion, massive on the left side, anechoic mass size 2 cm. posterior to left lobe of liver. Computed Tomography showed well capsulated fluid collection posterior to left lobe liver anterior to stomach (fig. 17), dilated pancreatic duct (fig. 18).

Sputum AFB for 3 days was negative, pleural fluid showed dark greenish color, cell 310 cm^3, PMN 63 %, LYM 37 37 %, Protein 4120 mg %, Sugar 107 (BS 110), amylase 9710 U/L, Serum amylase 578 U/L (Normal 30-110 U/L)

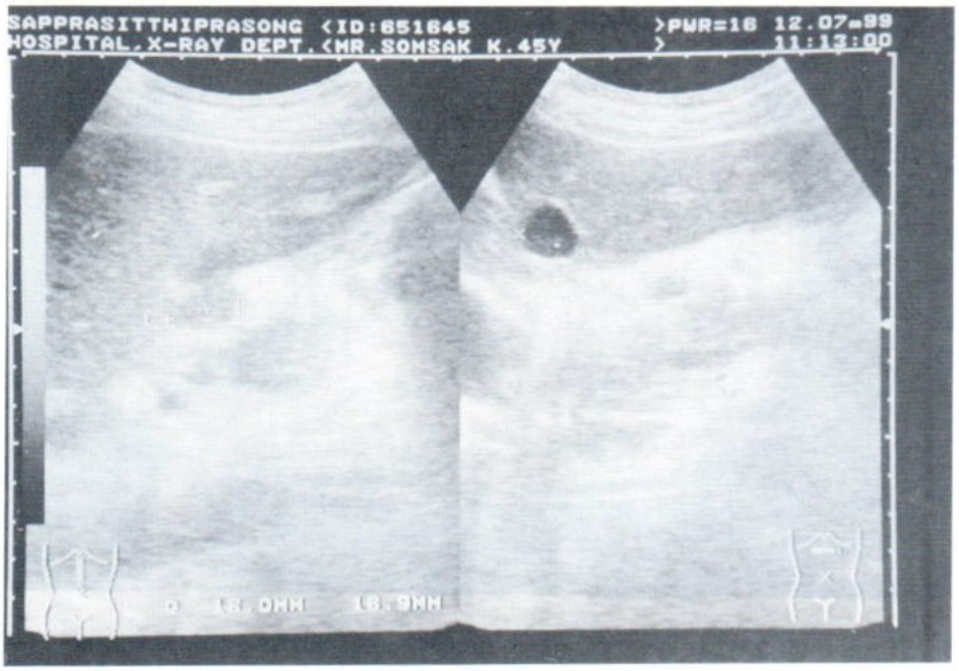

Fig. 1. Low echoic to anechoic mass, well defined border at, or near caudate lobe of liver, adjacent liver parenchyma showing mild low echoic change.

Bs = Blood Sugar

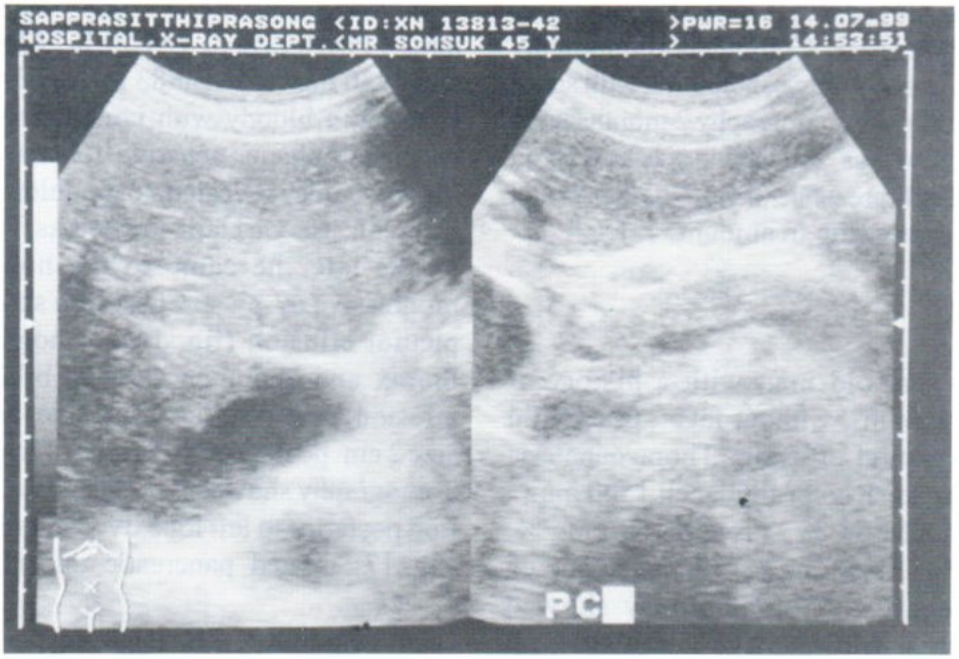

Fig. 2. The low echoic mass was increase in size, pancreas showed normal size and echo, mild prominent pancreatic duct.

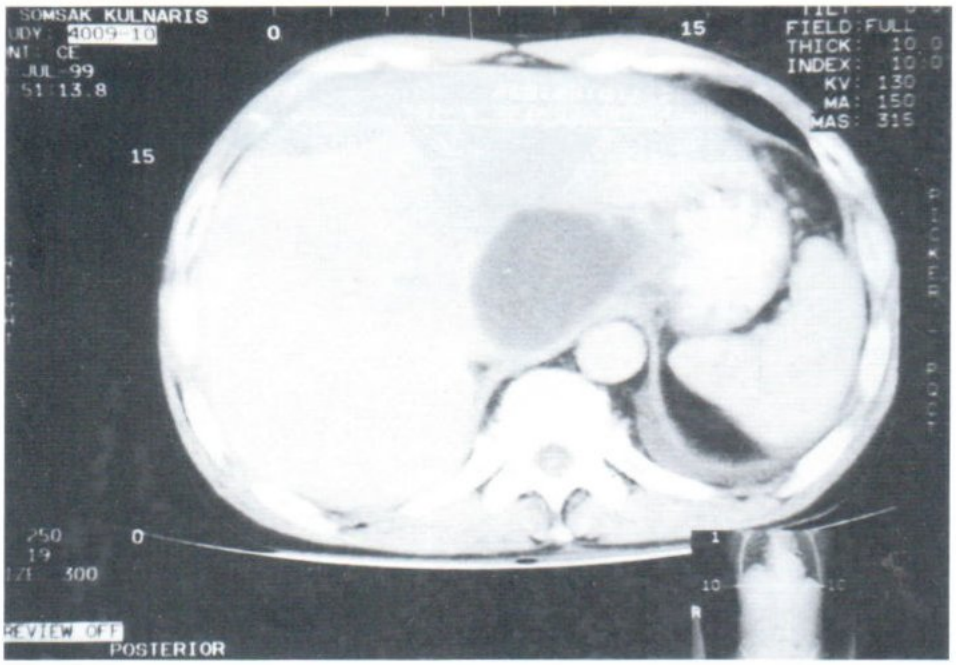

Fig. 3. CT scan with IV contrast enhancement, there is well defined border mass at superior recess of omental bursa.

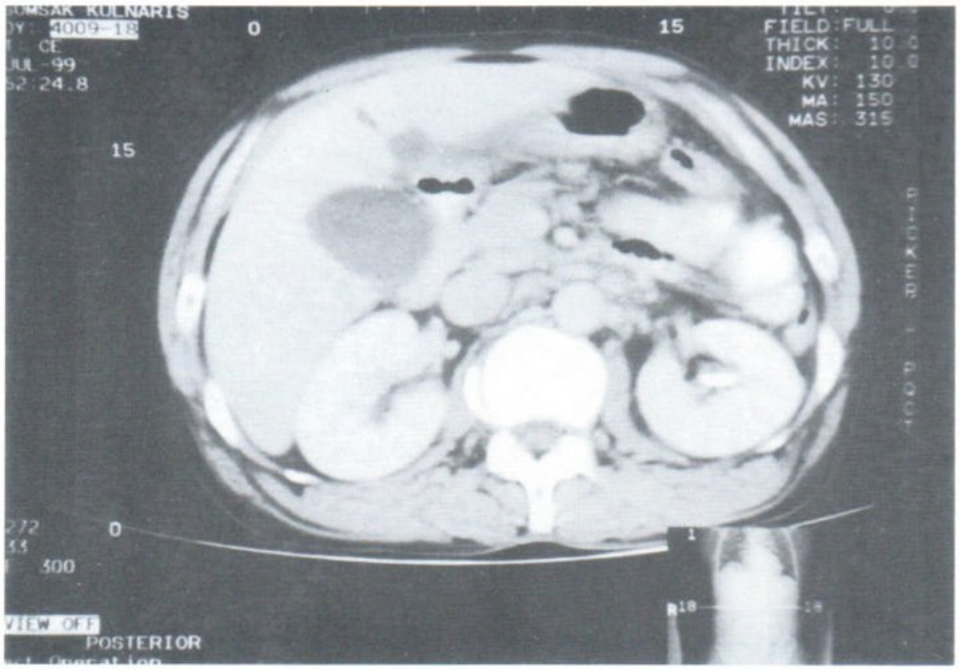

Fig. 4. Inferiorly to slice in fig. 3, also fluid is noted along the porta hepatis and posterior border of left lobe of liver.

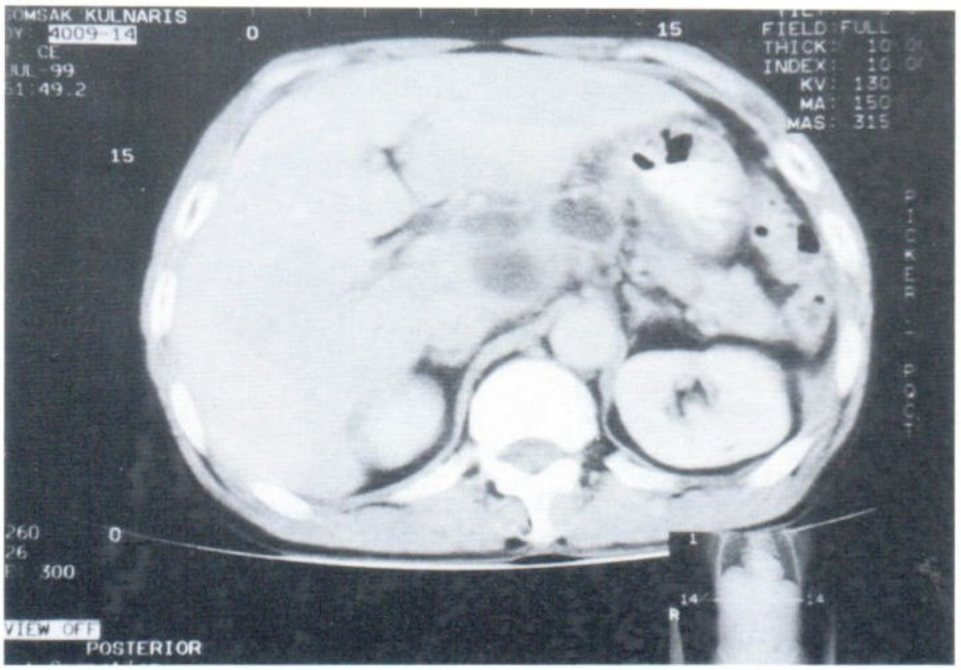

Fig. 5. Small pseudocysts at pancreatic body, the inferior portion of pseudocyst at the superior recess of omental bursa is also seen in this CT slice.

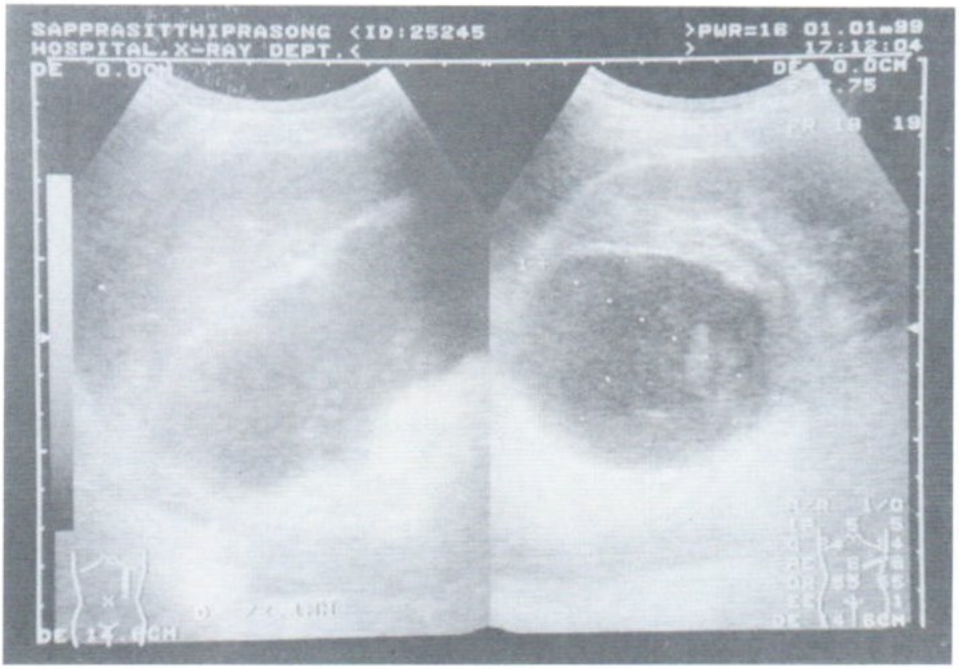

Fig. 6. Encapsulated fluid echoic mass at the upper pole of left kidney.

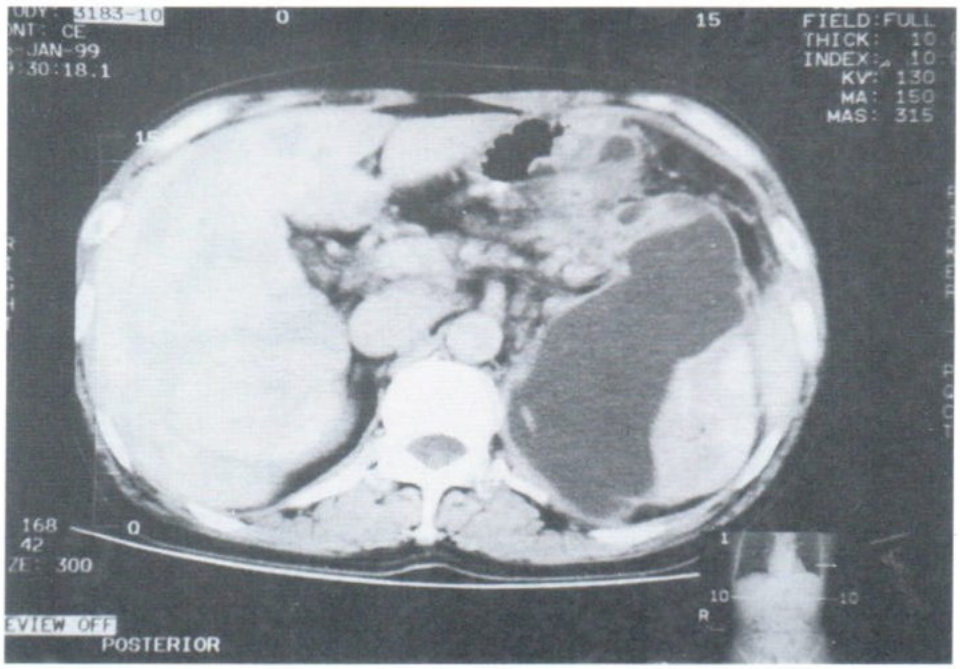

Fig. 7. CT scan showed subcapsular pseudocyst at the upper pole of left kidney.

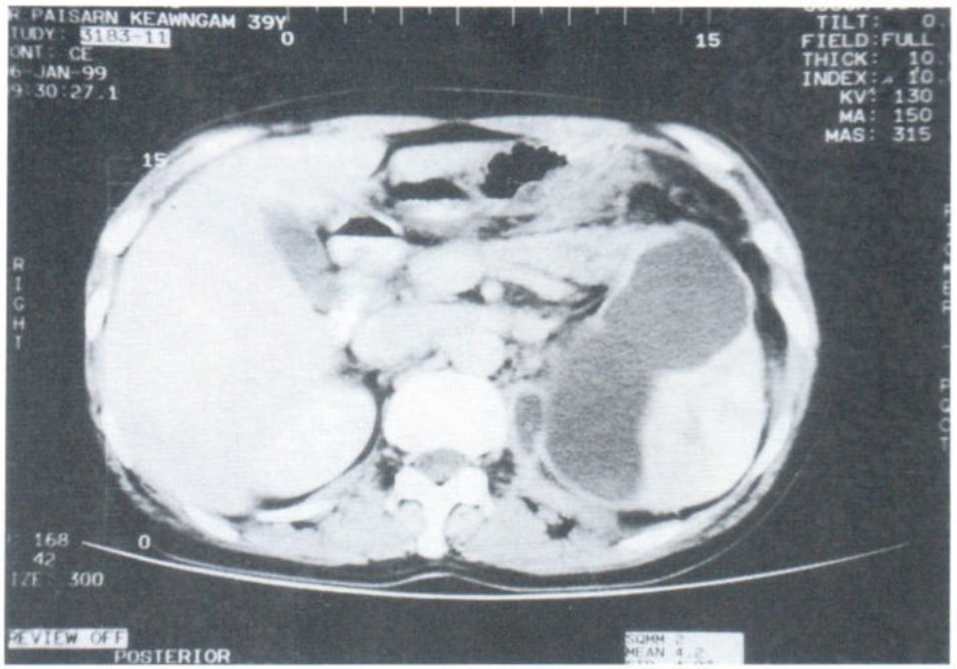

Fig. 8. At pancreatic tail level, there was well demonstrable continuity between subcapsular pseudocyst of left kidney and pancreatic tail.

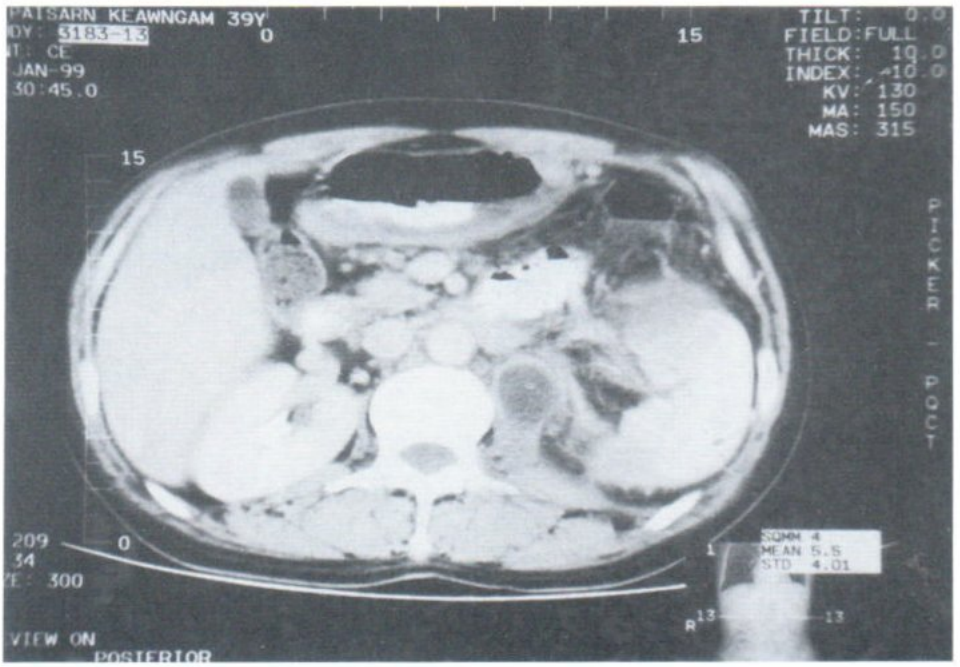

Fig. 9. Small pseudocyst at area of left psoas muscle.

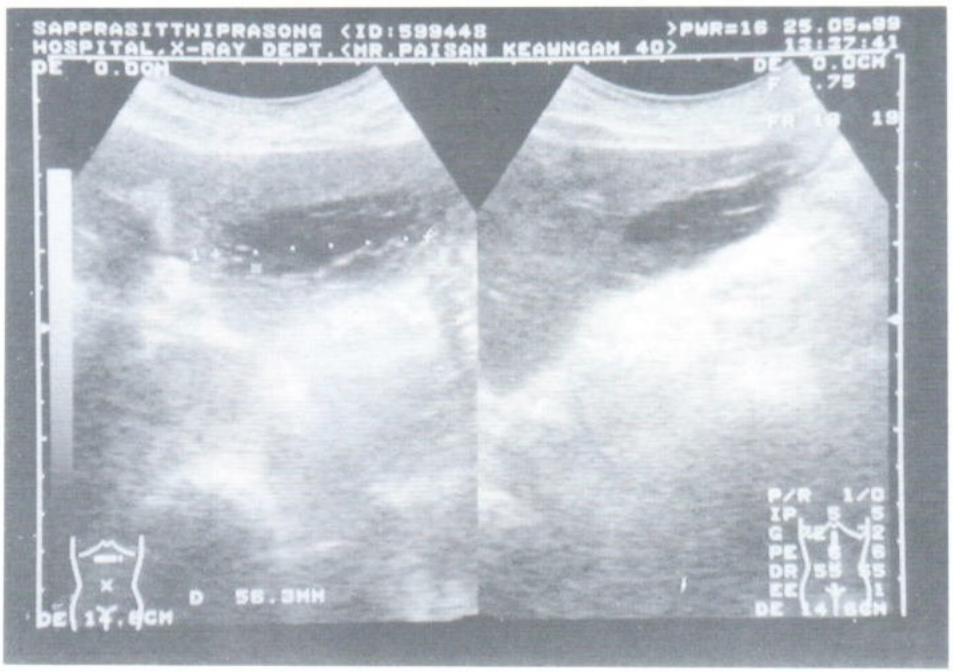

Fig. 10. Extrapancreatic fluid collection at the left lobe of liver.

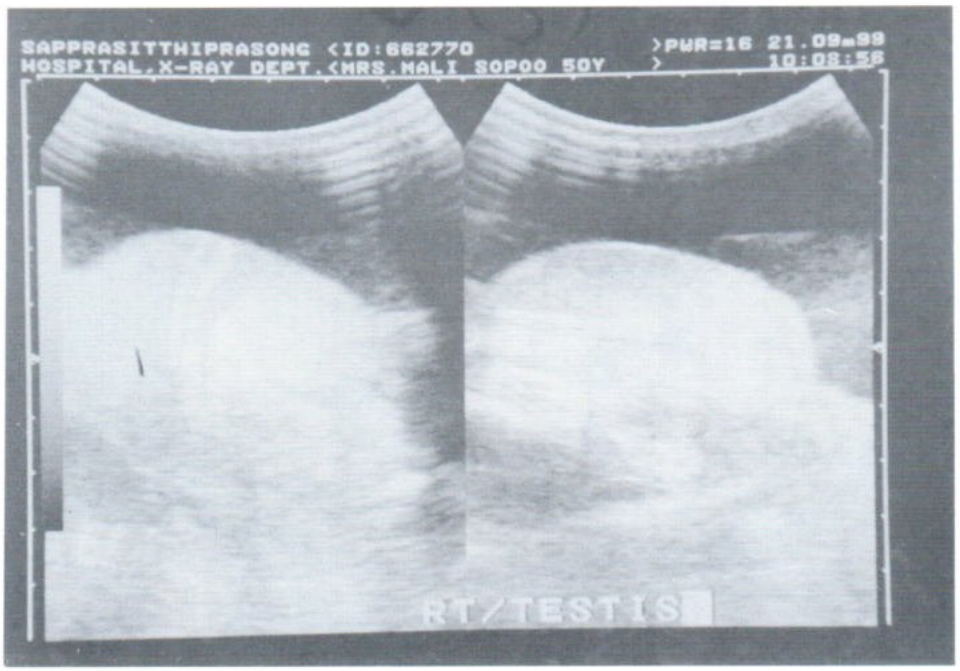

Fig. 11. Hydrocele at right scrotal sac.

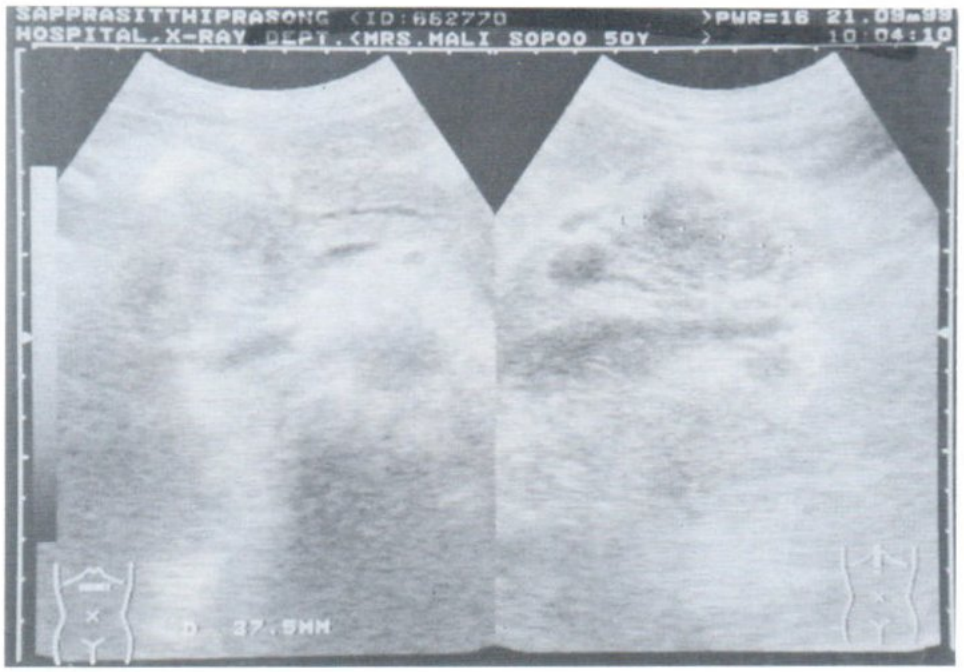

Fig. 12. Low echoic mass at pancreatic head, and mild dilated pancreatic duct.

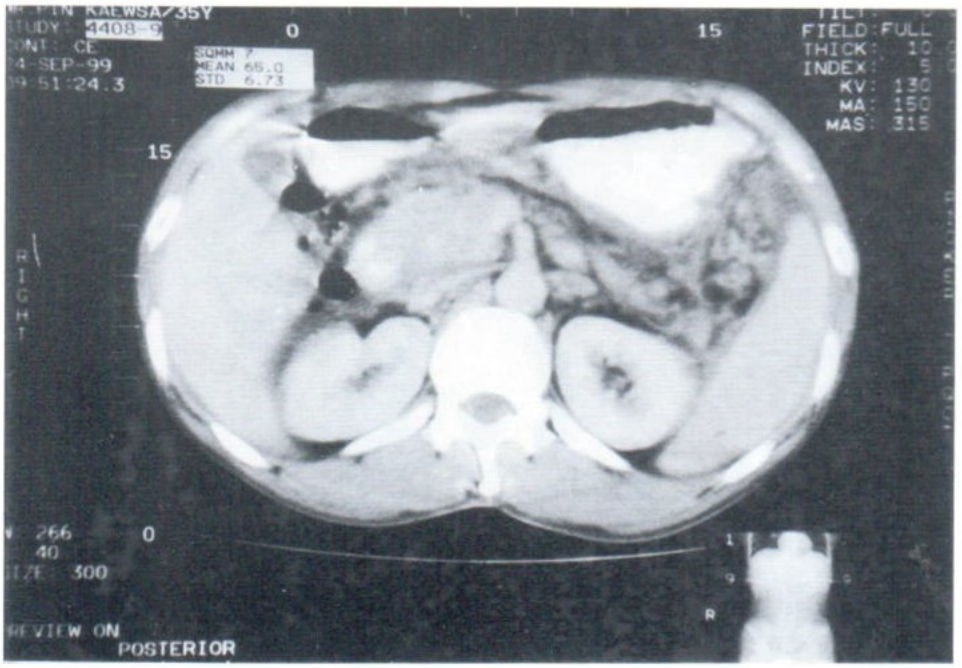

Fig. 13. Focal enlargement of pancreatic head, small pseudocyst at mesentery.

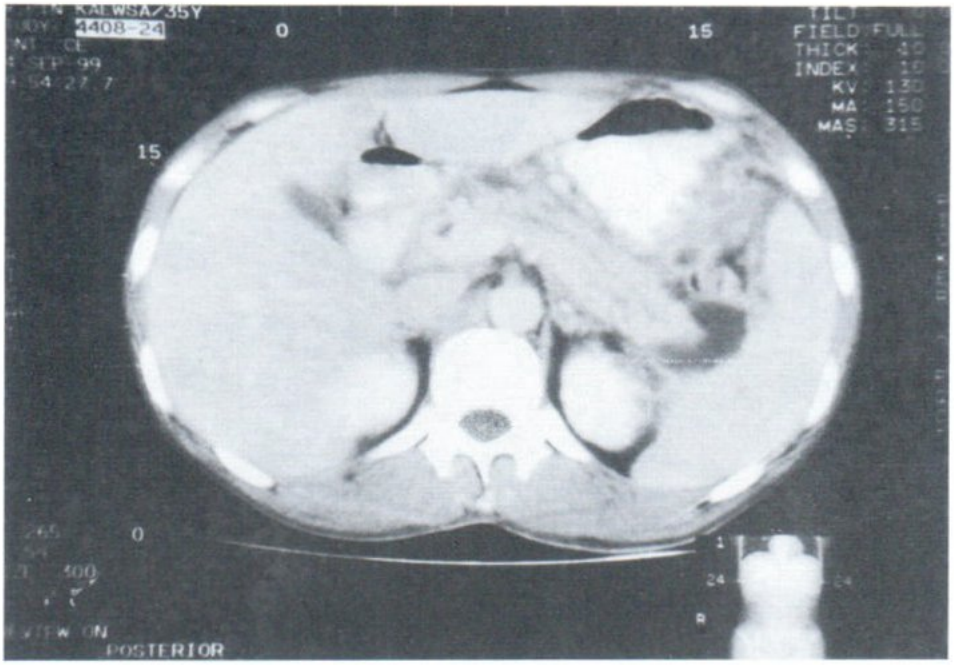

Fig. 14. Fluid collection, or pseudocyst at splenic hilum, mild dilated pancreatic duct.

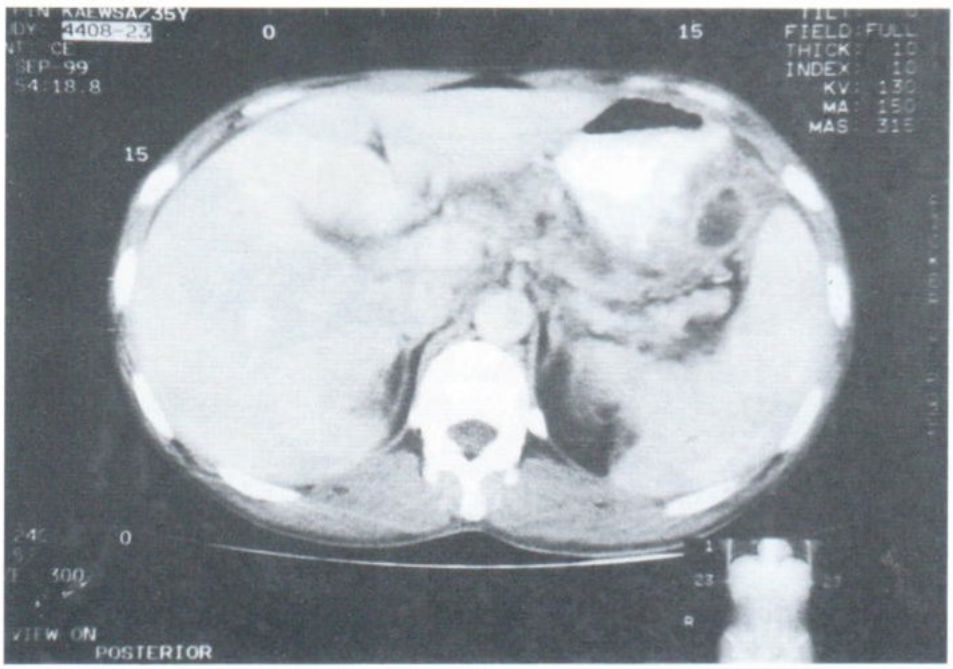

Fig. 15. Small pseudocyst at lesser sac.

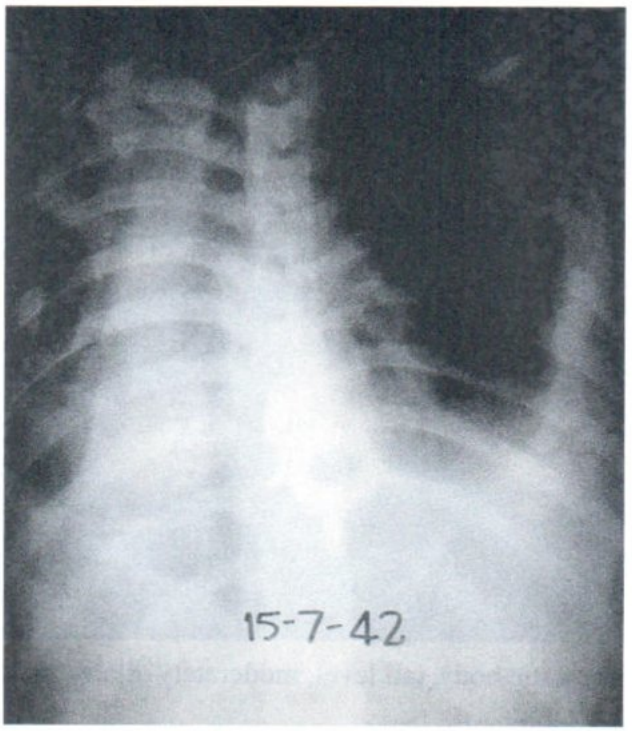

Fig. 16. Bilateral pleural effusion, some loculated component on the right side.

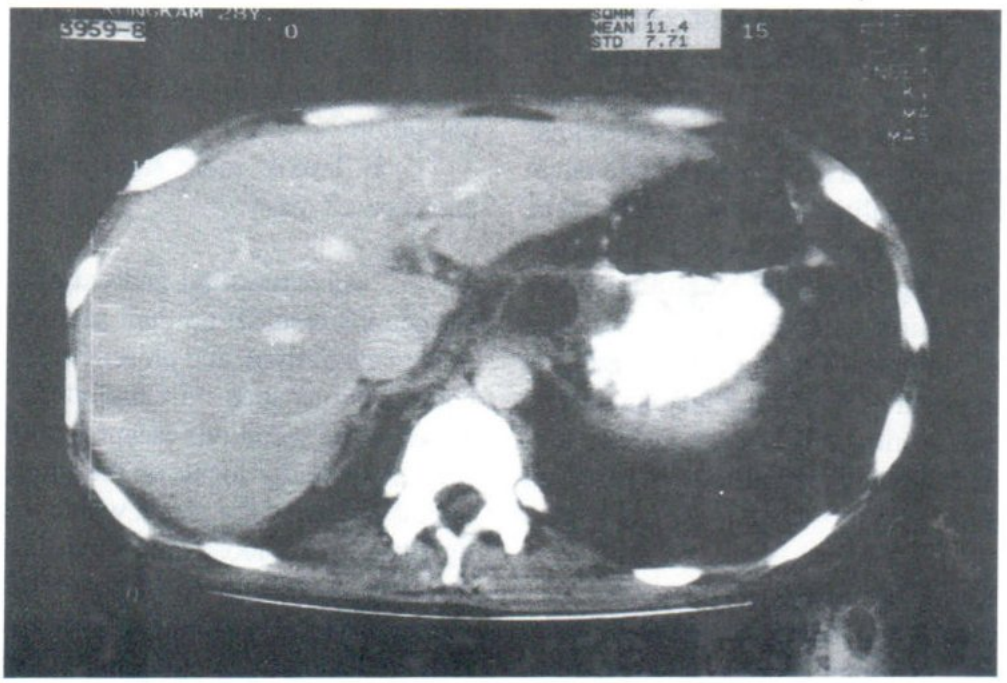

Fig. 17. Well defined pseudocyst, possibly in the hepatogastric ligament.

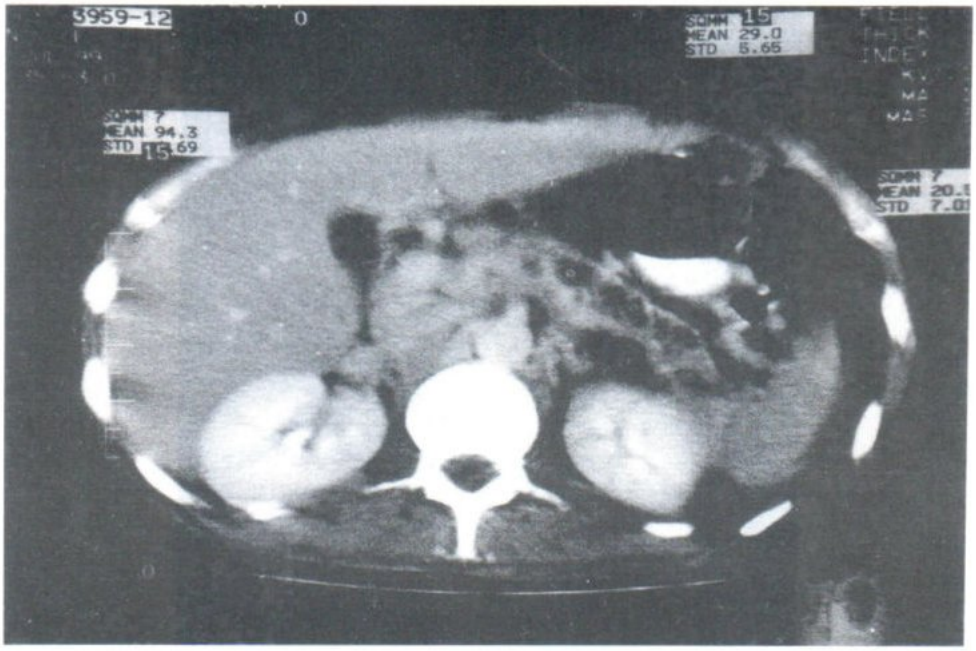

Fig. 18. At pancreatic body, tail level, moderately dilated pancreatic duct is evidence.

DISCUSSION

Pancreatitis is one of the most complex and challenging of all acute abdominal disorders. Its clinical manifestations are as numerous and diverse as its etiologies. No other acute abdominal disorders is accompanied by such a profound range of metabolic abnormalities. A broad spectrum of imflammatory changes may occur in acute pancreatitis ranging from mild edematous interstitial inflammation to fulminant necrotizing pancreatitis. Computed Tomography imaging is helpful as a method of predicting the outcome or severity of pancreatitis at the onset. Balthazar et al. devised the following grading system based on CT finding :

A. Normal pancreas.

B. Focal or diffuse enlargement of the gland (includes nonhomogeneous attenuation of the gland, dilatation of duct, and foci of fluid within the gland, as long as, there is no extrapancreatic edema).

C. Peripancreatic edema and intrinsic abnormalities of grade B.

D. Single ill-defined fluid collection or phlegmon.

E. Two or more fluid collections or the presence of gas.

Pancreatic fluid and extrapancreatic fluid collections result from duct rupture with escape of pancreatic fluid, and present the most common complications seen on Computed Tomography. When these secretions escape from the pancreas, they are typically locate on the anterior or anterolateral surface of the gland, which is covered only by a thin layer of loose connective tissue. The fluid initially leaks into the immediately adjacent spaces: the lesser sac and the left anterior pararenal space. The lesser sac is a potential space anterior to the pancreas and is separated from the pancreas by only a thin layer of connective tissue and the parietal peritoneum, explaining its common

involvement in pancreatitis. Fluid from the lesser sac rarely enters the greater peritoneal cavity due to closure of the foramen of Winslow.

The rare escape of fluid into the greater peritoneal space produces pancreatic ascites. Less frequent involve sites of extrapancreatic inflammatory process include

a) The right anterior pararenal space.

b) The perirenal space after penetrating Gerota's fascia.

c) The posterior pararenal space with spread to the pelvis and upper thigh.

d) The left lobe of liver via the lesser sac and fissure of the ligamentum venosum.

e) The spleen.

f) Between the crura of the diaphragm into the mediastinum.

More frequently in chronic than in acute pancreatitis, this fluid collection tends to be surrounded by a capsule of dense fibrous tissue assuming a cyst-like appearance (Pseudocyst). Most pseudocysts are located in the pancreas and peripancreatic region. The omental bursa is the second most common location of pseudocyst, according to Siegelman et al.[12] The inflammation causes closure of Winslow 's foramen, and the fluid will fill the entire omental bursa or be confined to a local region of the bursa. Uncommonly, the fluid will go to the superior recess of the omental bursa and produce a well defined fluid collection adjacent to the caudate lobe of liver as in the case reported. If a pseudocyst is large enough, it may split the leaves of the omentum producing a mass that project below the surface of the stomach in an anterior position. The inflammatory fluid may also digest through the hepatogastric ligament, splenorenal ligament and even beneath the capsule of solid organ such as liver, spleen,kidney. In case II, the pseudocysts involved the left kidney, left lobe of liver and left psoas muscle. The fluid collection originating from the pancreatic tail focally disrupted gerota's fascia and subsequently the renal capsule to reach the renal parenchyma. Sonography examination of the abdomen was not able to demonstrate the continuity between the pseudocyst and the pancreatic tail, however, primer sonography study was suspected to be pancreatic pseudocyst due to prominent size of pancreatic duct, even though normal size and echo appearance of the pancreas, and the adjacent mesentery appeared to be thickening. Later Computed Tomography study, other signs of pancreatitis was well demonstrable. According to Folco Scappaticci and Stuart K. Markowit,[5] since 1980, 11 cases of intrahepatic pseudocysts arising as complications of pancreatitis have been reported. They also reported one case of intrahepatic pseudocyst complicating pancreatitis in the year 1995. The mechanism have been described for a pseudocyst progression into the hepatic parenchyma. When only the left lobe is involved, it is likely that the fluid initially present in the lesser sac, spreading along the hepatogastric ligament and into the liver. When pancreatitis involves the head of the gland, the potential exists for the spread of disease into the hepatoduodenal ligament. As the common bile duct and the porta vein course within this structure into the porta hepatis, this underlying anatomy provides a mechanism by which intrahepatic pseudocyst formation can develop. In the autopsy case described by Quevedo, Achilles and de Franco,[10] pseudocyts in the liver were found to have developed as pancreatic fluid drained into the liver along the porta vein and it's major branches. In case two, fluid collection along the left lobe liver was seen, and small amount of fluid was seen, crepting along the porta hepatis in case one.

Scrotal swelling may result form a pathologic condition of intrascrotal contents, the scrotal wall or a more generalized disease process. In case three, hydrocele in the scrotum is likely descending from fluid in the abdomen, pancreatic ascites. A sonography of the abdomen

revealed the pancreatic head "mass", mild dilated pancreatic duct, however, sonography failed to demonstrate small pseudocysts 1-2 cm. in the omentum and in the splenic hilum which was well depict on Computed Tomography study. Small pseudocyst at the splenic hilum can be explained that the distal portion of the splenic artery and vein enters the splenic hilum contained within the splenorenal ligament. Because of these anatomic relationships, the spleen and splenic vessels may be involved by pancreatitis. Although rare (frequency 1%-5%), splenic involvement by pancreatitis includes intrasplenic cyst, abscess, hemorrhage, infarction, splenic rupture, and vascular injury. The case of penoscrotal edema due to acute necrotizing pancreatitis have been reported by Kevin K.L Choong.[7] The etiology of his case remains uncertain, but he considered to be an allergic cause.

Chest finding in pancreatitis, includes pleural effusion, usually on the left side with elevated amylase level, empyema, pericardial effusion, mediastinal abscess, pseudocyst, ARDS, and pulmonary edema.

Others complication can occur with pseudocyts, these include a) rupture into the peritoneum cavity, with these rupture the pseudocyst may be colonized and cause an infection b) abscess, fistula c) vascular problems as occlusion, pseudoaneurysm, or spontaneous hemorrhage. Pseudoaneurysm can occur in any vessels in the peripancreatic area, but the most common vessel is the splenic, followed by the gastroduodenal and branches of the pancreaticoduodenal arteries.

The natural history of pancreatic pseudocyts[11] ; 50 % resolve spontaneously and are not clinically significant, 20% are stable and 30% cause complications. In the patients with pseudocysts lasting 7 to 12 weeks, the number of spontaneous resolution decrease. If a pseudocyst is well defined and had a thick fibrous wall, internal drainage is indicated. Internal drainage by cystotomy is the greatest success rate and the lowest complication and recurrence rate. Bradley, Clements, and Gonzalez have recommended that surgical intervention should not be performed in the first 6 weeks because of the high incidence of spontaneous resolution. Between 6 and 13 weeks, the pseudocyst wall becomes well defined , thus internal drainage is possible. Waiting longer than 13 weeks creates a greater risk of spontaneous complications.

In conclusion, despite the rarity of such an entity, clinical, sonography and Computed Tomography of pancreatic pseudocyst, extrapancreatic fluid collection in an uncommon area, should not be mistaken for abscess, mass, or other cause of fluid collections, and correct diagnosis is not difficult by careful imaging. Other signs of pancreatitis, elevated amylase serum level or drainage fluid should arouse suspicious of this condition.

REFERENCES

1. A. Blandino, E. Scribano, G. Aloisi, et al. Subcapsular renal spread of a pancreatic pseudocyst. Abdominal Imaging 1996;21: 73-74.
2. Bradley, EL, Clements, JL, and Gonzalez, AC. The natural history of pancreatic pseudocyst. A unified concept of management. Am J Surg 1979;137:135.
3. Elliot K. Fishman, Philippe Soyer, Donald F. Bliss, et al. Splenic Involvement in Pancreatitis: Spcectrum of CT Findings. AJR 1995;164:631-635.
4. Emil J. Balthazar. CT Diagnosis and Staging of Acute Pancreatitis. Radiol Clin North Am 1989;27:19-37.

5. Folco Scappaticci, and Stuart K. Markowitz. Intrahepatic pseudocyst complicating Acute Pancreatitis: Imaging finding. AJR 1995;873-874.
6. John R. Haaga. The pancreas. In: John R. Haaga, Ralph J. Alfidi, eds. Computed Tomgraphy of the Whole Body Volume 2. St. Louis. Washington, D.C. : The C.V. Mosby Company, 1988:905-945.
7. Kevin K. L. Choong. Acute Penoscrotal Edema Due to Acute Necrotizing Pancreatitis. J Ultrasound Med 1996; 16 : 247-248.
8. Kunio Okuda, Shujiro Sugita, Etsuo Tsukada, et al. Pancreatic pseudocyst in the Left Hepatic Lobe: A Report of Two Cases. Hepatology 1991;13:359-363.
9. Matthew A.Mauro and Robert J. Stanley. In : Joseph K. T. Lee, Stuart S. Sagel, Robert J. Stanley, eds. Computed Body Tomography. New York: Raven press, 1983:213-241.
10. Quevedo FC, Achilles P, de Franco Mf. Propagacao de. Pseudocistos do pancreas pava O figado ebaco : relato de dois casos. Rev Hosp Clin Fac Med S Paulo 1975;30: 371-374.
11. Ralp Weisslerder, Mark J. Rieumont, Jack Wittenberg. Gastrointestinal imaging: Primer of Diagnostic imaging. Mosby : A Times Mirror Company, 1997;223-224.
12. Siegelman, SS, et al. CT of fluid collections associate with pancreatitis. AJR 1980;134:1121.
13. Wolfgang Dahnert. Differential Diagnosis of Hepatic, Billiary, Pancreas, and Spleen disorders: Radiology Review Manual. Williams & Wilkins: Awaverly Company, 1996;487-488.

Message from

Professor Dr. Kawee Tungsubutra

Editor-in-Chief, The Asean Journal of Radiology

Dear Friends ,

This is the 3rd Number of Vol VI of the Asean Journal of Radiology. We are applying to have our journal being accepted to have its appearance in the Index Medicus. I hope it will be accepted soon.

Most of the papers are reports from the members of the Royal College of Radiologists, Thailand. I would like to invite papers from other countries not limited to the Asia.

Kawee Tungsubutra.

Kawee Tungsubutra
SEPTEMBER - DECEMBER 2000.

ASSESSMENT OF RADIATION SAFETY FROM VOLATILIZATION OF ^{131}I IN THE TREATMENT OF HYPERTHYROIDISM AND THYROID CANCER

Puangrat BURANAPONG, Kun SUTTSIRI*, Nat ASAWACHATROJ, Prajak THANAPIBULPOL, Pentip KHUNARAK*, Darunee PEEKHUNTOD*, and Pachee CHAUDAKSHETRIN

ABSTRACT

Oral administration of ^{131}I treatment doses to hyperthyroid and thyroid cancer patients is the most hazardous procedure in nuclear medicine due to possible volatilization of ^{131}Iodine. Internal radiation exposure to medical personnel and patients involving the use of ^{131}I were analysed and assessed at the Department of Radiology by air sampling method. The air sampling was performed on a daily basis in front of an iodine fume hood where treatment doses ranging from 18.5-740 MBq were openly given to 169 hyperthyroid patients during a period of 42 days. At Siriraj Hospital, two thyroid cancer patients are admitted together to the same room due to shortage of room. Room partition to control external radiation exposure is achieved by relocating two lead screens between the patients' beds. To assess internal radiation exposure to the patients, concentration of ^{131}I in air in the room was determined for two days during an isolation period in two pairs of treated patients. It was found that the daily concentration of ^{131}I in air in front of the fume hood ranged from 0.9 to 262.7 Bq/m^3, and the maximum concentration of ^{131}I in air in the thyroid cancer patients' room was 546.9 Bq/m^3. All values were well below the established Derived Air Concentration (DAC) for ^{131}I, 700 Bq/m^3. It could be demonstrated that an individual intake of ^{131}I in the thyroid gland would be less than the Annual Limit on Intake (ALI). It is concluded that where internal body burden of ^{131}I is concerned, it is safe for medical personnel to openly administer treatment doses to hyperthyroid patients, and it is practically safe for two thyroid cancer patients to share the admitting room provided that sufficient shielding is established between their beds to control external radiation exposure.

INTRODUCTION

Oral administration of sodium iodide ^{131}Iodine treatment doses to hyperthyroid and thyroid cancer patients is the most hazardous procedure in nuclear medicine practice due to possible volatilization of radioactive iodine. Iodide solution, particularly in acidic form, when exposed to air will be easily oxidised. The resulting iodine (see equation 1) which is poor water- soluble then become volatile.

$$4I^- + O_2 + 4H^+ \rightarrow 2I_2 + 2H_2O \quad \ldots (1)$$

The risk to medical personnel from airborne radioactivity depends upon the radionu-

Department of Radiology, Faculty of Medicine Siriraj Hospital, Mahidol University,
* Division of Health Physics, Office of Atomic Energy for Peace, Bangkok

clide, its chemical form, its concentration in the air, and the duration of time that persons are exposed to it. Primary method in protecting personnel and the public from airborne radioactivity is to minimize the release of radioactivity to the atmosphere. As a good practice, vials of radioactive iodide solution should be kept tightly capped. The iodide content should be maintained at a basic pH. The volatile fraction can be further reduced by refrigerating the stored vials and keeping them in the dark. Also, when preparing and dispensing the treatment doses, it is advisable to minimize agitation of the vial, and to manipulate the doses in a fume hood.

At the Division of Nuclear Medicine, approximately 400 hyperthyroid and 150 thyroid cancer patients are treated in a year by an oral administration of the sodium iodide ^{131}Iodine. The objective of this study was to analyze and assess radiation safety from volatilization, if any, of radioactive iodine employing air sampling method. Concentration of ^{131}I in air was measured in two restricted areas as follows:

1. in front of the iodine fume hood where the treatment doses are openly given to the hyperthyroid patients to evaluate the safety for local medical workers, and
2. in an isolation room where two thyroid cancer patients are admitted together to evaluate the safety for the patients.

To assess the radiation safety from the volatilization of ^{131}I, measured air concentration of ^{131}I was then compared to its Derived Air Concentration (DAC)#.

MATERIAL AND METHOD

AIR SAMPLING

A vacuum pump (General Electric A-C Motor) was used to sample the air at a flow rate of 0.025 m^3 /min through a glass micro fibre filter (4.7 cm Whatman Grade GF/C) whose function is to filter out any particulate dusts. Volatile radioactive iodine which goes through the fibre filter will pass on to, and be trapped by an activated charcoal filter (4.7 cm TEDA impregnated charcoal). At the end of the daily sampling, both the fibre and charcoal filters were removed from the pump, and radioactivity on them was counted using a high purity germanium detector equipped with a multichannel analyzer and a PC computer. Figure 1 shows a diagram of the sequential processes.

MEASUREMENT OF THE CONCENTRATION OF ^{131}I IN AIR IN FRONT OF THE IODINE FUME HOOD

Approximately 4,440 MBq (120 mCi) of ^{131}I is prepared each week as a stock solution used for the treatment of hyperthyroidism having a fixed concentration of 37 MBq/ml on Monday. Processes of preparing and dispensing of the dose are manipulated remotely in a closed manner using a locally-built dispensing set[2] which is placed in the iodine fume hood. The only part which is open to the atmosphere is a bottle of prescribed amount of ^{131}I from which the patient will suck the dose through a straw (Fig. 2). To evaluate the volatilization of ^{131}I during the oral administration of the doses to the patients, air sampling was performed on a daily basis in front of the fume hood where the treatment doses ranging from 18.5-740 MBq (0.5-20 mCi) were openly given to 169 hyperthyroid patients during a period of 42 days (from July 1, 1997 to January 16, 1998). Durations of time that the workers were in contact with ^{131}I in each day were from 2-30 minutes.

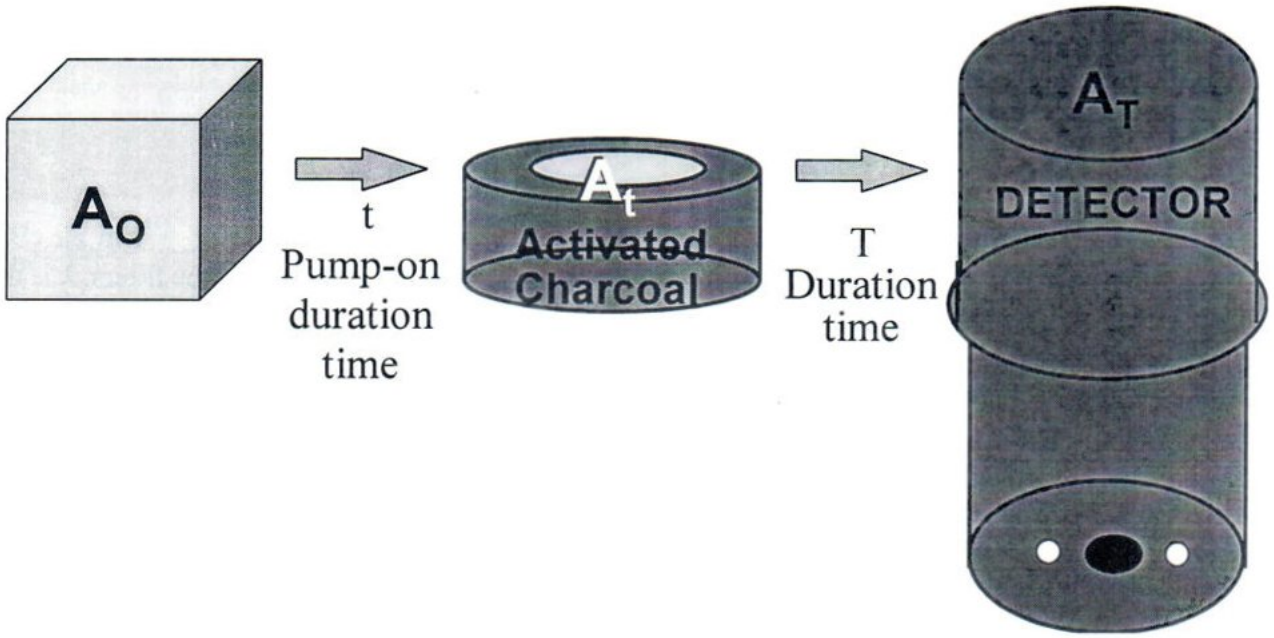

Fig. 1. Processes of air sampling and counting. A_0 is air to be sampled. ^{131}Iodine is trapped by the activated charcoal filter A_t during the pump-on duration time t. Radioactivity on the filter is counted by a germanium detector, and corrected for decay by the elapsed time between end of the sampling and the start of counting (duration time T).

Fig. 2. Air sampling in front of the fume hood during an oral administration of ^{131}I to a hyperthyroid patient.

MEASUREMENT OF THE CONCENTRATION OF ^{131}I IN AIR IN THE THYROID CANCER PATIENTS' ROOM

At Siriraj Hospital two thyroid cancer patients are admitted to the same room due to lack of room. Generally the patients receive 3,700 or 5,550 MBq of ^{131}I on Tuesday and will be discharged from the hospital on Friday. Room partition to control external radiation exposure to the patients is achieved by relocating two lead screens (height: length: thickness = 85: 120: 2 cm per screen) between the patients' beds. Two more lead screens are also placed at the end of each bed as shielding provision for visitors or passers-by. Figure 3 shows a diagram of the isolation room for admitting two thyroid cancer patients. However, as the two patients stay in the same room for 4 days after receiving the treatment doses, their inhale air might be the cause of internal radiation exposure to them. To assess the radiation safety for the patients, concentration of ^{131}I in air in the room was monitored for 2 days during an isolation period in two pairs of treated patients. Pump-on duration time on each day was not exactly 24 hours owing to technical inconvenience. As the isolation period, the most hazardous period, for patients being treated with upto 7,400 MBq (200 mCi) of ^{131}I is about 2 days,[3] no attempt was made to sample the air beyond this period.

CALCULATION OF THE CONCENTRATION OF ^{131}I IN AIR

The concentration of ^{131}I in air is calculated by equation (2).

$$C = R.\lambda. \exp(\lambda T) / V.E.F (1-\exp(-\lambda t)) \quad \ldots\ldots\ldots (2)$$

where C is the concentration of ^{131}I in air (Bq/m^3), R is the count rate (cps) of the filters, λ is the decay constant of ^{131}I (5.9671×10^{-5} min^{-1}), T is the duration time or elapsed time between end of the sampling and the start of counting (min), t is the pump-on duration time or sampling time (min), V is the flow rate of the pump (0.025 m^3/min), E is the counting efficiency of the detecting system (0.013), and F is the photon yield of ^{131}I (0.82 for 365 keV).

RESULTS

The measurement of daily airborne ^{131}I in front of the iodine fume hood revealed that during the sampling period of 42 days the concentration of ^{131}I in air ranged from 0.9 to 262.7 Bq/m^3 (mean = 51.8) as shown in Fig. 4. Even the maximum concentration of ^{131}I was well below the DAC of ^{131}I (700 Bq/m^3). For the concentration of ^{131}I in air in the thyroid cancer patients' room as tabulated in Table 1, it was observed that among the two pairs of treated patients, the worst situation occurred in the first pair whereby one patient vomitted several times for 3 days due to radiation side effect. The patient informed that his vomitus was cautiously collected in a plastic garbage bag and was put into a lead-lining bin provided in the room. Nevertheless the maximum concentration of ^{131}I in air in the first day after the administration of the treatment doses was found to be 546.9 Bq/m^3, which was under the DAC limit.

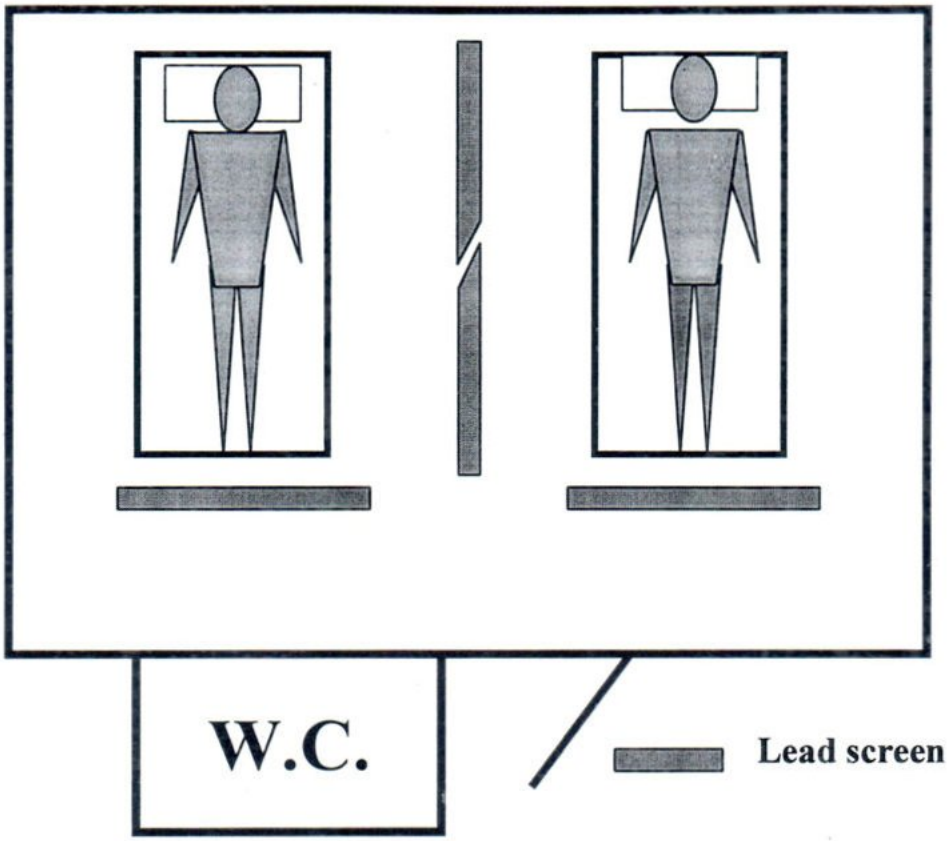

Fig. 3. Diagram of an isolation room for admitting two thyroid cancer patients.

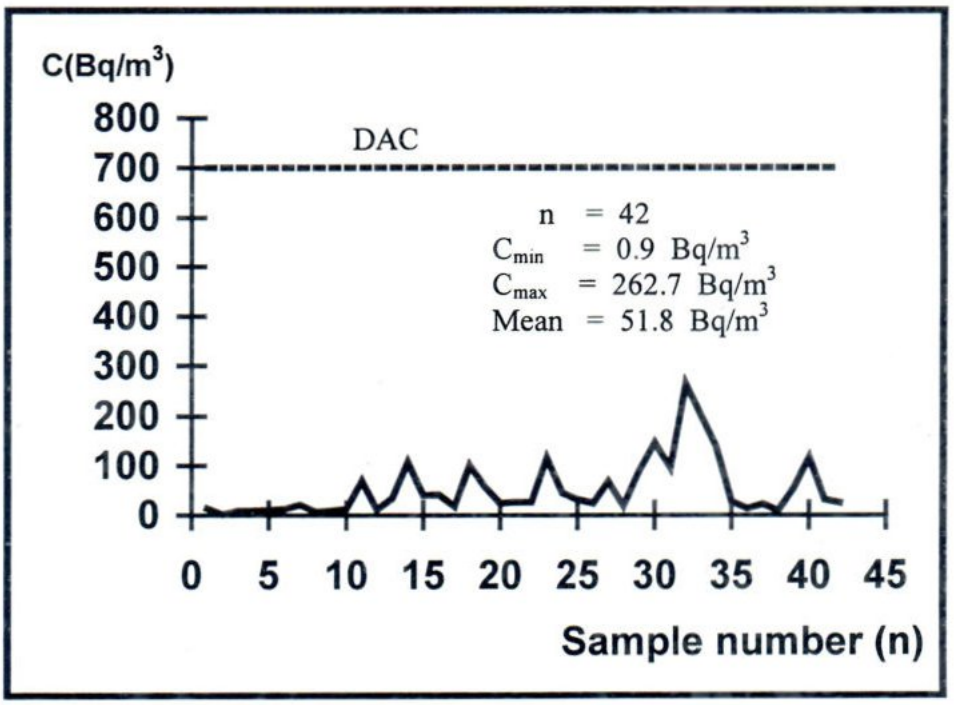

Fig. 4. Daily concentration of ^{131}I in air (C) in front of the iodine fume hood.

Table 1. Concentration of ^{131}I in air in the thyroid cancer patients' room.

Pair of patients	Administered doses in 2 patients (MBq)	Day	Pump-on duration	Concentration of ^{131}I in air in the room (Bq/m^3)
1	5,550 & 5,550	1	17 hr	546.9*
		2	23 hr 50 min	385.0*
2	3,700 & 5,550	1	19 hr 22 min	172.0
		2	23 hr 10 min	107.2

*There was patient's vomitus in the bin.

DISCUSSION

As the concentration of ^{131}I in air in front of the iodine fume hood where the treatment doses were openly administered to hyperthyroid patients, and in the room where two thyroid cancer patients shared it fell below the DAC, it could be concluded that there was little volatile ^{131}Iodine in the areas. This is so because present sodium iodide ^{131}Iodine solution, as commercially available, has been reformulated by changing the pH to basic form and adding buffers, antioxidants and stabilizers to the solution resulting in the reduction of volatilization of the iodine. Nevertheless it is a good practice to manipulate the iodide solution in the fume hood and to minimize the exposure of ^{131}I solution to air as much as possible. At Siriraj Hospital the process of preparing the stock solution of the treatment dose for the treatment of hyperthyroidism, and the dispensing of the prescribed amount of the dose are remotely and closely performed. Only the dispensed dose is open to the atmosphere to facilitate the administration of the dose to the patient.[2] In the case of the treatment of thyroid cancer, the dose is orally administered to the patient in a totally closed manner using a dispensing set locally designed.[5] Thus our concern is in the admittance of two radioactive patients to the same room. In doing so the two patients should be protected from the external radiation exposure by providing enough shielding or increasing the distance between their beds as much as possible. However this study revealed that the internal exposure to the patients themselves due to inhalation was not a problem.

From the measured concentration of ^{131}I in air in the restricted areas, body intake of ^{131}I for those who are in the areas can be calculated from the following equation:

$$\text{Body intake} = CI\tau \quad \ldots\ldots\ldots (3)$$

where I is human inhalation rate (2×10^{-2} m^3 / min), and τ is the time in contact with ^{131}I (min). It can be seen that the body intake depends on the concentration of ^{131}I in air and the time a person spends in contact with the ^{131}I. ^{131}I intake in the thyroid, which is normally assumed to be 30% of the body intake, and the committed dose equivalent for the thyroid can thus be estimated. Table 2 demonstrates two most risky situations where the medical workers who gave the treatment doses to the hyperthyroid patients experienced in this study, i.e.

(1) the measured concentration of ^{131}I in air in one day was maximum at 262.7 Bq/m^3 where the time spent in contact with ^{131}I was 7 minutes, and

(2) the time in contact with ^{131}I on another day was as long as 30 minutes where the measured concentration of ^{131}I in air was found to be 89.0 Bq/m^3.

From these data, the thyroid intake of ^{131}I and committed dose equivalent for the thyroid of the workers could be estimated (Table 2), and found to be under the dose limits established by the International Commission on Radiological Protection (ICRP Publication 54),[4] as shown on the last row of Table 2.

Table 2. ^{131}I intake in thyroid and committed dose equivalent for thyroid in comparison to dose limits[5] : Two risky situations encountered in front of the fume hood.

Situation	Concentration of ^{131}I in air (Bq/m^3)	Time in contact with ^{131}I (min)	^{131}I intake in thyroid (Bq)	Committed dose equivalent for thyroid* (mSv)
1	262.7	7	11.0	0.0032
2	89.0	30	178.0	0.0046
Limit[5]	700 (DAC)	2,000 x 60	2×10^6 (ALI for inhalation)	400

* Committed dose equivalent per unit intake for thyroid = 2.9×10^{-4} mSv/Bq (ICRP Publication 54[4])

CONCLUSION

To evaluate the radiation safety for the medical workers and the patients, air samples were obtained from two restricted areas where the workers administered the ^{131}I treatment doses to hyperthyroid patients and in the room where two thyroid cancer patients were admitted together. Analyses of the air samples indicated that where internal body burden of ^{131}I was concerned, it was safe for medical workers to openly administer the treatment doses to the hyperthyroid patients, and it was practically safe for two thyroid cancer patients to share the room provided that enough shielding is established between the patients' beds to control the external radiation exposure.

ACKNOWLEDGEMENT

The authors thank Ms. Nucharee Putrasreni for the preparations of the illustrations, and the Office of Atomic Energy for Peace for technical support.

REFERENCES

1. Bushberg JT, Leidholdt Jr. EM: Radiation Protection. In: Sandler MP, Coleman RE, Wackers FJTH, et al. Diagnosis Nuclear Medicine, 3rd ed. New York, Williams & Wilkins A Waverly Company 1988; 1: 270-271

2. Buranapong P, Kaewnil V, Pleehachinda R. ^{131}I dispenser for the treatment of thyrotoxicosis: a semi-closed therapeutic system. Presented in the 35th Annual Meeting of the Japanese Society of Nuclear Medicine, Oct. 4-6, 1995, Yokohama-City, Japan. Abstract no. 2029 in the Journal of the Japanese Society of Nuclear Medicine 1995; 32: 891
3. Radiation Safety Handbook, Royal Prince Alfred Hospital, Camperdown, NSW, page 10.3
4. ICRP Publication 54. Individual Monitoring for Intakes of Radionuclides for Workers: Design and Interpretation. Annals of the ICRP 19(1-3) 1988
5. Chaudakshetrin P, Buranapong P, Pleehachinda R. Closed system: a developed method of ^{131}I oral administration for therapeutic dosage. Journal of Radiological Technology 1995; 20(1): 13-18

The Derived Air Concentration (DAC) is the concentration of a radionuclide in air that, if breathed under conditions of light activity for 2,000 hours (working hours in one year), would result in the inhalation of an Annual Limit on Intake (ALI). The ALI is the activity of a radionuclide that, if inhaled or ingested, would produce a committed dose equivalent of 0.5 Sv (50 rem) in any individual organ or tissue or a committed effective dose equivalent of 0.05 Sv (5 rem). From inhalation of airborne ^{131}I pertained to restricted areas, the DAC is 700 Bq/m^3, and the ALI is 2 x 10^6 Bq.[1]

DEVELOPMENT OF INSTANT KITS FOR ^{99M}Tc-LABELLING OF ANTI-CEA MONOCLONAL ANTIBODY AND HUMAN IMMUNOGLOBULINS FOR SCINTIGRAPHY.

Vipa BOONKITTICHAROEN, Ph.D., Duangpen PUCHINDA, M.Sc., Puthiporn CHOUPLYWECH, B.Sc., Wirawat JALAYONDEJA, B.Sc., Chanika SRITARA, M.D., M.Sc., Rojana SIRISRIRO, M.D., Puangtong KRAIPHIBUL, M.D.

ABSTRACT

Simplicity and rapidity are highly desirable features in the development of ^{99m}Tc-labelled radiopharmaceuticals. On the basis of 2-mercaptoethanol reduction, three instant kits were formulated for preparation of ^{99m}Tc-labelled anti-CEA monoclonal antibody (IOR-CEA) used in the detection of colorectal cancers and ^{99m}Tc-labelled immunoglobulins (Sandoglobulin and Venoglobulin) for imaging of infection / inflammation in musculoskeletal system. The kits were sterile and demonstrated to be pyrogen free and had a shelf life of at least 1 year. Efficient labelling (>95% efficiency) could be achieved in 15 min at room temperature. All radiolabelled products exhibited 4-hour biodistribution patterns similar to those reported in literatures, i.e high blood background owing to long half life of IgG in plasma and high renal uptake because of in vivo cysteine transchelation. IOR-CEA was more resistant to cysteine challenge than Sandoglobulin and Venoglobulin. This facilitated the abdominal imaging using IOR-CEA. While the high renal activity in associating with Sandoglobulin and Venoglobulin did not interfere with the investigation of extremities. The costs for kit preparation were 40 times cheaper than those from commercial sources.

The instant kits developed in this study permitted the expensive radioimmunoscintigraphy within the reach of developing countries like Thailand where per capita incomes are far below the global standard.

INTRODUCTION

Development of simple methods for in-house preparation of radiopharmaceu-ticals is desirable for practical uses of the diagnostic agents in clinics. ^{99m}Tc-labelled monoclonal antibody (Mab) and human immunoglobulin G (HIG) have presently emerged as a class of site-specific radiopharmaceuticals in nuclear medicine diagnosis of malignant diseases[1] and detection of infection / inflammation process.[2] The reagents are safe for patient injection since they cause no

Division of Radiotherapy and Nuclear Medicine, Department of Radiology, Faculty of Medicine, Ramathibodi Hospital, Mahidol University, Rama VI Road, Bangkok 10400, Thailand.

Correspondence to: Vipa Boonkitticharoen, Ph.D
Division of Radiotherapy and Nuclear Medicine Department of Radiology Ramathibodi Hospital, Rama VI Road Bangkok 10400, Thailand Fax: 201-1191 Tel: 201-1657 E-mail: ravbk@mahidol.ac.th

biolo-gical hazards like the use of radiolabeled blood cells. Among a large number of methods used for labeling the antibody molecules with ^{99m}Tc,[3] reduction-mediated direct labelling method appears to be technically simple and produces a highly stable product with preserved immunological function.[4] The most attractive feature of the method is the high labelling efficiency which oviates the need for post-labelling purification. Several instant kits are now available commercially but at high prices.

We had previously conducted studies to understand the chemistry of ^{99m}Tc labelling for a number of antitumor Mabs and polyclonal HIG by reduction-mediated direct labelling method.[5] In this study, instant kits were formulated for labelling an anti-CEA monoclonal antibody (IOR-CEA) and two HIGs (Sandoglobulin and Venoglobulin) from different sources. The kits were evaluated for their radiochemical purity, stability towards cysteine challenge, apyrogenicity, shelf life, and in vivo biodistribution.

MATERIAL AND METHOD

ANTIBODIES AND IMMUNOGLOBULINS

IOR-CEA (IgG_1), M170 (IgG_1) and EMD (IgG_{2a}) are murine monoclonal antibodies which react to different types of tumors. IOR-CEA, an anti-CEA antibody, donated by the Center of Molecular Immunology (Havana, Cuba) was chosen for kit development because of its good radioimmunochemistry.[6] M170 reacting to cytokeratin on most human adenocarcinomas was a gift from Biomira Inc. (Edmonton, Alberta, Canada). EMD, an anti-epidermal growth factor (EGF) receptor was kindly donated by Dr Baum (Goethe University Hospital, Germany). Sandoglobulin (Sandoz Pharma Ltd, Basle, Switzerland) and Venoglobulin-I (Alpha Therapeutic Corporation, Los Angeles, U.S.A.) are polyclonal immunoglobulins having the same IgG subclass distributions as those IgG's in normal plasma.

ANTIBODY REDUCTION AND RADIOLABELLING

Under aseptic condition, IOR-CEA, Sandoglobulin and Venoglobulin at concentrations between 7-10 mg/ml in neutral phosphate buffered saline (PBS) were reduced by 2-mercaptoethanol (2-ME) with molar excess of 500:1 and 1000:1 at room temperature for 30 min. The reduced antibodies were purified on a sterile G-50 Sephadex column (Pharmacia, Uppsala, Sweden). Five hundred μg of antibody sample was labelled with 370 or 740 MBq of ^{99m}Tc. The medronate kit containing 1 mg of methylene diphosphonate (MDP) and 0.068 mg of SnF_2 in 1 ml solution was used to form ^{99m}Tc-MDP chelate for antibody labelling.

Radiochemical species were determined by instant thin layer chromatography (ITLC).[7,8] One μl of the labelled antibody solution was spotted onto a 1 x 8 cm ITLC strip. By using different chromatographic materials and solvents (Table 1), percentage of radioactivity was determined for different forms of radiochemical species, i.e. free pertechnetate ($^{99m}TcO^-_4$), ^{99m}Tc-MDP, hydrolysed reduced technetium (HR-^{99m}Tc) and ^{99m}Tc-labelled IgG. Radiolabelling efficiency was defined as percentage of ^{99m}Tc radioactivity tagged to IgG molecules.

Table 1. Instant thin layer chromatographic system for measuring different radiochemical species.[7,8]

Media	Solvent	Impurity	Location
Whatman 31 ET paper	Acetone	$^{99m}TcO_4^-$	Solvent front
ITLC-SG	Normal saline	$^{99m}TcO_4^-$ + ^{99m}Tc-MDP	Solvent front
HSA-impregnated ITLC-SG	EtOH:NH_4OH:H_2O (2 : 1 : 5)	HR-^{99m}Tc	Origin

HR-^{99m}Tc = hydrolysed reduced technetium

CYSTEINE CHALLENGE ASSAY

Stability of the ^{99m}Tc-labelled antibody was challenged with cysteine at concentrations 0, 0.0138, 0.138 and 1.38 mM for 1 hour at 37°C. Chromatographic analysis was performed on a 1 x 8 cm strip of Whatman No. 1 paper using 0.1 M PBS, pH 7, as an eluant. After development and drying, the strip was cut into two halves for gamma counting. In this system, labelled antibody remains at or near the origin, labelled cysteine migrates to the solvent front.[9]

ANIMAL BIODISTRIBUTION STUDIES

One hundred µl of ^{99m}Tc-labelled antibody solution containing 30 µg of IgG with activity around 1850 KBq was injected intraperitoneally into 5 normal balb/c female mice weighing 19.5 ± 2.3 g. Four hours after injection, the animals were sacrificed by spinal dislocation and samples of blood, the entire liver, spleen, heart, stomach with contents, femur, both kidneys and a sample of thigh muscle free of fat were removed. All tissues were rinsed in cold saline immediately after removal, patted dry and weighed before counting against a standard of the injectate.

LIMULUS AMEBOCYTE LYSATE (LAL) TEST.

The amount of bacterial endotoxin present in the frozen kit was determined by LAL test (Biowhittaker, Walkersville, MD, U.S.A) which utilizes a co-lyophilized mixture of LAL and a synthetic color producing substrate to detect endotoxin by measuring the colored product, p-nitroaniline at 405 nm. The test was performed with a 96-well microplate. On the basis of endotoxin standards, endotoxin unit (EU) in the antibody sample could be calculated. By U.S.P. standard,[10] no patient will receive more than 175 EU of endotoxin in a worst-case scenario.

SHELF LIFE OF THE INSTANT KITS.

The three instant kits, i.e. IOR-CEA, Sandoglobulin and Venoglobulin, were stored at -20° C and thawed after 1, 3, 6, 9, 12 months of storage to investigate for their physical appearance and labeling efficiency.

RESULTS

ANTIBODY REDUCTION AND CYSTEINE CHALLENGE

Optimal concentration of 2-mercaptoethanol (2-ME) was firstly established for each antibody. To achieve clinically useful specific activities, i.e. 740-1480 MBq/mg, 500:1 molar excess of 2-ME was required for generating ^{99m}Tc reactive sites in Sandoglobulin while IOR-CEA and Venoglobulin required twice as much of 2-ME (Table 2). ^{99m}Tc- labelled antibodies mediated by 2-ME reduction yielded the products which were stable for several hours after preparation. Less than 10% of ^{99m}Tc were lost when the labelled antibodies were incubated for 24 hours at 37° C either in PBS or serum proteins (Data are not present). Nevertheless, ^{99m}Tc-labelled antibodies were reported to be susceptible to in vivo trans-chelation via cysteine and excreted by kidney.[9,11] To understand the nature of ^{99m}Tc binding site induced by 2-ME, 4 antibodies of different reduction sensitivity (i.e. Sandoglobulin> Veno-globulin > IOR-CEA > EMD)[5] were challenged to a range of cysteine concentrations varying from 0, 0.0138 to 1.38 mM. On an overall basis, ^{99m}Tc-labelled Mabs were more stable to cysteine (0.138 mM upward) than polyclonal HIGS ($p<<0.001$) (Table 3). Order of stability could be ranked as follows : IOR-CEA > EMD > Sandoglobulin > Venoglobulin.

Table 2. 2-Mercaptoethanol(2-ME) - reduction of the antibody molecules for ^{99m}Tc-labelling.

Molar ratio 2ME : IgG	^{99m}Tc added (MBq / mg)	Labelling efficiency (%) IOR-CEA	Sandoglobulin	Venoglobulin
500 : 1	740	48.17 ± 6.40	99.39 ± 0.16	98.56 ± 0.23
	1480	NA	99.13 ± 0.14	90.45 ± 7.88
1000 : 1	740	99.66 ± 0.08	99.28 ± 0.22	99.00 ± 0.10
	1480	99.05 ± 0.38	98.85 ± 0.34	98.38 ± 0.54

NA = not available.

Table 3. In vitro stability to cysteine challenge of ^{99m}Tc-labelled monoclonal antibodies and human immunoglobulins. The data, mean ± SE(N = 5), present the percentage of radioactivity transchelated to cysteine molecules.

Cysteine : IgG	Concentration of Cysteine (mM)	Monoclonal Antibodies IOR-CEA (IgG_1)	EMD (IgG_{2a})	Polyclonal Antibodies Sandoglobulin	Venoglobulin
0	0	5.57 ± 0.07	4.20 ± 0.50	3.88 ± 0.20	3.03 ± 0.19
5 : 1	0.0138	4.92 ± 0.15	6.91 ± 1.15	4.83 ± 0.35	6.98 ± 0.19
50 : 1	0.138	14.21 ± 0.93	14.41 ± 0.36	26.65 ± 1.84*	40.79 ± 3.56*
500 : 1	1.38	34.40 ± 1.04*	50.04 ± 1.42*	55.50 ± 0.92*	74.48 ± 2.21*

* Significant difference with $p << 0.001$

RADIOCHEMICAL PURITY AND IN VIVO BIODISTRIBUTION

The instant kits developed in this study yielded ^{99m}Tc-labelled antibodies of high radiochemical purity (>95%). Less than 5% of the activity appeared as impurities in forms of $^{99m}TcO^-_4$, ^{99m}Tc-MDP and HR.-^{99m}Tc (Table 4). Therefore, no remarkable uptake by thyroid, stomach or reticuloendothelial system could be observed upon injection.

In animal study, high blood background and high kidney uptake were common findings for all labelled antibodies investigated here (Table 5). ^{99m}Tc-labelled IOR-CEA which was more resistant to cysteine transchelation was found to have lower kidney uptake than Sandoglobulin and Venoglobulin ($p<<0.001$). Similar biodistributions were observed between two Mabs (IOR-CEA, M170) which belong to the same IgG_1 subclass, although their 2-ME reduction sensitivities were different.[5] Interestingly, Venoglobulin which was more vulnerable to in vitro cysteine transchelation displayed lower kidney activity than Sandoglobulin ($p<0.05$). Significantly higher blood background and heart activity were also noted ($p<<0.001$). The presence of ^{99m}Tc-labelled human serum albumin (HSA) was postulated to be the cause. In compounding Venoglobulin, 0.2 g of HSA was added per g of IgG as a carrier.[13] In our laboratory, effective labelling of ^{99m}Tc to HSA could also be achieved by 2-ME reduction at 500:1 molar excess. Since ^{99m}Tc-labelled HSA is a blood pool agent for dynamic cardiac function studies,[14] this might be accounted for the remarkable blood and heart activities for Venoglobulin sample. Because HSA is a normal blood component, excretion of ^{99m}Tc-labelled HSA by kidney can not be observed early.[14] On the contrary, kidney has been suggested as a site for catabolism of ^{99m}Tc-labelled IgG by direct approach.[11] Lower kidney uptake of ^{99m}Tc-labelled Venoglobulin in comparing to Sandoglobulin ($p<0.05$) indicated a more favorable in vivo stability for IgG in Venoglobulin. Instability of ^{99m}Tc-HSA towards in vitro cysteine challenge might be responsible for the loss of activity from the Venoglobulin sample.

Table 4. Distribution of different radiochemical species for the three instant kits.

Readiochemical Species	Instant Kit			Site of uptake
	IOR-CEA[a]	Sandoglobulin[b]	Venoglobulin[b]	
$^{99m}TcO_4$	0.84 ± 0.31	0.53 ± 0.12	0.09 ± 0.03	Blood, thyroid, stomach salivary gland, etc[12]
^{99m}Tc-MDP	0.69 ± 0.13	1.10 ± 0.10	0.34 ± 0.01	Bone[12]
HR-^{99m}Tc	0.55 ± 0.14	2.07 ± 0.31	1.10 ± 0.18	Reticuloendothelial system (liver, bone marrow, spleen)[12]
^{99m}Tc-IgG	97.92 ± 0.39	96.30 ± 0.66	98.47 ± 0.24	Colon cancer[(a)] Infection / inflammation[(b)]

Table 5. The four-hour biodistributions of ^{99m}Tc-labelled monoclonal antibodies and human immunoglobulins in normal balb/c mice. The data, mean ± SE (N = 5) are expressed as percentage of injected dose per gram of tissue.

Organ	Murine Monoclonal Antibody		Polyclonal Human Immunoglobulin G	
	IOR-CEA (IgG_1)	M170 (IgG_1)	Sandoglobulin	Venoglobulin
Blood	16.60 ± 1.53	14.25 ± 0.78	13.32 ± 1.86	19.61 ± 1.21
Liver	5.02 ± 0.51	5.86 ± 0.38	3.82 ± 0.47	5.12 ± 0.36
Spleen	4.95 ± 0.34	5.41 ± 0.42	4.50 ± 0.43	5.63 ± 0.18
Heart	4.78 ± 0.42	3.92 ± 0.23	4.45 ± 0.28	7.79 ± 0.34
Stomach	2.46 ± 0.27	3.13 ± 0.17	3.09 ± 0.45	2.38 ± 0.27
Kidney	8.47 ± 0.57	8.88 ± 0.52	23.24 ± 2.27	16.00 ± 0.83
Femur	1.79 ± 0.17	2.04 ± 0.33	1.47 ± 0.20	2.10 ± 0.56
Muscle	1.68 ± 0.18	1.12 ± 0.16	1.04 ± 0.12	1.10 ± 0.10

APYROGENICITY AND SHELF LIFE

For commercially avialable instant kits, the modified antibody is supplied in lyophilized form which is quite suitable for large scale manufacturing. In kit preparation for in house use, it is more convenient to prepare the frozen kit. Procedure for kit preparation by aseptic technique is described in Table 6. Apyrogenicity of the instant kit was assessed by bacterial endotoxin level using chromogenic LAL assay. For each antibody, three batches of instant kits were assayed for endotoxin level. Endotoxin units in each kit were well below the limit recommended by U.S. Pharmacopia[10] (Table 7). All the frozen kits stored at -20° C were highly stable. Neither changes in labelling efficiency nor in physical appearance of the antibody solution could be observed over a peroid of one year (Table 8).

Table 6. Standard procedure for preparing instant kits for labelling the anti-CEA monoclonal antibody and human immunoglobulins with ^{99m}Tc.

I. Antibody reduction under aseptic condition

1 Adjust or concentrate in case of diluted solution, the 10mg antibody to a concentration of 5-10 mg/ml.

2 Add 2-ME to provide a 1000 : 1 of 2 ME : IgG molar ratio and allow the reaction to proceed for 30 min at room temperature with intermittant shaking.

3 Purify the reduced antibody with a prechilled Sephadex-G50 column (2 x 8 cm) using N_2-purged PBS as mobile phase.

4 Assay the antibody peak by spectrophotometer at 280 nm, based on $E^{1\%}_{1cm} = 14.3$.

5 Adjust the concentration of the reduced antibody to > 0.5 mg/ml[5] and sterilize the antibody solution by 0.22 μm membrane filter (hydrophilic Durapore Membrane, Millipore).

6 Fractionate the antibody solution into 2 ml aliquots.

7 Purge the antibody sample for 2 min with sterile N_2 gas before freezing at -20° C.

II. Radiolabelling by sterile technique

8 Thaw the frozen sample.

9 Add 15 μl of MDP-SnF_2 to the antibody sample and mix gently.[5]

10 Add 740 MBq ^{99m}Tc-pertecnetate to antibody / MDP mixture and allow the reaction to undergo at room temperature for 15 min.

11 Assess labelling efficiency (should be >95%) by ITLC.
(The labelled antibody was highly stable for many hours after labelling.)

Table 7. Apyrogenicity test by chromogenic limulus amebocyte lysate (LAL) assay.

Instant kit	Endotoxin (EU/mg IgG)
IOR-CEA	less than 59.9 ± 42.4
Sandoglobulin / Venoglobulin	less than 9.7 ± 0.2

Endotoxin limit : USP < 175 EU / mg.[10]

Table 8. Long-term stability of the three instant kits assessed by ^{99m}Tc-labelling efficiency.

Month of Storage	Labelling Efficiency (%)		
	IOR-CEA	Sandoglobulin	Venoglobulin
1	98.36 ± 0.08	94.05 ± 1.09	97.81 ± 0.81
3	98.35 ± 0.08	98.42 ± 0.81	97.82 ± 0.02
6	97.06 ± 0.13	97.37 ± 0.16	99.16 ± 0.39
9	96.25 ± 0.62	99.15 ± 0.74	99.29 ± 0.18
12	98.84 ± 0.12	97.01 ± 0.19	98.72 ± 1.74

All the instant kits stored over a period of one year appeared as clear solutions after thawing.

DISCUSSION

Considerations in development of instant kit for in-house preparation of radiopharmaceutical using short-lived radionuclide like ^{99m}Tc based upon the following factors : (1) yield of the desirable radiochemical species; (2) simplicity, reproducibility and cost of the instant kit; (3) biodistribution behaviour of the radiopharmaceuticals; (4) shelf-life and apyrogenicity. For the three labelling kits formulated in this laboratory, effective labelling was highly reproducible. No changes in labelling efficiency observed over 12-month storage. The procedures for kit preparations were simple and rapid. It took one day to reduce the antibody to make a batch of instant kits for 3-4 month use. Radiolabelling required only 15 min of reaction at room temperature. Post labelling purification was not required since labelling efficiency exceeded 95%. The kits were pyrogen free and safe for patients injection. IOR-CEA kit and Venoglobulin kits are now used by our institute for detection of colorectal cancers[15] and localization of infectious foci in musculosketal system.[16] Both kits had shelf life of not less than 1 year. In comparing to the price of a commercial kit for infection / inflammation imaging, the cost for preparation of Venoglobulin kit as well as Sandoglobulin was 40 times cheaper.

IOR-CEA, Sandoglobulin and Venoglobulin displayed typical biodistributions in balb/c mice, i.e. high blood background and high kidney uptake, which were the common findings for ^{99m}Tc-labelled antibody by direct approach.[4, 17-20] However, high liver uptake was reported in animals bearing tumor,[4,19] or with abcess[17, 18, 20] as well as in patients.[15, 16] Beaty et al[21] demonstrated that much of the liver activity was related to metabolism of the immune complex sequestrated from the blood stream. Absence of antigen-antibody complex in normal mouse model could be accounted for low liver uptake for the kits developed in this study. IgG has long resident time in blood circulation (human IgG = 23 day,[22] mouse IgG = 4 day.[22]) This could explain the observation of high blood background at 4 hours after injection. In our institute, high blood pool activity was neither a problem for imaging of infection / inflammation process in the musculoskeletal system[16] nor prevented the sucessful localization of colorectal cancers owing to their

high target-to-background ratios.[15]

Our labelling kits, like those reported in literatures,[4, 23] were quite stable towards in vivo oxidation of the reduced ^{99m}Tc to free pertechnetate or transchelation to serum proteins except for sul -fhydryl containing molecules such as cysteine[9, 11] which is present at high concentration in plasma (10 μM[24]) and tissue (10-100μM.[25]) Antibody catabolism in kidney or transchelation of the radiolable was identified as the cause of high renal uptake.[11] In vitro cysteine challenge assay did not predict in vivo stability of Venoglobulin kit due to the presence of ^{99m}Tc-labelled HSA. Nevertheless, lower kidney uptake of Venoglobulin in comparing to Sandoglobulin suggested that ^{99m}Tc-labelled Venoglobulin might be a better imaging agent.

Localization of the human IgG is postulated to be dependent of increased vascular permeability, bacterial recognition, Fc mediated binding to both granulocytes and microorganisms at the infectious site.[26] Some IgG such as Sandoglobulin may receive enzymatic treatment during manufacturing and leads to damaged Fc regions.[27] Dormehl et al[18] observed the greater uptake by the inflammatory foci of the Gammagard IgG with intact Fc than Sandoglobulin IgG of which the activity of Fc portion was impaired during production. For Venoglobulin, the production process involves no enzymatic modification. The molecule is reported to retain its full biological functions in opsonizing, complement binding and Fc-receptor binding of polymorphonuclear cells.[13] For these reasons, Venoglobulin kit was chosen for clinical uses.

ACKNOWLEDGEMENTS

This study was partly supported by World Health Organization (WHO) and the International Atomic Energy Agency (IAEA).

REFERENCE

1. Britton KE. Towards the goal of cancer-specific imaging and therapy. Nucl Med Commun 1997; 18:992-1007.
2. Chianelli M, Mather SJ, Martin-Comin J, Signore A. Radiopharmaceuticals for the study of inflammatory processes. A review. Nucl Med Commun 1997; 18:437-55.
3. Reilly RM. Immunoscintigraphy of tumours using ^{99m}Tc-labelled monoclonal antibodies : a review. Nucl Med Commun 1993; 14 : 347-59.
4. Mather SJ, Ellison D. Reduction-mediated technetium-99m labelling of monoclonal antibodies. J Nucl Med 1990; 31 : 692-7.
5. Boonkitticharoen V, Puchinda D, Ngonrath Na Ayudhya A, Kraiphibul P. Factors affecting chemistry of reduction - mediated ^{99m}Tc-labelling of monoclonal antibodies and immunoglobulins. J Med Assoc Thai (In press).
6. Boonkitticharoen V, Puchinda D, Chouplywech P, Jalayondeja W. Reduction-mediated ^{99m}Tc-labelling of antitumor monoclonal antibodies : Effect of increasing specific activity on antibody binding kinetics. J Med Assoc Thai 1998; 81:74-9.
7. Robbins PJ. Chromatography of Technetium-99m Radiopharmaceuticals A Practical Guide. New York : The Society of Nuclear Medicine Inc, 1984.
8. Throll JH, Freitas JE, Swanson D, et al. Clinical comparison of cardiac blood pool visualization with Tc-99m red blood cells labelled in vivo with Tc-99m human serum albumin. J Nucl Med 1976; 19 : 796-803.
9. Hnatowich DJ, Virzi F, Winnard P, Fogarasi M, Rusckowski M. Investiga tions of ascorbate for direct labelling of antibodies with technetium-99m. J Nucl Med 1994; 35 : 127-34.
10. United States Pharmacopia. 22nd ed, Rockville : Mack Printing Co., 1989; 1493-5.

11. Mardirossian G, Wu C, Rusckowski M, Hnatowich DJ. The stability of ^{99m}Tc directly labelled to an Fab' antibody via stannousion and mercaptoethanal reduction. Nucl Med Commun 1992; 13:503-12.
12. Ponto JA, Swanson DP, Freitas JE. Clinical manifestations of radiopharmaceutical formulation problems. In: Hladik WB, Saha GB, Study KT, eds. Essentials of Nuclear Medicine. Baltimore : William & Wilkins, 1987; 268-89.
13. Alpha Therapeutic Corporation. Venoglobulin-I. Product Monograph. Los Angeles : 1991.
14. Vanbilloen HP, Verbeke KA, De Roo MJ, Verbruggen AM. Technetium-99m labelled human serum albumin for ventriculography : a comparative evaluation of six labelling kits. Eur J Nucl Med 1993; 20: 465-72.
15. Sirisriro R, Boonkitticharoen V, Kraiphibul P, et al. Detection of colorectal carcinoma by anti-CEA monoclonal antibody (IOR-CEA1) labelled with ^{99m}Tc scintigraphy. Hepato-Gastroenterol (In press).
16. Sritara C, Sinphurmsukskul O, Boonkitticharoen V, et al. Clinical evaluation of technetium-99m labelled human polyclonal immunoglobulin G for imaging of bone and joint infection. Asean J Radiol (Submitted for publication).
17. Oster ZH, Som P, Rhodes BA, et al. Abscess scintigraphy with ^{99m}Tc-human immunoglobulin (IgG) using a one-step labelling method. Nucl Med Biol 1993; 20: 225-30.
18. Dormehl IC, Louw WK, Hugo N. Biodistribution and accumulation in inflammatory lesion of different thiol reduction-mediated ^{99m}Tc-IgG preparations in baboon model. Nucl Med Commun 1994; 15: 475-82.
19. Gooden CSR, Snook DE, Maraveyas A, Rowlinson-Busza G, Peters AM, Epenetos AA. Direct technetium-99m labelling of three anticancer monoclonal antibodies : Stability, pharmacokinetics and imaging. J Nucl Med 1995; 36: 842-9.
20. Claessens RA, Boerman OC, Koenders EB, et al. Technetium-99m labelled hydrazinonicotinamido human non-specific polyclonal immunoglobulin G for detection of infectious foci: a comparison with two other technetium-labelled immunoglobulin preparations. Eur J Nucl Med 1996; 23:414-21.
21. Beatty JD, Beatty BG, O'Conner-Tressel M, et al. Mechanisms of tissue uptake and metabolism of radiolabelled antibody-Role of antigen : antibody complex formation. Cancer Res (Suppl) 1990; 50: 8408-458.
22. Kerr MA, Thorpe R. Immunochemistry. The LABFAX series. Oxford: Blockwell Scientific Publications, 1994.
23. Hawkins EB, Pant KD, Rhodes BA. Resistance to direct Tc-99m-protein bond to transchelation. Ant Immun Radiopharm 1990; 3: 17-25.
24. Aebi S, Assereto R, Lauterburg BH. High-dose intravenous glutathione in man. Pharmacokinetics and effects of cysteine in plasma and urine. Eur J Clinical Invest 1991; 21: 103-10.
25. Cooper AJL. Biochemistry of sulfur-containing amino acids. Ann Rev Biochem 1983; 52: 187-222.
26. Calame W, Feitsma HI, Ensing GJ, et al Detection of a local staphylococcal infection in mice with technetium-99m-labelled polyclonal human immunoglobulin. J Nucl Med 1991; 32: 468-74.
27. Hopkins SJ. Sandoglobulin. Drugs of Today 1985; 21: 279-82.

บริษัท กรุงศิลป์วิวรรณ จำกัด
SONGSITTIVAN CO.,LTD.
Tel. 910-1999 Fax : 910-1888